DYNAMIC MECHANICAL PROPERTIES OF FIBRES

by

ARTHUR A. HARRY

A THESIS

presented to

THE UNIVERSITY OF GLASGOW

FOR THE DEGREE

OF

DOCTOR OF PHILOSOPHY

AUGUST 1965.

ProQuest LLC.
789 East Eisenhower Parkway
P.O. Box 1346
Ann Arbor, MI 48106 – 1346

C O N T E N T S

ACKNOWLEDGEMENT.

The author wishes to express his sincere gratitude to Professor R.Meredith, D.Sc., F.T.I., F. Inst. P., F.R.S.E. for his valuable guidance and encouragement during the course of this work.

Thanks are due also to all the members of the staff of the Fibre Science Department, the University of Strathclyde for their keen interest and assistance in arranging suitable working conditions. The author wishes to express his thanks also to all his colleagues for their co-operation at all times.

Finally, the author is indebted to Chemstrand Ltd.,for the financial assistance which made this work possible.

A B S T R A C T.

The dynamic mechanical properties of rod like polymer specimens, plastics, and rubbers have been studied in some detail during the last decade. Nevertheless, comparatively less information is available on fibres of normal textile counts. This project, therefore, was undertaken with a view to investigating the dynamic mechanical properties of severl natural and synthetic fibres of normal textile counts ever a wide range of temperature and /or humidity. For this purpose two experimental techniques have been developed in the Fibre Science laboratory at the University of Strathclyde.

One of the experimental techniques is similar to that used by Meredith and Hsu[40] for measuring the dynamic bending properties of dry fibres in vacuo over a range of temperature. Certain modifications in the design of the apparatus have been made in order to minimise conduction losses through the fibre mounting system so that in vacuo the temperature recorded by the sensing element was as close as possible to the temperature of the fibre.

The other experimental technique is similar to that employed by Yoshino and Takayanagi[75] for measuring the dynamic tensile properties of films and monofilaments. To make dynamic tensile measurements possible on fibres of normal textile counts and fibres from tyre cords over a wide range of temperature and/or humidity the apparatus was designed in the

laboratory and made in the work shop with finer strain gauge systems and other necessary accessories.

A detailed description of the apparatus and working procedures have been given in the thesis.

Measurements were carried out on several fibres like wool, silk, Fibrolane, ramie, Fortisan, viscose rayon, acetate, Tricel, Acrilan 16, Orlon, three types of polypropylene, eight types of nylon 66, Terylene, Dacron and finally three types of polyblend fibres.

The results are discussed in the light of the information available to date on dynamic mechanical properties, NMR spectroscopy and infra-red spectroscopy on high polymers.

Optical, physical and tensile properties of some of the synthetic fibres have also been studied to find the correlation of these properties with the observed dynamic mechanical properties.

Finally the effect of heat setting of Acrilan 16, nylon 66 type 900 and Terylene on the optical, physical and mechanical properties of these fibres have been studied.

CHAPTER 1 INTRODUCTION

INTRODUCTION

1. General Introduction.

The physical properties of high polymers at any given temperature are determined to a great extent by the internal mobility of the chains of which they are composed.[1] It is therefore of considerable practical, as well as theoretical, interest to know the types of molecular motions present in a given polymer and how these motions are related to the composition and structure of the polymer as well as to the temperature.

Three of the most useful physical methods for studying internal motions in polymers chains are nuclear magnetic resonance, (NMR), dielectric dispersion and dynamic mechanical measurements. Dynamic mechanical methods consist of measuring the in phase and out of phase deformational responses of a polymer specimen subjected to an applied alternating stress. Dielectric methods consist of measuring the response of dipoles in a material to oscillating electric fields. Nuclear magnetic resonance method consists of measuring the response of a material to a small radio frequency magnetic field while the specimen is maintained in a strong steady magnetic field. In many ways it is analogous to dielectric dispersion measurements in that they both measure a resonance phenomenon between the dipoles and applied field. In dielectric measurements electric dipoles and electric fields are involved, while in NMR measurements, magnetic dipoles and magnetic

fields are involved. However, one of the most important differences between the two methods concerns the dipole rotation which is brought to resonance with the applied oscillatory field.

In dielectric measurements, the dipole oscillating under the action of the electric field consists of a group of atoms, and its rotation is restricted by the viscous contacts with the neighbouring molecules. The characteristic features of the dipole dispersion curve are determined almost entirely by these viscous forces.

In nuclear magnetic resonance measurements however, the dipoles are the nuclei of the atoms, and rotation of nuclear dipoles can take place through the rotation of the nucleus of the atom. In general, the atom itself does not move and hence, no viscous forces are involved.

The dielectric dispersion of polar polymers is a valuable tool for determining the rate of motion of dipoles. Nevertheless, the method is apparently restricted to polymers where the main chain contains judiciously placed polar groups. However, there are no such restriction in the nuclear magnetic resonance method and it is becoming a very popular technique for studying segmental mobility in polar and non polar polymers.

A study of physical properties of high polymers can never be complete without an understanding of the fundamental molecular structure of long chain polymers. For such a study, however, recourse is made

to the well established x-ray diffraction technique and to the more radical infra-red spectroscopic technique.

2. Viscoelastic Properties.

The classical theory of elasticity deals with mechanical properties of perfectly elastic solids. From Hooke's law for such solids the stress is always directly proportional to strain but is independent of the rate of strain. The theory of hydro-dynamics, however, deals with the properties of viscous liquids, for which in accordance with Newton's law the stress is always directly proportional to rate of strain but is independent of strain itself. These theories are idealisations and any real solid shows deviations from Hooke's law under suitably chosen conditions, and it is also probably true that any real liquid would show deviations from Newton's law if subjected to sufficiently precise measurements.

There are two important deviations. Firstly, the strain in a solid or the rate of strain in liquid may not be directly proportional to stress but may depend on stress in a more complicated way as is familiar when the elastic limit is exceeded for a solid. Secondly, the stress may depend on both the strain and the rate of strain together with higher time derivatives of strain. Such time dependent behaviour of materials reflects a combination of liquid-like and solid-like characteristics and is therefore, called viscoelastic.

If in a given experiment the ratio of stress to strain is a function of time alone, and not of the stress, the viscoelastic behaviour of the material is said to be linear. Its mechanical properties can be duplicated by a model consisting of a suitable combination of springs that obey Hooke's law and viscous dash-pots (i.e. pistons moving in oil) which obey Newton's law (Fig 1).

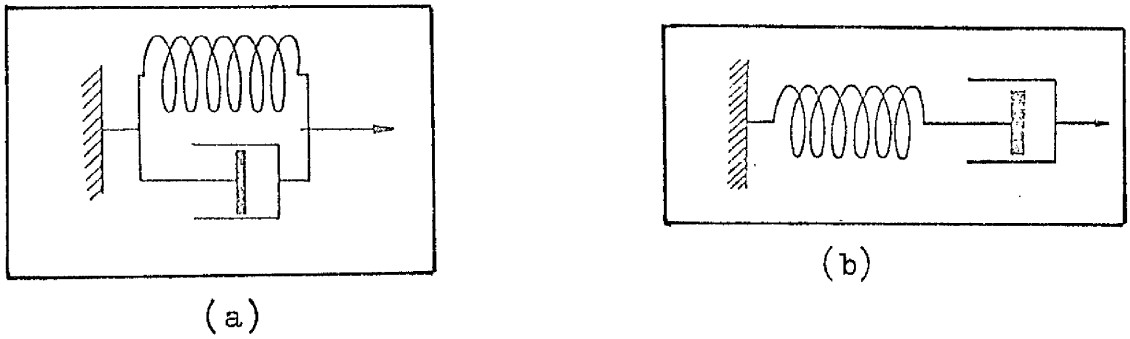

(a) (b)

Fig.1. (a) Voigt Model (Spring and dash-pot in parallel)
(b) Maxwell Model(Spring and dash-pot in series)

3. Dynamic mechanical measurements.

When a viscoelastic material is subjected to sinusoidally oscillating stresses of small magnitude so that the viscoelastic behaviour of material is linear, the strain will also alternate sinusoidally, but will be neither exactly in phase with stress (as it would for a perfectly elastic solid) nor $\pi/2$ out of phase (as it would for a perfectly viscous liquid) but will be some where between 0 and $\pi/2$, as shown in Fig. 2.

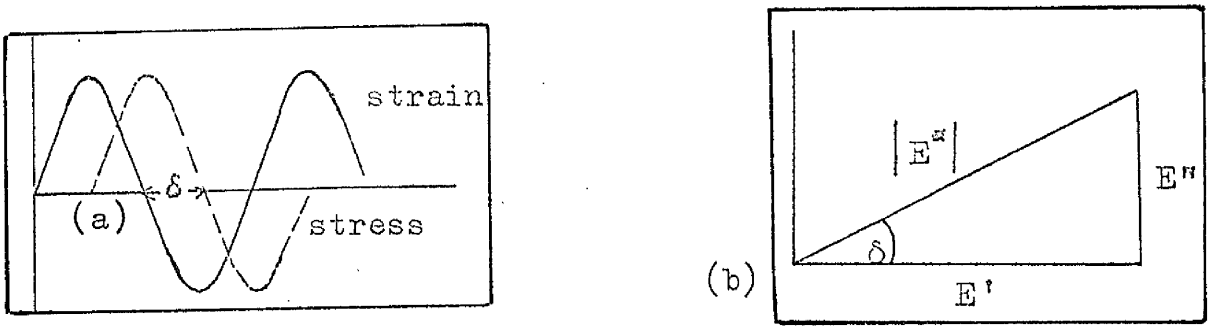

Fig.2. (a) Relation between sinusoidal stress and strain

(b) Vector diagram.

This behaviour is represented in equations 1 and 2

$$e = e_o \sin \omega t \qquad \ldots\ldots\ldots (1)$$

where e_o is dynamic strain amplitude and ω is the angular frequency of vibration, and

$$f = f_o \sin (\omega t + \delta) \qquad \ldots\ldots\ldots (2)$$

where f_o is the amplitude of stress and δ is the loss angle

Equation 2 can also be written as

$$f = f_o (\cos \delta \sin \omega t + \sin \delta \cos \omega t) \qquad \ldots\ldots\ldots (2a)$$

Equation (2a) implies that the stress in this case can be decomposed vectorially into two components. One is in phase with strain and the other $\pi/2$ out of phase.

Defining E' as the ratio of the component of stress in phase with strain to the strain (storage modulus) and E'' as the ratio of the component of stress out of phase with strain by $\pi/2$ to the strain (loss modulus), then

$$f = e_o (E' \sin \omega t + E'' \cos \omega t) \qquad \ldots\ldots\ldots (2b)$$

and $$E' = E^* \cos \delta , \qquad E'' = E^* \sin \delta \qquad \ldots\ldots\ldots (3)$$

where E^* is defined as the ratio of stress amplitude to strain amplitude i.e., f_o / e_o

Therefore, $E^{*2} = E'^2 + E''^2$, ... (4)

and

$$\tan \delta = E'' / E',$$

where $\tan \delta$ is called 'the loss tangent 'or' dissipation factor' and δ is the phase angle between stress and strain (Fig. 2b)

Introducing the operator i, equation (4) may be written as

$/ E^* / = E' + iE''$, where $/ E^* /$ represents the absolute value of the complex number $(E' + iE'')$.

The dynamic mechanical measurements at any given frequency thus provide two independent quantities, the storage modulus and loss modulus. The modulus, however, may be a shear, a Young's (bending or tensile), or a bulk modulus depending upon experimental equipment. The dissipation factor is a very useful parameter (dimensionless) and is proportional to the ratio of energy dissipated per cycle to the maximum potential energy stored during each cycle. These properties are very sensitive to phase transitions, crystallinity, cross-linking, phase separation and molecular aggregation and many other features of molecular structure of polymer chains and the morphology of the bulk materials. In the study of the structure of high polymers, as mentioned earlier, the most far reaching techniques in current use are those of dynamic mechanical testing, infra-red spectroscopy, and nuclear magnetic resonance (NMR) spectroscopy. These techniques, particularly when studied cojointly over a wide temperat range, are capable of giving some insight into the probable behaviour of

the amorphous components in polymers.

However, in order to exploit the full potentialities of dynamic mechanical tests alone, measurements should be made over a wide range of temperatures and frequencies and probably humidities as well. Since no single instrument can possibly cover a range of frequencies say 10^{-5} to 10^{4} cps., many types of instruments have been used by various research workers. These instruments for fibres, yarns, and films range from the less sophisticated torsion pendulum to the more sophisticated pulse propagation technique involving the use of an expensive and elaborate electronic equipment. Nevertheless, much useful information may be obtained in a short time by measuring the dynamic mechanical properties at a fixed frequency and over a wide range of temperature and/or humidities. With this object in mind the present investigation of fibres was carried out on two instruments, one capable of measuring the dynamic bending properties of dry fibres over a range of temperatures at frequencies between 50 - 400 cps, and the other capable of measuring the dynamic tensile properties of fibres over a range of temperatures and/or humidities at a frequency of 20 cps.

Before dealing with the actual experimental procedure involved in the present investigations, it may be useful to discuss some basic theories of mechanical properties and review the relevant literature thereon.

4. Chemical bonding : Molecular motion : Segmental relaxation : Energy dispersion.

The theories presented in this chapter are based on those proposed by some of the research workers like Gordon[2], Ferry[3], Nielson[4], Bueche[5], Goodman[7], Tobolsky[6], Yasaka Wada[8], and Treloar[9].

The mobility of a polymer chain is the collective mobilities of its individual bonds. The bonds can be visualized as tiny flexible steel springs between pairs of atoms, springs which vibrate, and when vibrated too strongly may strain to breaking point, moreover, the springs rotate about their axes and bend and waggle. The vibrating and bending motions are known to occur with frequencies of about 10^{11} or so revolutions per second. These modes interact with and absorb the energy of electromagnetic vibrations in the infra-red and far infra-red regions and spectral studies provide the key to their understanding.

However, rotation about the bonds in the back bone of a high polymer is the most important mode of molecular motion in determining physical and mechanical properties of polymers. According to the recent theory of rotation and rotational isomerism, all bond rotations have to overcome certain energy barriers opposing their course, even the so called free-rotations postulated in organic chemistry. Below a certain temperature, depending on the height of the energy barrier, complete rotation is 'frozen out' of molecular mechanics and only torsional vibrations between insuperable barriers remain in the bond under consideration.

Compounds containing C = C bonds give rise to cis and trans isomers which are stable at ordinary temperature because of the high energy barrier required to over come the anti-rotation barrier inherent in the electronic structure of C = C bonds. The low barriers in the rotation about single C - C bonds usually only become effective at liquid air temperature in preventing rotations, so that isomers cannot be isolated at normal temperatures. However, with reinforcement of the barrier by steric hinderance to rotation by suitable substitution ~~with~~ big groupings enables compounds to be resolved into isomers stable at room temperature. Superimposed on the electronic structure and the steric hinderance barriers, a third kind of barrier in the form of dipole forces is also effective. The rate at which such a process takes place (K) in isolated molecules is related to the absolute temperature by the Arrhenius equation.

$$K = Ae^{-E/RT} \qquad \ldots\ldots\ldots (5)$$

where E = energy of activation

A = a constant

R = gas constant.

Because of the shape of the exponential function, equation (5) does, of course, predict that there is a considerable range of temperature over which rotation becomes progressively more pronounced, rather than a sharp critical temperature at which it sets in suddenly.

While this is true of gases, in condensed phases (liquids and or solids). however, sharp transitions are encountered. This is because in liquids and or solids the molecules are packed close together and therefore affect each others rotational barriers.

The foregoing account of rotational transition in ordinary small molecules, though very brief, makes it clear that such transitions will occur when high polymers are heated to melt (in the case of melting polymers) or vice versa. These transitions include crystal melting, first order crystalline transitions, glass transitions and secondary glass transitions. The properties of poly crystalline materials must obviously be determined by the structure as a whole (of both crystalline and non-crystalline components). However, there are certain features of the mechanical behaviour that are influenced mainly by the non - crystalline components. It is accepted that because the chains, in the amorphous polymers or in the non-crystalline parts of crystalline polymers, are less constrained than those in a close packed lattice, they are more readily able to undergo local vibrational and rotational movements with corresponding configurational changes. Therefore, such movements will readily occur when fibres are subjected to mechanical stresses. For each material there is a characteristic short region of temperature above which the amorphous substance is ductile but below wh it has a substantially glassy character; this region is termed the second-order (or glass) transition temperature, T_g , and it is found to occur

for most common synthetic fibres somewhere between -40° and 150° C varying somewhat in each case with the diagnostic method used and the degree of crystallinity and orientation already present. It has been generally assumed that the transition temperature T_g, represents a point above which significant local segmental motions become possible, and this view is supported by growing evidence from NMR investigations, which provide a means of following changes in the position of bonded hydrogen atoms. On the other hand, molecular motion of a lower order called secondary glass transitions are perceptible in certain polymers even down to -180°C. The interpretation of these changes is the central problem of much of the research on the amorphous regions. The smaller molecular motions detected by NMR at very low temperatures are being ascribed to oscillations or partial rotations of certain small groups in the amorphous regions, these motions becoming complete only at higher temperatures.

Transitions due to molecular motion in the non-crystalline regions are also observed for many natural fibres like cellulose, wool, and silk. Just which segments or parts of segments that are responsible for such transitions, however, is at present far from clear.

The natural relaxation rates at any given temperature assooiated with deformations in a polymer involving segmental motions in the non-crystalline regions, lead to special rate-dependent effects.

This occurs when the applied forces are large enough to cause deformation faster than those which can be accommodated by the natural relaxation rate of segments. This is explained by the fact that dynamic moduli exceed the static ones. The effect of rate of loading at small deformations on physical properties can be conveniently studied by imposing sinusoidal vibrations of various frequencies on the specimen. At each temperature there is then a resonant frequency, at which the imposed frequency matches the average time taken by a segmental jump. In dynamic mechanical testing when the applied frequency matches the average segmental relaxation rate of the polymer chains, maximum absorption of energy takes place. Such energy absorption in the glass transition region results in tan δ rising to a peak. The loss maximum peak is obtainable either as the temperature is varied at fixed frequency (segmental frequency variable, applied frequency fixed), or as the frequency is varied at constant temperature (applied frequency variable, segmental frequency fixed) Fig.3 illustrates this with typical temperature and frequency scales.

The dynamic elastic moduli rise from a low value in the rubbery state to a high value in the glassy state, either as the frequency is raised or as the temperature is lowered. In the glass transition region the rate of change of moduli is a maximum.

Similar energy dispersions due to secondary glass transitions are perceptible at lower temperatures or higher frequencies.

It is apparent from Fig.3, that the temperature at which a loss maximum appears will shift with frequency or vice versa. Nielson[4] has calculated the shift in temperature of maximum damping for a decade change in frequency, as a function of energy of activation. His values show that the higher the energy of activation or the lower the reference temperature, the smaller is the temperature shift in the damping peak. Nielson's calculated values are in general agreement with the existing experimental data on mechanical dispersion of semi-crystalline polymers compiled by Yasaka Wada[8]. In the glass transition regions where the energy of activation is generally high, most common polymers have a shift of about 7° - 8°C for a decade change in the frequency. The secondary peaks have a smaller energy of activation and correspondingly larger shifts occur in the temperature maximum with change in frequency.

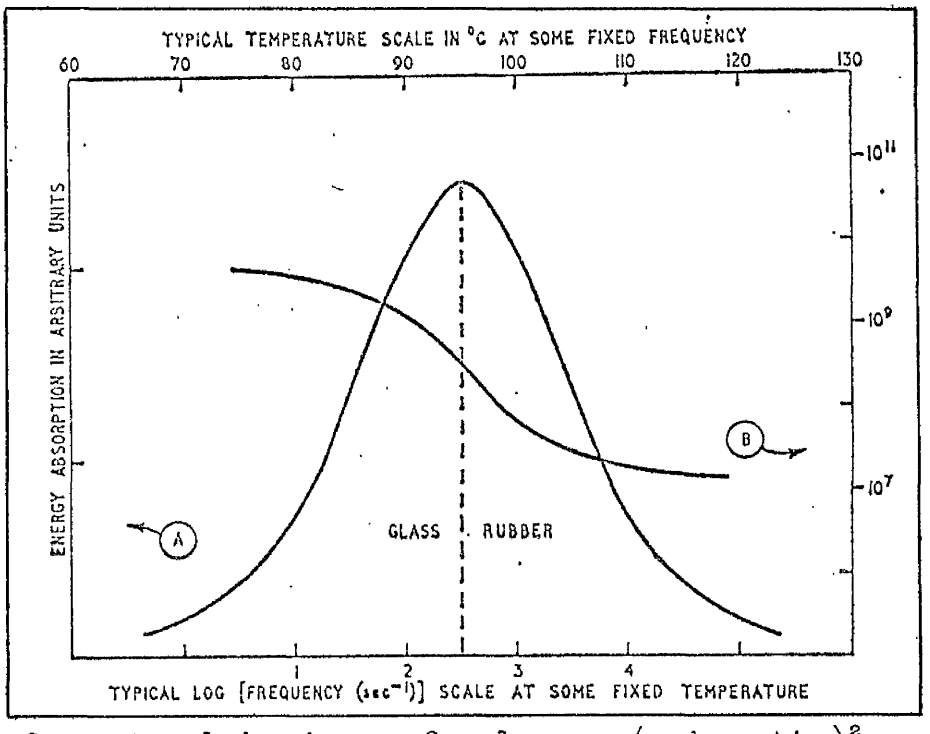

Fig.3. Relaxation behaviour of polymers (schematic)[2].
Curve A, energy loss. Curve B, Young's modulus. Both curves are functions of temperature (upper scale) or frequency(lower scale). The vertical line denotes the dynamic glass-to-rubber transition.

5.Criteria for Primary and Secondary Dispersions.

The primary dispersion or dispersion due to glass transition being caused by movements of large sections of chain molecules in the amorphous phase, may be expected to follow the following criteria proposed by Yasaka Wada[8].

(1) The loss peak height should increase with increase in the fraction of the amorphous phase.

(2) The activation energy should be relatively large, say several tens Kcal / mole as estimated from that of perfectly amorphous polymers, owing to the large unit of motion.

(3) The thermal expansion curve should have a point of discontinuity in slope (T_g) in the vicinity of the loss peak temperature at very low frequencies.

(4) T_g should be roughly two-thirds of the crystalline melting point T_m , when measured in absolute temperature scale. This relationship, however, is only an emperical one, but has been confirmed for many substances exhibiting the glass transition.

The mechanism of the secondary dispersion has not yet been fully understood. However, many research workers attribute the secondary dispersion of a specific polymer to the rotation of a specific group of atoms in a chain molecule. Tentatively, it is at least valid to say that the secondary dispersion comes from local motion of segments in the amorphous phase, and the dispersion may be expected to obey the

following criteria.

(5) The loss peak should increase with increase in the relative amount of the amorphous phase.

(6) The dispersion should be observed at lower temperatures than the primary one.

(7) The activation energy should be smaller than that of the primary dispersion, roughly estimated as ten Kcal /mole or so.

It is now generally agreed that semi-crystalline polymers exhibit a more complex dynamic mechanical behaviour than was formerly believed. Since the facts reveal a very wide region of temperature, extending over a range of at least 100°C, and frequently as much as 300°C, in which relaxation process accompanied by changes in elastic moduli occur, it may be interesting to mention a rather extreme point of view of Treloar[9]. He feels "particularly when two or more distinct relaxation processes can be resolved, the question of which, if any, of the observed processes should be regarded as the glass transition becomes arbitrary, if not meaningless. Wilbourn[10] has worked on the basis that the glass transition is the process corresponding to the onset of mobility of the main polymer chain. Such a definition, puts the onus on the interpretation of the observed properties rather than the properties themselves, and leads, on Wilbourn's own admission, to many difficulties." He further goes on to say that "From a purely phenomenological stand point, no absolute criteria for discriminating between observed

transitions is possible, and it appears to the writer (Treloar) that the concept of glass transition, though valuable as a help in interpreting the general pattern of behaviour, is not necessarily applicable to the detailed fine structure of the relaxation spectrum, and provides no information that is not already available in the experimental data".

CHAPTER 11 LITERATURE SURVEY

LITERATURE SURVEY

The field of dynamic mechanical testing of polymers is fairly new, but it has been considered to be one of the most important techniques from both practical and scientific stand points.

Since the effect of temperature and/or humidity on dynamic bending and tensile properties has been the subject of study in the present investigation, it may be useful to review briefly the work of some of the research workers on this subject.

1. Dynamic bending properties.

Peirce[11] was the first to use a free vibration method to measure the flexural rigidity of cotton fibres through Searle's double pendulum technique.

Warburton[12] obtained higher values of bending modulus of horn Keratin in absorption than in desorption over a range of 0 to 30% regain. He also observed that the variation of bending modulus with regain was very much greater than that of tensile modulus as observed by Woods[13] but compared favourably with the variation of torsional rigidity as measured by Speakman[14].

Lochner[15] observed that for wool and cellulose acetate fibres under forced vibration in a vacuum, the damping capacity in bending was higher than that in torsion.

The dynamic bending modulus and damping capacity of wool, untreated,

acid carbonised, and carbonised and naturalised were measured by Lincoln.[16]

Van Wyk[17] established that the dynamic bending modulus of wool, mohair and human hair reduced to a third of their values, from dryness to saturation. The shape of the curve relating bending modulus to absorbed water was found to be similar to that of torsional rigidity. He reports that due to fibre swelling the stiffness of the fibres was reduced by approximately one half of the extent to which the bending modulus was reduced on the absorption of water.

Horio et al[18] observed that a direct linear relationship existed between the dynamic bending modulus and the orientation of the fibre as measured by double refraction. The loss tangent also increased linearly with orientation at low frequencies but became independent of orientation above 90 cps. This was ascribed to the increase in number of secondary bonds with orientation. At low frequencies these bonds cause internal friction, but at high frequencies they behave as fixed points due to their inability to respond to rapid changes.

Horio and Onogi[19] using forced vibration technique obtained a value of $3.3\ 10^{10}$ dyn/cm^2 for the bending modulus of cellulose acetate filaments. It was also noted that the modulus was independent of frequency over a range of 45 to 11,000 cps.

The influence of air damping on resonant frequency was calculated with the help of equations deduced by Stokes[20], by Karrholm and Schröder[21].

Experimental verification was performed on model circular viscose rayon using cantilever vibration method. It was shown that Young's modulus by bending was 1.5 times that by stretching. Values of the moduli for wool, nylon and human hair were obtained. They observed two resonant frequencies around the principal axes of inertia in the case of the elliptical hairs and the ratios of these frequencies were equal to the ratios of the axes of the ellipse. In another paper Kärrrholm[22] reports the dynamic bending modulus for viscose rayon filaments with different amounts of formaldehyde content. A maximum value of the modulus was observed at about 5% fixed formaldehyde content. Her results indicated that below 5%, the number of cross-links increased steadily, where as above 5% the length of the cross-link was greater.

Okajima and Suzuki[23] used a vibrating reed method to measure the bending modulus of viscose rayon. The mean resonant frequency of four readings taken at right angles to one another was used to calculate the bending modulus. The four resonant frequencies obtained at right angles to one another were, of course, dependent on the shape of the fibre cross section.

Schröder[24] has described a simple mechanical device to determine the dynamic bending stiffness of single fibres. Tyre cord rayon was found to be less stiff than cotton fibres used in tyre cords. However, due to inherent characteristics of cotton the stiffness values showed a larger scatter.

Wakelin[25] has reported that the dynamic bending modulus increased by a factor of 3.5 for nylon 66 monofilaments and 5.8 for Dacron monofilaments for a one to six increase in the draw ratio. At the same draw ratios, the quasi-static tensile modulus was generally lower than the dynamic bending modulus, the difference being greater for nylon 66 than for Dacron and being more pronounced at the low draw ratios. This has been attributed to the effect of stress relaxation. For a homogeneous isotropic material with a Poisson's ratio of 0.5., the ratio of the Young's modulus to three times the shear modulus should be unity. However, this ratio was found to be about 3 for nylon 66 and greater than 5 for Dacron at a draw ratio of 6. These results, along with those obtained at lower draw ratios, indicate that both filaments became progressively more anisotropic with drawing.

Marlow[26] found the dynamic bending modulus of nylon 66 monofilaments to increase linearly with increasing draw ratio. His values obtained at 20 - 2000 cps were slightly lower than the dynamic tensile modulus obtained at 0.1 cps by Adams'[27]. This considerable measure of agreement is considered as indicative of the equality of the moduli of compression and extension in bending.

Kawaguchi[28] using a vibrating reed method has studied the dynamic mechanical behaviour of dry undrawn monfilaments of a number of polyamides, over a temperature range -140°C to 200°C at about 100 cps. He observed four dispersion regions characterised by loss peaks at -120°, -40°, +90°C

and near the melting temperature. It is believed that the high temperature α peak reflects the onset of chain mobility accompanying the crystalline melting process, and the α' peak occurring at about 90°C is ascribed to the motion of large chain segments caused by the breaking of inter-molecular bridging in the amorphous regions. Since the properties of the proton groups in the molecular chain have been found to influence the β dispersion at -40°C, it is attributed to the segmental motion involving non-hydrogen bonded amide groups. The γ peak at -120°C is attributed to the onset of co-operative movement of CH_2 groups.

The mechanical dispersion of various polyamides has been most fully investigated by Woodward, Crissman and Sauer[29]. All their experiments were carried out on rods of about 12 cm length and 0.6 cm diameter using a modified transverse beam apparatus. In earlier studies carried out over -193°C to about 257°C range [30] all the polyamide samples investigated were found to exhibit three damping peaks around -103°C, -23°C and 77°C (γ, β and α peaks respectively) and at the highest temperature an upswing in the mechanical loss or damping was also observed. These changes were accompanied by decreases in the dynamic modulus going from lower to higher temperatures. However, in a later investigation[31] they demonstrated that thorough drying of polyhexamethylene adipamide at elevated temperatures under vacuum caused the β peak in the -23°C region to disappear, implying that the water contents of some of the samples previously studied were ill-defined.

However, their recent investigations[29] were carried out on five polyamides at resonant frequencies ranging from 100-2000 cps at temperatures in the -173°C to 177°C region. Speciments of polyhexamethylene adipamide containing 0, 0.9, 3.3 and 6.4 wt% water were also studied and they found with increasing water content, the γ loss peak and associated modulus dispersion at -103°C in dry material decreased, the α loss peak and modulus dispersion at 97°C in dry material shifted to lower temperatures reaching a value of 7°C for 6.4% water, a third damping peak β appeared at -33° to -28°C and the modulus in the -123° to -23°C region increased while above and below this the reverse was true. A polyhexamethylene adipamide specimen containing 10.5 wt% methanol exhibited only one broad peak at about -18° to -13°C.

The molecular interpretation given to these results is as follows:

The principal mechanical loss peak and associated modulus change in the 27° to 97°C region for polyamides has been attributed to segmental motions in the amorphous regions as a consequence of the breaking up of hydrogen bonds (or polar forces of attraction) between chains. It is believed that their results for the series of polyhexamethylene adipamide specimens containing various amounts of water is in agreement with this interpretation. This view is also further supported from their investigations that replacing the protons on the amide groups with relatively non-polar substituents, such as methyl groups from methanol,

disrupts and or decreases the interchain bonding and thus lowers the transition temperature. The damping peak in the -33°C region for a polyhexamethylene adipamide specimen containing water has been attributed to segmental motions in the amorphous regions involving the co-operation of methylene groups and non-hydrogen bonded amide links.

The complete disappearance of the β peak in the heat treated dry specimen has been attributed to an increase in ordering and hydrogen bridging in the amorphous region.

The γ peak and modulus dispersion in the -108° to -103°C region has been explained as due to segmental motion in the amorphous regions of a small number of methylene groups between amide groups. In the specimens containing water the decrease in the γ peak is thought to be due to interference of the water molecules with the moving hydrocarbon segments. It is also interesting to learn from their results that increase in water content in poly hexamethylene adipamide appears to increase the rigidity of the polymer chains in the -123° to -23°C range.

Kawaguchi[32] has measured the dynamic mechanical properties of polyethylene terephthalate as a funtion of temperature at -70° to +150°C at 100-200 cps, - using a cantilever vibration method. He observed two transition regions, one around 90° to 120°C and the other around -40°C. With increasing degree of crystallinity and orientation the transition peak at 90°C shifted to a higher temperature, where as the transition

peak at -40°C showed a tendency to shift toward lower temperature. Also with increasing degree of crystallinity the temperature dependency of elastic modulus at room temperature and the value of the loss maxima at -40°C decreased. With changes in water content of the material the height of the low temperature peak increased, but the temperature at which the maximum occured remained unchanged.

Kline and Sauer[33] using rod like speciments of polyethlene terephthalate (PET, density 1.386 g/cm , crystallinity 52%) studied the effect of radiation and moisture on dynamic mechanical properties in the range of temperature -193° to 257°C and frequency range from 100 to 1300 cycles/sec. For un-irradiated PET as received three principal dispersion regions have been reported; a low temperature damping peak near -33°C, a loss peak near 107°C and above 207°C the damping again was found to rise as the region of crystalline melting was approached. A corresponding drop and or inflection was noted in elastic modulus for each of these temperature regions. When the water content of the specimen as received (0.3%) was reduced they observed an increase (slightly) in height of the low temperature damping and possibly a shift to a slightly higher temperature of the peak. The main peak near 107°C, however, changed little if any in size. The final transition in the temperature region of 177° to 207°C showed a slight shift in both damping and modulus data to still higher temperature, probably as a consequence of increased crystallinity.

When the water content of the sample was increased to more than 0.8% beyond the dried water content value, the low temperature peak ($-23^{\circ}C$) increased some what in value from that of the unconditioned sample. They also observed that the primary damping peak shifted noticeably to a lower temperature with added water and the area under the peak also decreased. The inflection point in the modulus curve, which appeared at a higher temperature for the dried sample, as compared with the unconditioned sample now appeared at a lower temperature consistant with the shift in the damping peak.

Comparing their findings with those of Ward[34] and Thompson[35] they conclude that the damping peak near $107^{\circ}C$ is associated with the motion of large number of segments in the amorphous regions, probably involving at least the phenylene carboxyl bond in addition to the glycol residue. Since Reddish[36] has also noted in his dielectric measurements that this peak shifts to lower temperatures with added water content it is thought to be analogous to the shift in the glass-rubber transition peak of nylon 66 with added water and or other small molecules. In nylon 66 however, the temperature shift is greater and this probably is thought to be due to greater amount of water that nylon absorbs under similar conditions.

Dutch, Hoff and Reddish[37] have made a comprehensive study of the dynamic mechanical and dielectric properties of acrylic polymers (poly methyl metha-acrylate, poly methyl -α-chloroacrylate) and find these two properties to be intrinsically correlated.

They have proposed the hypothesis that each of several mechanical and dielectric dispersion regions found in a given polymer is associated with a definable structural feature, i.e. a group of atoms in the polymer, such that each group gives rise to a mechanical dispersion and, if polar, also to a dielectric dispersion in the same temperature and frequency range; it should also be possible to trace the same dispersion from one polymer to another, provided they all contain the same group.

Hoff, Robinson and Wilbourn[38] carried out further investigations on dynamic mechanical properties of a series of polymethacrylics and polychloroacrylics over a wide temperature range at about 200 cps using a cantilver vibration method. The main softening region is shown to be influenced by the presence of polar atoms in both the main and side chains and by spatial size and flexibility of the side chains. The secondary dispersion occurring just below the main softening region is shown to be associated with rearrangements of the polar -CO.O- groups in the side chains. Some new low temperature transitions reported, one of which at -30°C is characteristic only of poly-cyclohexyl methacrylate and polycyclo-hexyl-chloroacrylate and they attribute it to intramolecular flexibility within the cyclo-hexyl ring. Another process is reported to occur at about -150°C for those polymers whose side chain alkyl components possess sufficient flexibility to enable them to take up more than one spatial configuration. Such

flexibility is shown to be characteristic of the n-propyl,n-butyl, sec-butyl esters in both series and of the β-chloroethyl, neopentyl carbinyl, and stearly esters in the poly methacrylic series.

Sauer et al[39] subjected rod like specimens of crystalline and amorphous polypropylene to transverse vibrations and measured the dynamic mechanical properties from -100°C to near melting point. Three dispersions were observed - a high temperature transition associated with large scale motion of polymer chains, - a room temperature transition associated with primary glass transition of the amorphous phase of the polymer, and a low temperature transition attributed to the onset of small scale chain motion in the amorphous regions. The low temperature transition occurred at about -50°C in amorphous polypropylene compared with -110°C in polyethylene. This difference is attributed to the hinderance of main chain rotation caused by the presence of a methyl group on alternate carbon atom in polypropylene.

Meredith and Hsu[40] have studied dynamic bending properties over a range of temperature from -70°C to +170°C of single textile filaments of nylon 66, Terylene, Orlon and viscose rayon in dry state under vacuum using an electrostatic method. They observed maximum loss modulus at -50°C, +115°C for nylon 66, at -60°C +155°C for Terylene, at 70°C and 110°C for Orlon and -20°C and 90°C for viscose rayon. Applying the rate process theory to these transition regions they have calculated the

activation energies. They conclude that the value of activation energies they have obtained support their interpretation that the low temperature transition is associated with segmental motion and the high temperature transition involves breaking of secondary bonds, e.g. hydrogen bonds in nylon 66.

2. Dynamic Tensile and Torsional properties.

Meyer and Lotmar[41] subjected some natural fibres to forced longitudanal vibrations by an acoustic method. At high frequencies they report that the dynamic young's modulus of linen, ramie and hemp increased slightly with increasing static tension.

Tipton[42] measured the dynamic moduli of several yarns and mono - filaments under standard laboratory conditions and various static and dynamic strains. He reports that the modulus generally increased with static strain and decreased with dynamic strain. The increase of dynamic modulus with increasing static strain in monofilaments, is attributed to increased molecular orientation. At very small static strains, Tipton observed small initial drops in modulus and attributed these to increase in moisture regain which occur on straining a yarn. Highly twisted yarns, however, did not exhibit a drop in modulus, but an increase and this was attributed to lateral compression of fibres and a resultant lowering of regain. The decrease in modulus with increasing dynamic strain is thought to be due to the fact that the

forces of contact between adjacent fibres in a yarn increase and tend to cause movement and slippage amongst a greater number of fibres.

Palandri[43] using forced longitudinal vibration, found that the dynamic young's modulus of yarns made from long fibres, was independent of dynamic strain amplitude and of frequency above 100 cps in the range 20 to 200 cps. In yarns made from short fibres the dynamic Young's modulus was found to decrease with increasing dynamic strain amplitude.

The dynamic elastic moduli of cellulose fibres and rayons were measured as a function of extension by de Vries[44] at 65% RH and 20°C, the modulus remained fairly constant up to a certain critical extension and this varied as to whether viscose, acetate or rayon was under examination. Beyond the critical extension the modulus increased for all materials but the rate of increase depended again on the material under test. He found that the decrease in compliance (1/modulus) was proportional to the increase in the natural strain. His results suggested a correlation between the dynamic modulus and the chain molecule orientation. de Vries[45] further established a relationship between dynamic elastic modulus and birefringence of viscose, acetate and cuprammonium rayons. He reports that beyond a certain yield value of extensi the modulus was equivalent to the birefringence as a measure of the orientation of the filament.

Hamburger[46] found that for viscose rayon, cellulose acetate and nylon

yarns, the dynamic Young's modulus increased with static strain only beyond the yield point.

Fujino et al[47] measured the viscoelastic properties of viscose, acetate and cuprammonium rayons, silk and nylons under a static tension of 0.4 gm per denier and dynamic strain amplitude of less than 1% using several longitudinal vibration methods to cover a frequency range of several decades. In general they found that the storage modulus was constant over the frequency range 2×10^{-1} up to 2×10^{5} cps and increased slightly in the supersonic range. The loss modulus, however, increased at both ends of the frequency range. They concluded that for textile fibres the anomalous dispersion is not as great as that of various rubber like materials in the same frequency range.

Kawai and Tokita[48] measured the dynamic Young's modulus of silk at $8^{\circ}C$ and 71 % r.h. over a frequency range of 2 to 14×10^{2} cps and found the modulus of 9.8×10^{10} dyn/cm^2 remained constant.

Dunell and Dillon[49] measured the dynamic modulus and energy losses of single fibres of viscose and acetate rayons, silk, feather keratin and nylon using a forced longitudinal method. They found that storage and loss moduli were independent of frequency in the range 1 to 100 cps and the measured values of energy dissipated per cycle were proportional to the square of the dynamic amplitude in accordance with theoretical prediction.

Lyons [50] noted that for cotton and viscose rayon cords, the loss modulus was not independent of large dynamic strain amplitude. Between 65 to 360 cps at a dynamic strain amplitude of 0.3%. the dynamic modulus was independent of frequency. The dynamic Young's modulus was, however, found to decrease with increasing dynamic strain amplitude.

Chaikin and Chamberlain[51] found that the dynamic elastic modulus at 100 Kcps was four times as great for viscose rayon and Tenasco and about two and a half times as great for wool, human hair and nylon, as the static modulus. Higher values at higher rates of strain were atrributed to the fact that weak secondary bonds had no time to break and the stress was transferred directly to the main chain, while at lower rates of strain the mechanism of deformation is the unfolding of molecular chain in the non-crystalline regions, which involves the rotation of segments of the chains around single bonds having barriers of low energy of activation at slow rates of deformations the secondary bonds broke under applied stress. They also observed that by raising the r.h. from 25 to 65% at room temperature there was a significant decrease in Young's modulus of viscose rayon and human hair, while in nylon the decrease was smaller.

Asmussen and Andersen[52] using longitudinal vibrations on cellulosic fibres found that the dynamic Young's modulus was higher than the static modulus. From their investigations they report that humidity has a

lesser effect on the dynamic than on the static modulus.

Andersen[53] observed that the dynamic Young's modulus of viscose rayon and cotton in the frequency range of 25 to 40 cps was much less affected by changing relative humidity that the static modulus. By increasing the static strain the modulus of cotton was affected by humidity, while rayon was unaffected. Increasing temperature caused a fall of both the static and dynamic moduli of rayon. For cotton however, only the static modulus was found to increase.

Ballou and Silverman[54] used a sound velocity method for determining the tensile moduli of viscose and acetate rayon,nylon and other yarns at frequencies of 10 Kcps. They report for viscose rayon a decrease in modulus with increasing humidity and temperature. Finishes in general had little effect. However, boiling in soap solution tended to lower the modulus.

Dunell and Price[55] report that the curves of dynamic Young's modulus and loss factor against temperature for viscose rayon are nearly similar in shape to those for other high polymers. Percentage increase in modulus and changes in energy loss factor for viscose rayon were much smaller. The dynamic Young's modulus increased by 40% as the temperature was lowered from 0 to $-80^{\circ}C$, and a well defined energy loss maximum was observed at $-40^{\circ}C$. This was ascribed to the rotation of CH_2OH side chains which did not involve breaking of hydrogen bonds.

Tokita[56] reports a mechanical dispersion peak in dry viscose rayon at 80°C. At 65% RH, however, the dispersion was found to occur at 65°C and the energy of activation for the segmental motion in the amorphous parts was found to be about 190 Kcal/mole. The water molecules absorbed in the fibrous structure are supposed to be playing the role of a plasticizer. He observed no loss maxima for viscose rayon in the frequency range 0.047 cps to 100 Kcps. He also reports that the mechanical behaviour of viscose rayon is not affected much by the degree of crystallinity (70-75%).

Russel and van Kerpel[57] used a torsion pendulum technique to determine the dynamic rigidity modulus and damping of cellulose acetate and cellulose triacetate. Damping peak and associated modulus changes were observed at 175°C and -48°C for triacetate and 195°C and -55°C for secondary acetate.

The effect of acetyl content on the high temperature transition was studied by Nakamura[58] and his results were in agreement with the findings of Russel and van Kerpel that the transition temperature decreased with increasing acetyl content. At audio frequencies Nakamura also found a mechanical loss peak at 60°C for cellulose triacetate and he considered this peak to correspond with the 30°C transition reported in the dilatometric measurements. However, he observed no peak in the secondary acetate curve which could be correlated with the 55°C transition observed in the dilatometric methods.

Tokita and Kanamura[59] studied the effect of cross-linking on the dynamic properties of viscose rayon and cellulose acetate at 66% r.h. They report that when the cross-linking agents are long chain molecules, the intermolecular spaces in cellulose are widened and the dipole interaction of the strong polar hydroxyl groups between molecules are partly relieved and a small amount of cross-linking agent is sufficient to cause a decrease in the dynamic Young's modulus, loss tangent and apparent energy of activation for the dispersion region.

Using a torsional pendulum, Mackay and Downes[60] made measurements on the dynamic modulus of rigidity of wool fibres during the process of sorbing and desorbing, water (from the vapour phase). They report that when a large increase is made in the relative humidity surrounding a wool fibre, its dynamic torsional rigidity goes through a minimum value considerably less than the final equilibrium value. This is true for all except very gradual increases in humidity. The temporary reduction in rigidity modulus is attributed to the transient stresses produced as a result of differential swelling during the penetration of the water "front" into the fibre and these stresses are believed to cause temporary rupture of bonds which contribute to the rigidity.

Ree et al[61] working in the frequency range 1.75 to 31.5 cps observed that the internal friction of Saran was dependent on frequency. They also observed a maximum in the value of internal friction around 14.8°C. The dynamic and static moduli of Saran were found to increase sharply below 17°C.

Smith[62] and co-workers measured the dynamic modulus of Orlon yarn at different rates of strain varying from 1% to 300,000% per minute. In the low range of frequency they observed an increase in the dynamic modulus and the modulus was constant above 10 Kcps.

Eyring et al[63] subjected polyamide filaments to forced vibration over a frequency range of 0.06 to 6 cps and a temperature range of 0 to 65°C. The energy loss was found to be independent of frequency but it decreased exponentially with increasing temperature at constant frequency.

The effect of orientation on the dynamic Young's and shear moduli at 66% r.h. was investigated by Adams[27]. The dynamic modulus was observed to vary linearly with draw ratio above 1.4. The shear modulus decreased with draw ratio below 40% r.h. while at relative humidities above 40% an increase in shear modulus was observed.

Tokita[56] in his investigations on nylon 6 under standard laboratory conditions found that in general, an increase in frequency increased the dynamic Young's modulus, and it tended to approach a limiting value above 100 Kcps. Samples of different crystallinity approached nearly the same value of $2.2 \cdot 10^{10}$ dynes/cm^2, indicating that the dynamic modulus at frequencies higher than 100 Kcps was independent of the degree of crystallinity. However, in the frequency range 0.1 cps to 100 Kcps the increase in the dynamic modulus with drawing was considerable, and this

was attributed to the orientation of crystallites. Further, it was found that increase of degree of crystallinity and drawing results in shifting the dispersion region, as a whole, to longer time regions, and the shapes of the spectra of relaxation times were almost independent of the degree of crystallinity, while the heights of the peaks reduce with the degree of mechanical drawing. These facts are attributed to the steric hinderance against the segmental motion.

Ogawa et al[64] have studied the effect of heat treatment on the dynamic mechanical properties of Amilan (a Nylon 6 type polyamide fibre). They found heat conditioning for 1 hour at temperatures between 80° and 160°C increases the dynamic Young's modulus and the internal friction decreases with increasihg temperature of heat treatment. This was attributed to the increasing degree of crystallinity. For heat treatment above 160°C the reverse was found to be true, and below 80°C the dynamic mechanical properties were unaffected.

Dole et al[65] report that the glass transition temperature of nylon 66 and nylon 6 changed from 47°C for the amorphous polymer to above 75°C for the drawn fibre.

Fujino et al[66] examined the viscoelastic properties of several high polymers using longitudinal vibrations. They report that increasing the draw ratio increased the dynamic tensile Young's modulus. This effect is attributed to lateral bonding between chains in the amorphous

regions and not to the development of crystallisation.

Kawaguchi[67] measured dynamic parameters of nylon and Terylene filaments and compared the results with the predicted theory. The degree of orientation rather than crystallisation was thought to be the principal factor affecting the mechanical properties. It was proposed that the Young's modulus would increase to a maximum value of 5 times that of the isotropic body as the draw ratio was increased. On the other hand, the torsional modulus would decrease with increasing draw ratio, the completely oriented amorphous polymer exhibiting zero torsional modulus.

Thompson and Woods[35] have measured the dynamic tensile moduli and mechanical loss factors of polyethylene terephthalate filaments in different states of orientation and crystallinity between -80°C and 180°C and from 10^{-3} cps to 10^{4} cps. They have shown that at 1 cps the main transition temperature peak shifts from 80° to 125°C, with increasing crystallinity, its apparent activation energy meanwhile falls from 182 Kcal/mole to 97 Kcal/mole. However, a second transition at about -40°C with an apparent activation energy of 17 Kcal/mole is less affected by crystallinity. At that time of publication, they gave three possible interpretations for these transitions:

(i) Since the dielectric experiments of Reddish[36] suggested that the dipole observed in the low-temperature transition was that of a terminal-OH group, it might be inferred that the corresponding mechanical process was due to the mobility of chain end-groups, the upper transition being due to mobility in the main chain.

(ii) The upper transition in polyethylene terephthalate may be due to rotations in the stiff aromatic part of the chain, while the lower transition may be due to rotations in the less rigid aliphatic part. This need not be inconsistent with the dielectric data, for this second mode of movement might only be discernible electrically where the OH groups act as pointers. The principal arguments in favour of this interpretation are firstly, it seems unlikely that the end-group mobility could produce a mechanical loss process comparable in magnitude with the main upper transition, while it seems more reasonable to suppose that a secondary force of main chain flexibility could do so, and secondly, that if rotations in the stiff p-phenylene group provide high temperature transition, rotation in the more mobile ethylene group should, following the ideas of Deutsch, Hoff and Reddish[37] give another transition some where lower down the temperature scale.

(iii) The p-phenylene link may be rigid, so that all rotations occur in the alipahatic part of the chain. Then the lower transition might indicate the onset of partial rotation, and the upper transition the onset of fuller rotation. In this scheme each transition is

still related to a mode of flexibility, but the modes are distinguished by different extents of freedom in the same bonds, rather than by the on set of rotations in different bonds.

Ward[34] studied the molecular structure and the mechanical properties of a series of polyethylene terephthalate polymers using dynamic mechanical technique, nuclear magnetic resonance spectra, infra-red spectra and x-ray diffraction. For these polymers three transitions, α, β and γ were observed; α corresponding to the melting point, β ~~is clearly~~ corresponding to the glass transition. Consideration of his dynamic loss results alone were thought to suggest that the γ transitions (low temperature) is connected with motions in the aliphatic part of the chain and the β transition is connected in some way with the phenylene carboxyl bond.

From NMR results, however, he shows that the γ transition is restricted to very small inter molecular motions, whereas the β transition is associated with considerable motions of the molecules in the amorphous regions.

From infra-red data he has suggested that an additional preferred configuration of the $O - CH_2 - CH_2 - O$ group exists in the amorphous regions of the polyethylene terephthalate. Since crystallisation sets in above the β transition he thinks it may be reasonable to imply that this transition is associated with at least this configurational change.

Also from a detailed x-ray and optical examination of single crystals of cyclic trimer (ethylene terephthalate) he suggests that in the cyclic trimer molecules the carboxyl groups are placed in the cis positions with respect to the benzene rings. Thus, configurational changes may also involve the phenylene carboxyl bond.

Taking into account all these data, Ward concludes that the γ transition involves some very restricted rotation of the glycol residue and the β transition a considerable rotation of this residue, also involving paraphenylene linkages in the amorphous material.

Nohara[68] also has studied dynamic mechanical properties and nuclear magnetic resonance spectra of Terylene, nylon and other plastics. In the temperature range $-70^{\circ}C$ to $+200^{\circ}C$ he observed that the p-phenylene group in Terylene was undergoing hindered rotations at about $110^{\circ}C$ whereas the two methylene groups still rotated at lower temperatures.

Price et al [69] have investigated the dynamic mechanical properties of nylon, polyethylene and viscose and acetate rayons over a frequency range of 5 to 50 cps by forced longitudinal vibration method. They report that the dynamic modulus increases with decreasing the humidity from 98% to 28% r.h. They report that the dissipation energy per cycle, decreased with decreasing relative humidity.

Quistwater and Dunnell[70] measured the dynamic modulus and energy loss for nylon 66 at $35^{\circ}C$ over a wide range of humidity by forced longitudina vibration method.

The frequency range covered was about 3 to 30 cps. They observed dispersion of mechanical properties with changing humidity, the maximum in the loss factor, tan δ, occurring at about 70% R.H. The small variation of energy dissipation with change in frequency observed was such as to suggest that the dispersion region extends over a wide frequency range and that at low humidity an energy loss maximum could be expected at a frequency below one cycle per second. They propose that increase in the amount of water absorbed by nylon with increasing relative humidity leads to plasticization of the fibre and consequent increase in freedom of motion of chain segments in the amorphous region of the fibre. From the data of Bull[71] and Forward[72] et al they have calculated moisture regain values (moles of water absorbed per base mole of nylon ($-CO\ (CH_2)_4\ CONH\ (CH_2)_6\ NH-$) and find the maximum energy loss to occur at about 0.5 mole of water per base mole of nylon. Nylon 66 chains which are most favourably oriented in crystalline array can form two hydrogen bonds per base mole of nylon with neighbouring chains. In the amorphous region, there will be appreciably fewer than two hydrogen bonds per base mole and Quistwater and Dunnell argue that the 0.5 mole of water absorbed at maximum energy loss should be more than sufficient to break existing hydrogen bonds in the amorphous regions. They however, feel that new hydrogen bonds could form at points where water has not been absorbed, and significant increase in the freedom of motion of chains in the amorphous area may come only after a substantial fraction of the carboxyl and amino groups are associated with absorbed water molecule.

Since water is known to attack only the amorphous regions, it can be reasonably supposed that in the amorphous regions something nearer one than one-half mole of water per mole of nylon is absorbed at maximum energy loss. Therefore, following Schmieder and Wolf[73] and Tokita[56] they postulate that the observed energy dissipation in nylon is associated with the motion of molecular segments in the amorphous region. As this motion becomes freer because of the decrease in the possibility of hydrogen bonding between chains in the amorphous region with increase in water absorption, the amount of energy dissipated increased with increasing extent of internal movement. Simultaneously, however, the force required to produce internal movement decreases with decreasing chain interaction and sets a maximum on energy dissipation by this particular mechanism. If the chain interactions are sufficiently weakened, the energy loss decreased below this maximum. The decrease in modulus they observed accompanying the above process is consistent with the idea of chain interaction becoming weaker with absorbed water.

The same authors[74] extended their work by measuring the same properties at 9°C and 60°C over the same humidity and frequency range (10^{-4} to 10^{6} cps). The dynamic tensile modulus at 9°C was independent of frequency at relative humidities lower than 60% but increased with increasing frequency at higher humidities. The tensile modulus was similarly affected by frequency at 60°C. At this temperature a well defined maximum in the energy loss was observed, similar to that

obtained previously at 35°C but at a some-what lower moisture content. This effect, however, is expected since increase in temperature with moisture content would facilitate segmental motion to a greater extent than would increase in moisture content alone. A maximum in the energy loss (not well defined) was also observed at 9°C and 100% r.h.

Yoshino and Takayanagi[75] constructed a mechanical tan δ meter of direct reading type and measured the dynamic mechanical properties of oriented crystalline polyethylene teraphthalate, isotactic polypropylene and poly-acrylonitrile fibres over a range of temperature at 100 cps. They observed tan δ peaks at -35°C and + 140°C for polyethylene terephthalate, and 105°C for poly acrylonitrile fibres. For poly-propylene however, a rise in tan δ was observed at 20°C and at about 140°C.

Recently Crissman et al[76] made measurements on dynamic mechanical properties of various polymers in the -267° to 27°C temperature range at resonant frequencies of about 10^4 cps by using longitudinal vibration apparatus. The polymers they studied include polyethylene, nylon 66, three polymethacrylate esters, and five poly-α-olefins and related polymers. From their observation they conclude that polymethyl-meth acrylate and polyethyl-methacrylate indicate low temperature relaxation processes(-267°C and -221°C respectively) involving configurational rearrangements in the hydrocarbon portion of the ester side group. Their data provide no evidence for mechanical loss processes associated with

hindered rotation of the main chain methyl groups in the poly-methacrylate esters or polypropylene. Very weak relaxation processes or loss plateaus are reported to have been observed in the -250°C region for polypropylene, polyvinyl chloride, poly (d, l- propylene oxide), poly isobutyl methacrylate and possibly nylon 66, while for poly-4-methylpentane-1 a sizeable peak is reported at -248°C. However, they conclude that the mechanisms responsible for these loss peaks are not yet understood. No relaxation phenomenon was observed below -196°C for either polyethylene or poly-butene-1. For poly (d, l-propylene oxide) a loss maxima at -196°C to -153°C is reported, which is associated with probable chain motions accompanying the methyl reorientation process.

AtsuoKonda et al[77] have recently measured dynamic viscoelastic properties of drawn and heat treated samples of polyethylene terephthalate fibres.

From their observations they concluded that:

(1) The peak temperature of tan δ does not always increase with increasing crystallinity (different from the results of Thomson and Woods[35]).

(2) The peak value of loss tangent decreases with increasing crystallinity but, when the crystallinity is larger than about thirty percent, the peak-value depends more on the method and temperature of heat treatment.

(3) The lower the temperature of heat treatment the smaller is the size of the crystallites and as a result molecular chains in amorphous parts owing to restriction by many small crystallities are strained more, and the effect of straining becomes much more pronounced than the crystallinity itself, especially, when the crystallinity is large.

CHAPTER 111 EXPERIMENTAL

Apparatus for measuring dynamic bending properties of dry fibres in vacuo.

EXPERIMENTAL

1. The Effect of Temperature on Dynamic Bending Properties of Dry Fibres in Vacuo.

(i) Introduction.

A fibre in the form of a cantilever can be forced laterally into resonance by several methods, e.g. electro-mechanical, electrostatic, acoustic etc. In the present investigations on the dynamic bending properties of dry fibres, in vacuo, over a temperature range of $-70^{\circ}C$ to $180^{\circ}C$, an electrostatic method similar to the one used by Meredith and HSu[40] and Kubie[78] was adopted. The experiments were carried out in vacuo to avoid the necessity for corrections due to air damping.

The basic principle of this method consists of a clamped fibre in an electrostatic field between two electrodes, brought to resonance by super imposing on the electrodes an alternating field of the right frequency supplied from a variable frequency oscillator. The success of this method depends on the fibre acquiring full charge from the electrostatic field.

To determine the dynamic bending modulus and the loss tangent, it is necessary to know the resonance frequency, the band width and also the length, shape factor and mass of specimen.

(ii) Description of Apparatus and Instruments

From the circuit diagram in Fig.4 it will be seen, that the fibre

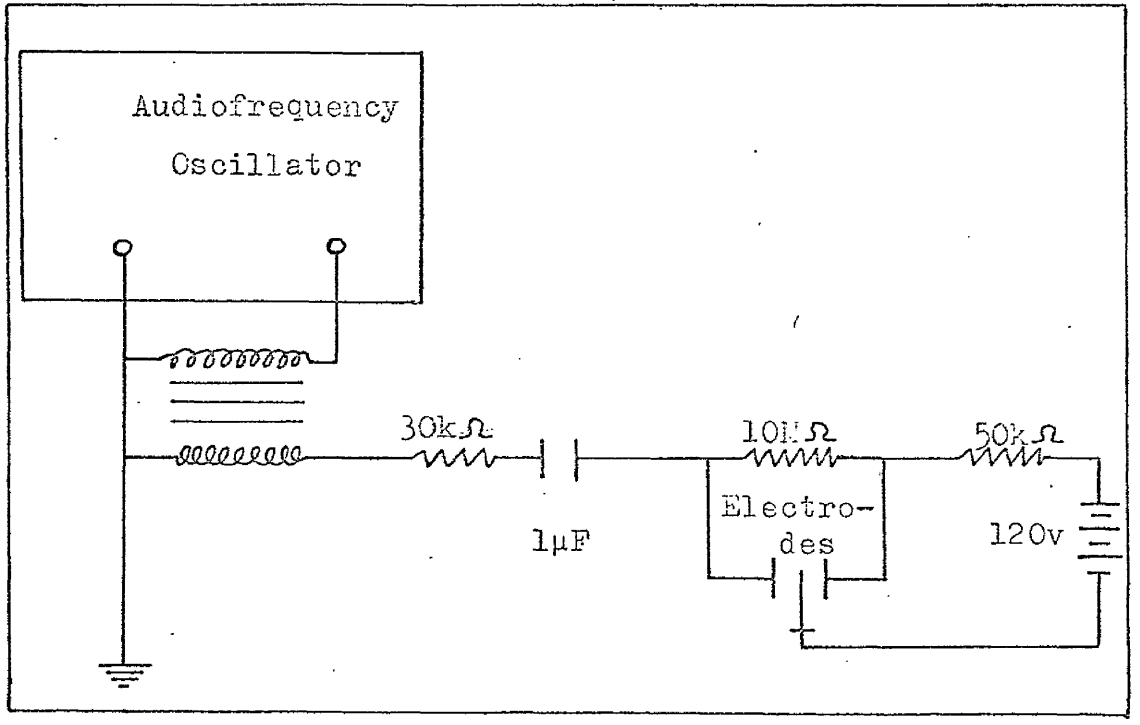

Fig.4. Circuit diagram of the electrostatic system.

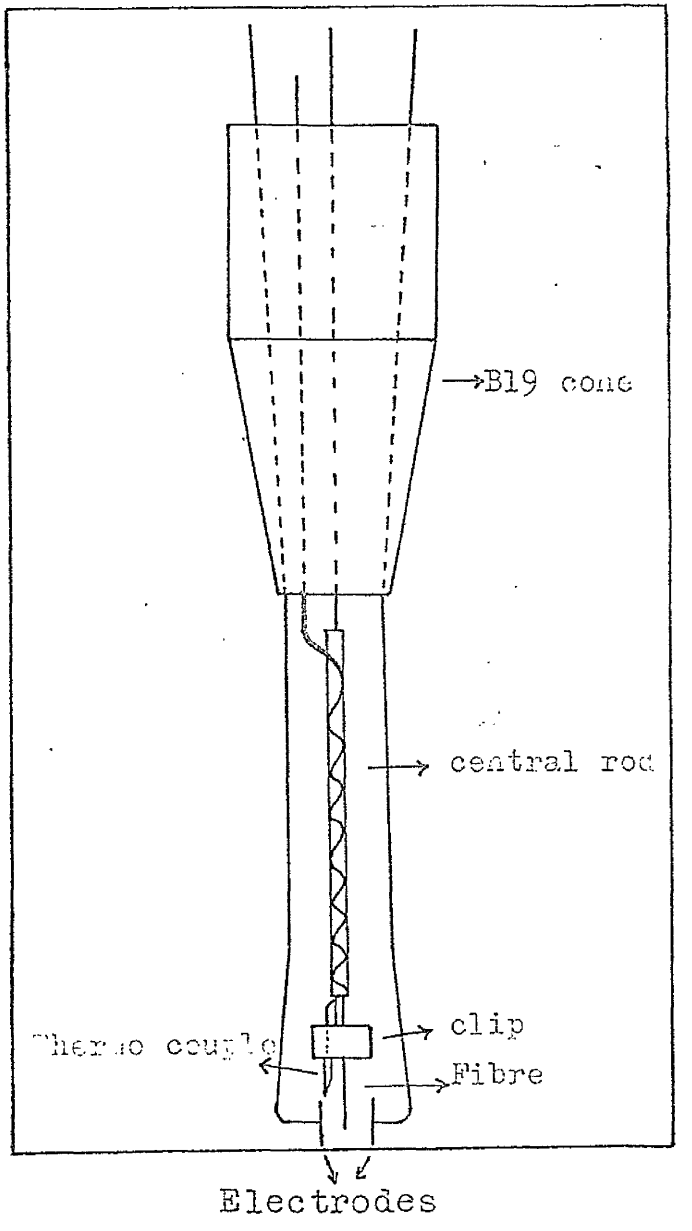

Fig.5. Fibre mounting head.

placed between the two electrodes is raised to a negative potential by a high tension DC source, and is subjected to an alternating voltage applied to the electrodes from the Muirhead decade oscillator through a step up transformer.

The applied DC voltage is not very critical but higher voltages are undesirable in vacuo, as they would tend to produce sparks across the electrodes. In the present experiments 120 volts DC was found suitable for all fibres. The AC voltage however, depends on the fibre dimensions. In general a fully charged fibre requires 5 to 50 volts to give a reasonable amplitude of vibration. An electrode spacing of 3 to 4 mm was found satisfactory for all fibres.

In the dry state at room temperature, synthetic fibres owing to high electrical resistance are difficult to charge. However, if heated to about 100°C they pick up charge easily and thereafter retain the charge well at all temperatures.

Under given experimental conditions the resonance frequency increases with decrease in specimen length. Although, in theory, the upper limit of frequency is determined by the natural frequency of the support carrying the fibre, in practice it is not possible to attain this limit. Before this limit is reached the fibre will have become too short for accurate measurements. The lower limit, however, is set by the amplitude of vibration which decreases with increase in fibre length.

In the present experiments the frequency range was confined to 50 to 600 cps.

Since the dynamic bending properties of fibres are measured in dry condition under vacuum, an air tight system carrying the fibre mounting head and an arrangement to create vacuum in the system are necessary.

As indicated in Fig. 5 the mounting head is a B. 19 ground glass cone carrying the two electrodes, a central rod with a fibre mounting clip at the end and the two wires of the thermocouple. These are fitted through appropriate holes made in the cone and are sealed off with epoxy resin and set at 106°C. The electrodes are made of brass foil (2 x 3 mm in area) and are placed 3 to 4 mm apart. The rods that carry the electrodes are enamelled 18 swg copper wires.

The central rod however, was made of fine quartz tube which carries a fibre mounting clip at one end. The other end of the quartz tube fits into the 18 swg copper wire just protruding from the B 19 cone serving as a connecting lead to the battery. The fibre mounting clip is connected to this lead by means of a very fine copper wire wound round the quartz tube. This precaution was taken in order that conduction loss through the central rod is negligible. A 36 swg copper constantan thermocouple wire, of sufficient length (to minimize conduction losses), was coiled round the quartz tube and its junction was placed as close to the fibre as possible to register the temperature of the fibres.

The temperature sensing junction of the thermo couple was wrapped with a fine polypropylene monofil in order to ensure that the fibre and the thermocouple junction absorb nearly the same amount of heat radiation in vacuo.

It was necessary to place the fibre well in the middle of the heating or cooling tube about 8" long. In earlier experiments however, a failure to observe this precaution resulted in apparent under estimation of the temperature recording. This was later found to be due to high conduction losses through the wires of the thermocouple and also probably through the fibre holder.

The thermocouple used in the experiments was independently calibrated against steam (100°C) and against sublimation point of solid carbon dioxide (-78.5°C). One junction of the thermocouple was maintained at 0°C using ice. The emf generated by the thermocouple was read on the Pye scalelamp galvanometer (No.7901/5). Later the temperature calibration curve for the temperature range of -80°C to 200°C was worked out by extrapolation using standard tables[79].

The refrigerating unit was a Townsen and Mercer minus seventy thermostat bath. Using solid carbon dioxide as the cooling agent and petroleum ether (B.P. 80° to 100°C) as the heat transfer medium the temperature was thermostatically controlled from 20°C to -70°C.

The cooling tube (Fig.6) has a B. 19 ground glass socket at the top

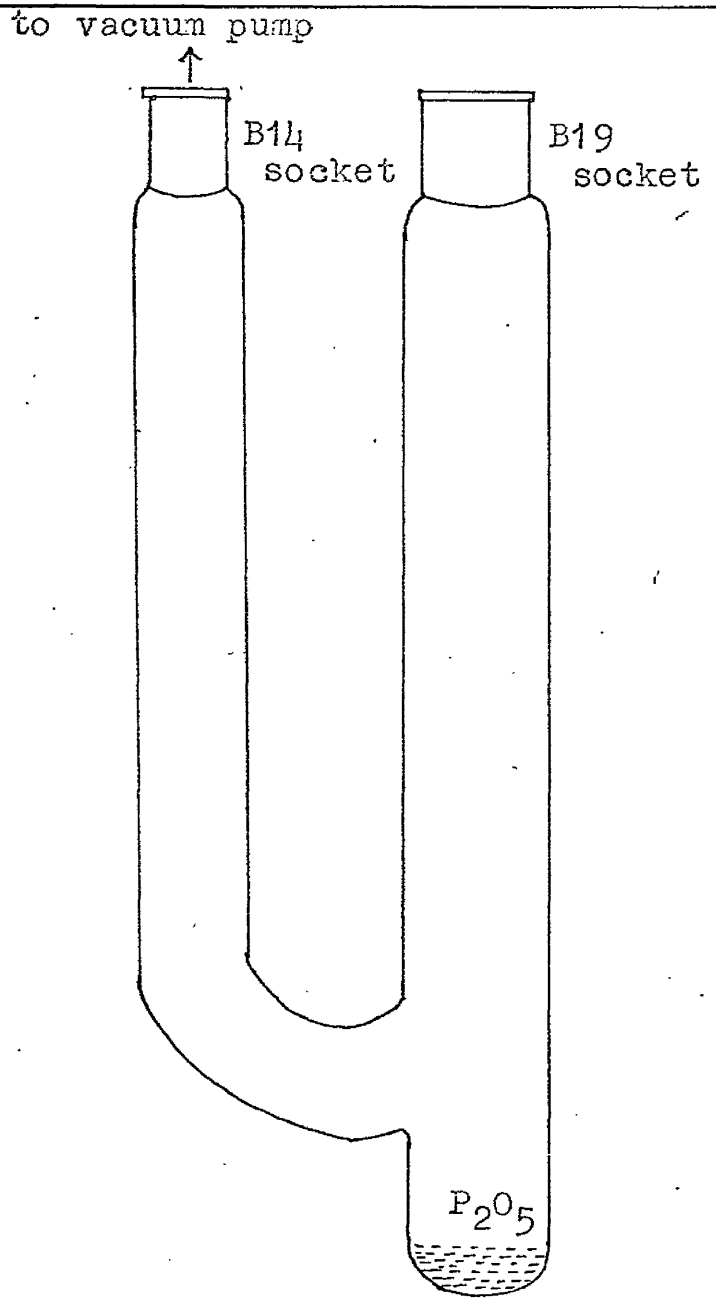

Fig.6. Cooling tube.

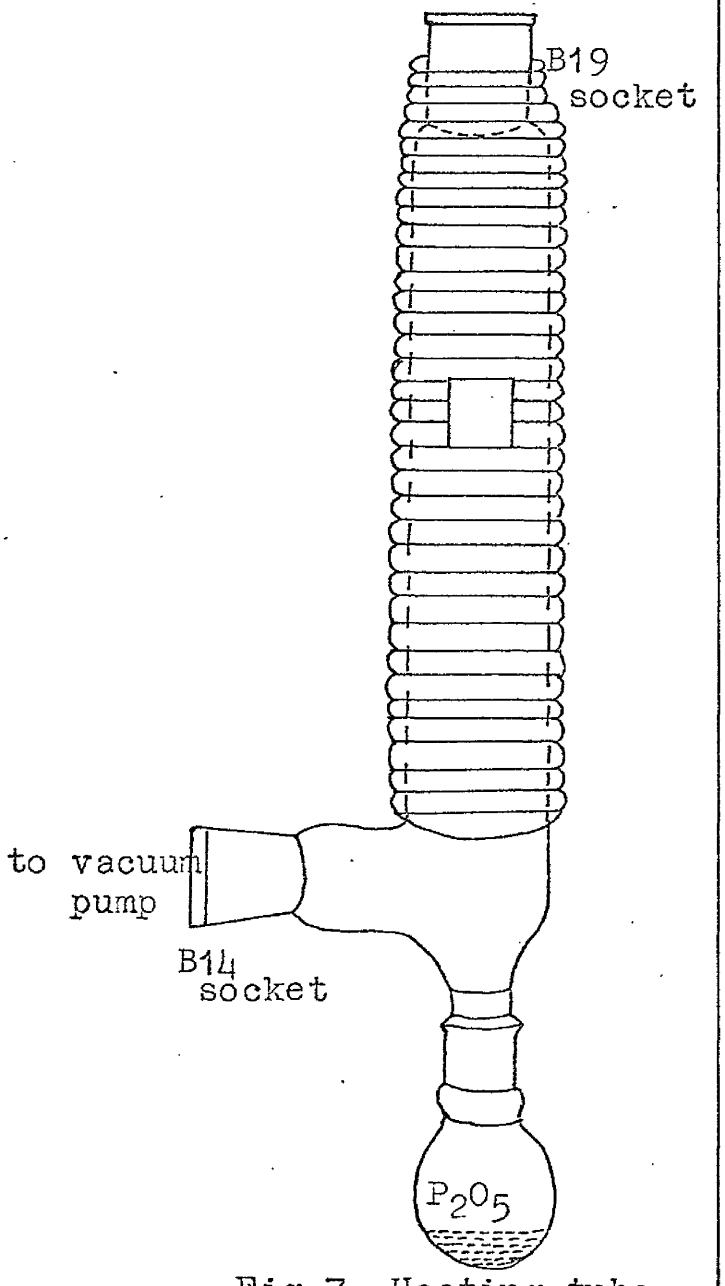

Fig.7. Heating tube.

to take the mounting head. The side vertical arm in the tube connects the system to a vacuum pump. The fibre was left inside the tube over P_2O_5 under vacuum for a sufficiently long time (24 hours) to ensure dry conditions before immersing the tube in the bath and lowering the temperature. The temperature of the fibre registered by the thermocouple inside the tube was read from the galvanometer. The refrigerator has a double window through which the vibrating fibre was viewed using a low-power microscope. Stroboscopic illumination from a Philips Stroboscope, PR 9103/O_2 was used to define the limits of vibration more clearly. Driving a stream of room air at the window ensures clear viewing of the fibre, by avoiding condensation of moisture on the window at low temperatures.

For measurements above room temperature a vertical glass tube shown in Fig. 7 was used. The glass tube was first covered with a layer of aluminium foil and asbestos paper and then wound uniformly with nichrome resistance wire. It was further heat insulated by Wrapping successive layers of asbestos string.

The heating tube was also fitted with a B.19 ground glass socket at the top to take the mounting head and a small side arm near the bottom to connect it to a vacuum pump. A small flask with P_2O_5 was fitted to the ground glass joint at the bottom end of the tube to ensure dry conditions inside the tube. The aluminium foil was earthed to prevent accumulation of static charges on the heating tube.

Two opposite windows at the appropriate place on the tube were left uncovered to enable viewing the fibre through the microscope and as before the fibre was stroboscopically illuminated.

Heat was provided to the tube by supplying the coils with the out put of a full wave rectifier. The temperature of heating was controlled by means of a continuously variable transformer (220 - 250 volts ac) that fed the rectifier circuit. The use of the rectifier was to eliminate the possible interference of the heating current with the alternating voltage used for exciting the fibre.

(iii) Experimental procedure

All fibres used in this investigation unless otherwise mentioned were conditioned in the heating tube over P_2O_5 in vacuo, for 10 minutes, at 180°C - 190°C under a small load of 2 mg/denier.

The fibre, after heat conditioning, was cooled under load (2 mg/ denier) to room temperature. The mounting head was then gently removed from the heating tube by releasing the vacuum and the fibre was cut between the electrodes to the required length with a pair of fine scissors. The mounting head was placed back in the heating tube and the vacuum was again restored. By heating the fibre again to the required temperature (5° to 10°C below the heat conditioning temperature), the measurements of resonance frequency and band width were made at 5° to 10°C interval as the temperature was steadily lowered to room temperature.

In this way the specimen was cooled to room temperature through the transition region in about 2 to $2\frac{1}{2}$ hours.

At room temperature the mounting head was transferred to the cooling tube and left under vacuum over P_2O_5 for 10 to 12 hours to ensure dry conditions. Measurements were then made in cold bath adopting the same procedure as above, while cooling the specimen steadily to the lowest temperature.

In these experiments vacuum was maintained to 0.015 mm of Hg by using a two stage Edward's vacuum pump and measured using a Pirani guage.

(iv) Quantities measured and methods of measurement.

The quantities measured in these experiments were the resonance frequency, the band width, and the length and mass per unit length of the specimen.

The resonance frequency is the natural frequency of the fibre when the amplitude of vibration goes through a maximum and was read directly from D 890-A Muirhead Wigan decade oscillator. The Muirhead oscillator is incorporated with a 2 kc crystal oscillator for calibration of the instrument to a very high degree of precision. The amplitude of vibration was measured with a micrometer eye piece reading 0.0425mm/ division in a low power microscope (x10 magnification and 2" objective lens).

The band width is the difference between the two frequencies that straddle the resonance frequency where the amplitude of vibration is $1/\sqrt{2}$ or 70% of the maximum. All measurements were made at the fundamental mode of vibration.

After the temperature experiments were over, the length of the fibre was measured at 20°C in the cooling tube using a travelling microscope reading to 10 microns.

To determine the weight of the fibre, it was cut off the holder using a razor blade and was weighed on a modified double cantilever balance at 20°C and 65% RH. The balance could weigh to 0.035 microgrammes. Since it was not always possible to cut the fibre flush to the holder, the residual length on the holder was measured to calculate the actual length of the fibre that is weighed.

2. The Effect of Static and Dynamic Strain, Temperature and/or Humidity on Dynamic Tensile Properties of Fibres from Tyre Cords.

(i) Introduction.

In the dynamic bending experiments on fine fibres in air there is considerable damping of the lateral vibrations. Karrholm and Schröder[21] have shown that the band width at resonance is affected for fibres of diameter less than 300 μ. Meredith and Hsu[40] have worked out in detail the theoretical corrections for air damping. For fine fibres the magnitude of this correction is, however, large.

In the dynamic tensile experiments, where sinusoidal forces are applied longitudanally to the fibre, air damping has no influence. Therefore the study of the effect of temperature and humidity on the dynamic mechanical properties of fibres from tyre cords were made on a mechanical tan δ meter of the direct recording type similar to that employed by Yoshino and Takayanagi[75].

The principle of their tan δ meter is "To fix both ends of the sample to two strain gauges of unbonded type. One of the strain gauges is used to transform the sinusoidal displacement into an electrical quantity proportional to the displacement and the other is transducer of the generated force. The absolute values of these electrical vectors representing force and displacement are adjusted to unity (full scale of volt meter) and vector reduction is achieved by opposing the out-puts of the two strain gauges. By this operation the value of tan δ can be directly read off the voltmeter. Regulation of the magnitude of the difference in the vector is brought about conveniently by controlling the DC input of the strain gauges. The dynamic tensile modulus is calculated from the ratio of the input voltages of the strain gauges v_2/v_1. When out-put voltages are regulated to unity the dynamic tensile modulus $E' = K\ (v_2/v_1)$, where K is a constant relating to the dimensions of samples and strain gauges".

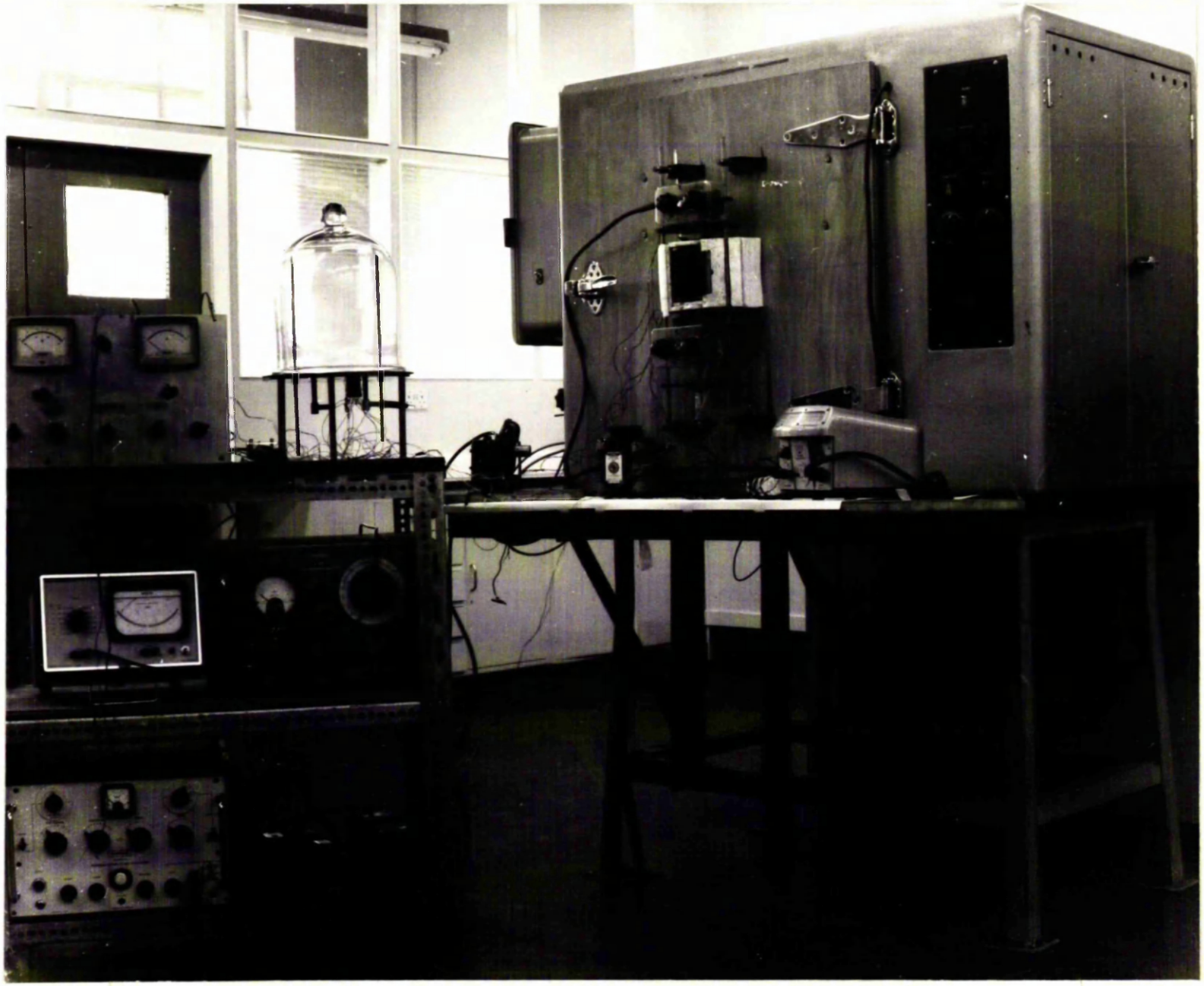

Apparatus for measuring dynamic tensile properties of fibres under different conditions of temperature and relative humidity.

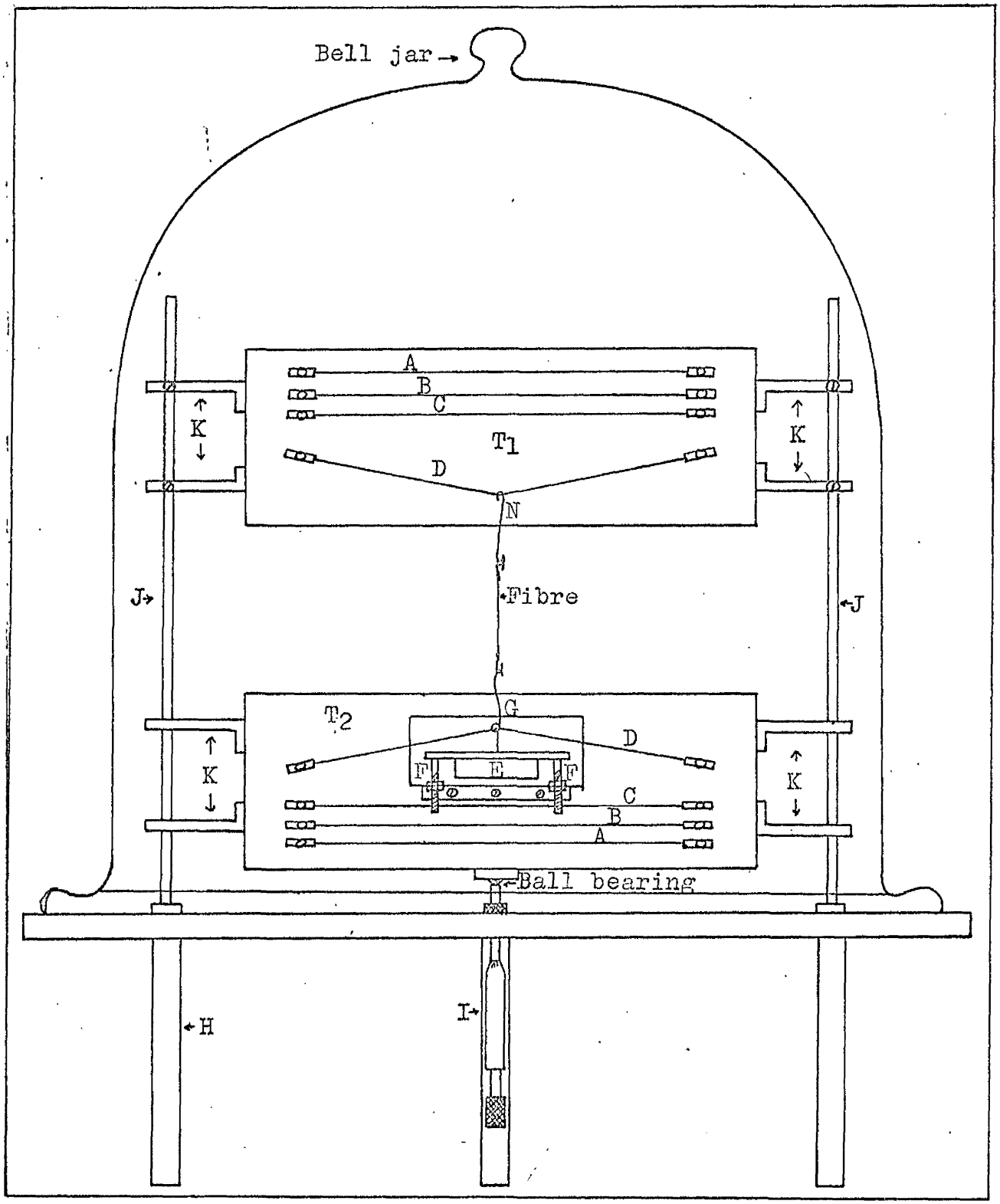

Fig.8. tanδ meter.

(ii) Description of apparatus and instruments.

The arrangements in the tan δ meter of the force and displacement sensing units T_1 and T_2 respectively, are shown in Fig. 8 . Each unit consists of four unbonded elements A, B, C and D of swg 50, Karma resistance wires. The wires that are approximately 10 cm long are silver soldered to brass tabs made from 1/2" length and 1/16" diameter brass tubing. The tabs are soft soldered to binding posts on Tuflon boards with elements A, B, and C mounted slack. The binding posts project $\frac{1}{4}$" from the Tuflon board to avoid chaffing of the elements against the board. Wires D are the force and displacement sensing elements in the two units T_1, and T_2 respectively. The sensing elements D are mounted in their respective units with 24^{o} sag which gives them a mechanical advantage of more than 2. The force or the displacement to be measured is applied to the respective centres of the elements through thin glass rods of 1 mm diameter. The tuflon boards are housed compactly into two boxes made from Perspex to avoid any damage from external source to the very delicate unbonded elements.

An opening is provided in the centre of the Tuflon board in the unit T_2, to accommodate the electromagnetic transducer (telephone mouthpiece) E. The transducer E is mounted on two bolts F to an angled brass metal which is fixed to the Tuflon board by means of screws. The bolts F are provided with rubber washers to damp the vibrations from the frame of the transducer.

A glass rod G, 4 cm long bent in the form of a coil in the centre for threading the element D is fixed vertically with Durofix to the centre of the diaphgram, and the top end of the glass rod bent in the form of a hook, is used for mounting the fibre. Required tension is applied to the element D by manipulating the bolts F that carry the transducer. The tension on this element should be such that it remains taut when sinusoidal vibrations from the transducer are imposed on it.

The units T_1 and T_2 are also provided with metal flanges, K, at the sides for mounting them on two vertical rods. In Fig.8 they are seen mounted on two vertical rods, J, on a tripod H. The tripod is made of a 10" dia. metal plate and is fitted with a micrometer I, from beneath the plate through a hole in the centre. The micrometer reads to 0.001 cms and the micrometer stud projects 2 cm above the metal plate. The strain gauge unit T_2 that is free to slide in the vertical rods, J, rests on the micrometer stud, and a ball bearing is embedded beneath unit T_2 to ensure point contact with the flat surface of the stud.

The unit T_1, however, can be secured firmly to the vertical rods, J, at any required height by means of screws provided on the side flanges K. A glass rod, N, suspended from the centre of the force sensing element, serves to mount the specimen between the units T_1 and T_2. Using the micrometer, unit T_2 can be lowered with respect to unit T_1 to subject the specimen to required static strain.

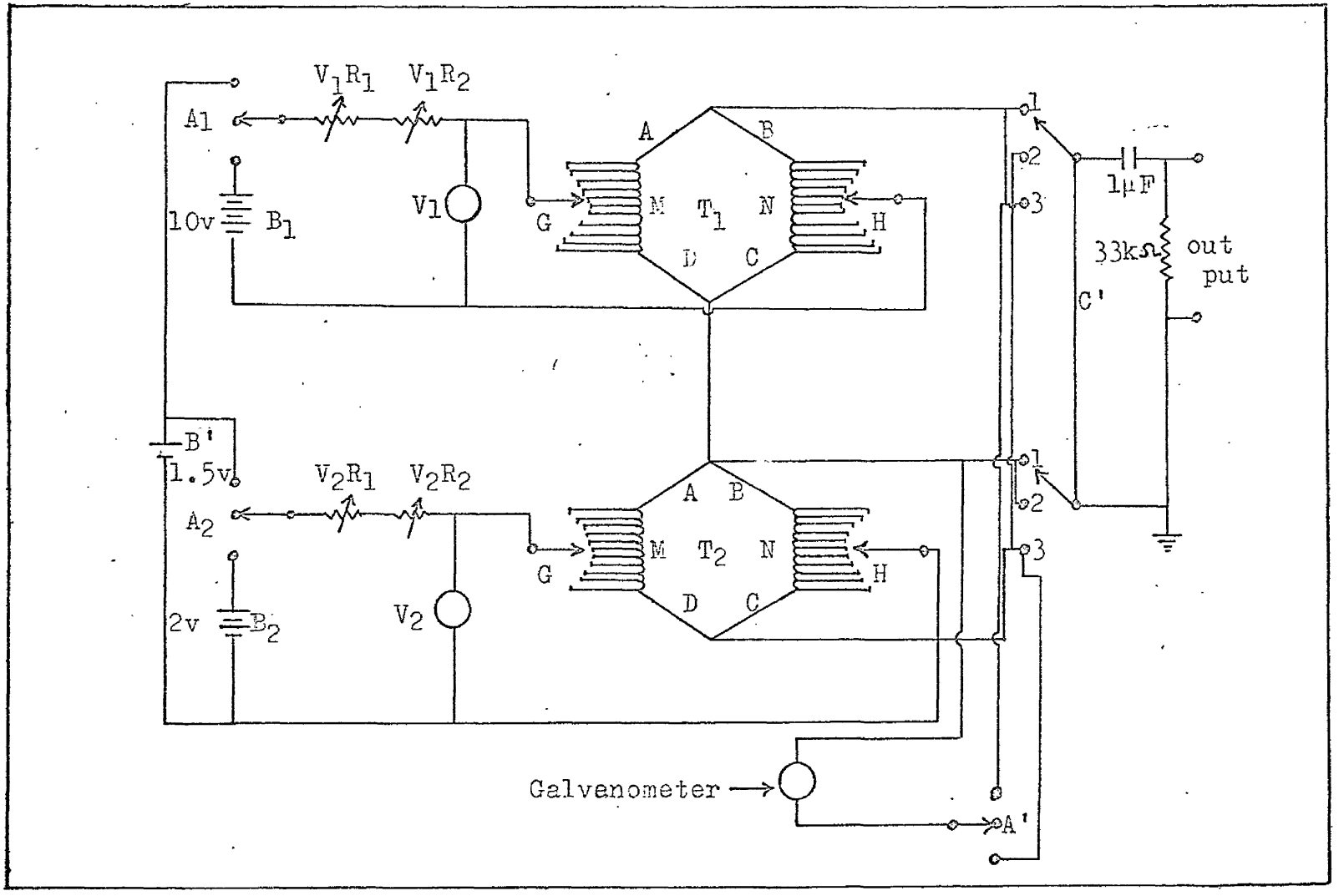

Fig.9. Circuit diagram for the tanδ meter.

The circuit diagram for the strair gauge portion of the apparatus is indicated in Fig.9 The four elements A, B, C and D in each unit are connected in the form of a Wheatstone bridge. Since it is difficult to solder elements of equal lengths, the bridges are brought to near balance by adding swg 36 Karma resisfance wire of short length to the appropriate arm of the bridge. Resistors M and N are used for fine and coarse balance respectively. G and H are single pole silver contact 11 position rotary switches for manipulating the bridges into balance.

The 10v battery B_1 and the 2v battery B_2 supply DC voltages to the bridge units T_1 and T_2, respectively. The fine and coarse variable resistors V_1 R_1 and V_1 R_2 in the bridge circuit T_1 and V_2 R_1 and V_2 R_2 in the bridge circuit T_2 respectively, are used for regulating the input voltages to the two bridge units. The 1.5v battery B′ is used exclusively when the bridges are being checked for their balance or for the response of their elements D (e.g. DC output/volt DC input/gram load or DC output/volt DC input/unit strain). The two three-way single pole switches A_1 and A_2 enable selection of the appropriate DC source to the bridges to be made as required. The input DC voltages to the two units are measured on the two DC voltmeters V_1 and V_2 incorporated in the circuit. The DC output of the two bridges, are also conducted through the switch A′ to a Pye scalelamp galvanometer, which can be brought into operation when required.

If a specimen that is under static strain between the two units T_1 and T_2 is subjected to longitudinal vibrations by driving the electromagnetic transducer by an oscillator, AC voltages will be produced in the two units. The AC output voltages from the two units will be proportional to the respective DC input voltages to the bridges and also in T_1, to the dynamic force applied to the force sensing element through the specimen and in T_2, to the dynamic strain applied to the strain sensing element by the transducer. It will be noted from Fig.8 that because of the geometry of construction of the two elements D in units T_1 and T_2, the force sensing element and the strain sensing element work in opposite phases. Therefore, inherently, the AC output from the two gauges will be 180° out of phase with each other. The specimen between the two gauges will however introduce an additional phase difference, the magnitude of which will depend on the characteristic viscoelastic response of the specimen to dynamic tensile testing under given experimental conditions.

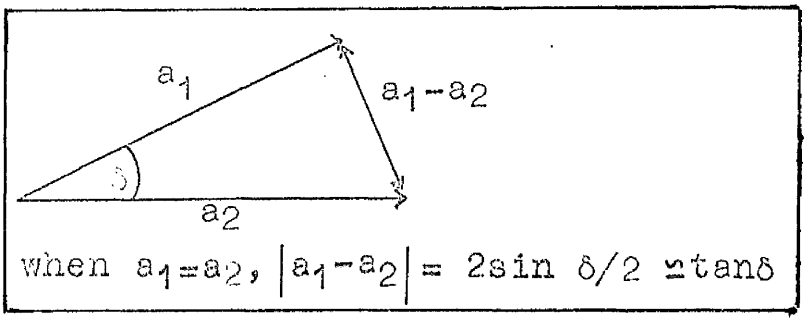

Fig. 10. Vectorial representation of the output voltages from T_1 and T_2

Fig. 10 is a vectorial representation of the output voltages from T_1 and T_2 and a_1 and a_2 are proportional to force and displacement respectively. If a_1 and a_2 are adjusted to unity and the two signals are mixed then the reduced vector $/a_1 - a_2/ \triangleq \tan \delta$ is obtained. The mixing of the two signals is conveniently brought about by conducting the output voltages to the three-way, two pole change over switch C' (Fig. 9). In positions 1 and 2 the switch C' picks up voltages from T_1 and T_2 respectively. In position 3, however, because the signals are opposed only the residual voltage of the two signals is picked up.

The main structural feature of this apparatus is that the vector reduction is conducted without pre-amplifying the respective electrical output from the two strain gauges proportional to force and displacement. By this method the possibility of introducing experimental error due to phase shifting effect from the amplifier is avoided. However, in order to make this possible, it is necessary to amplify the very small output voltage (less than one micro volt) by using a tuned amplifier of the highest sensitivity.

In the present investigation a D-788-A low frequency amplifier ~~analyser~~ with a selectivity (Q - factor) of 50 and a voltage gain 90 dB $\pm$ 3 dB was used. The amplified AC voltages were measured on a sensitive valve voltmeter (Marconi T F 2600). The block diagram of the tan δ meter is shown in Fig.11.

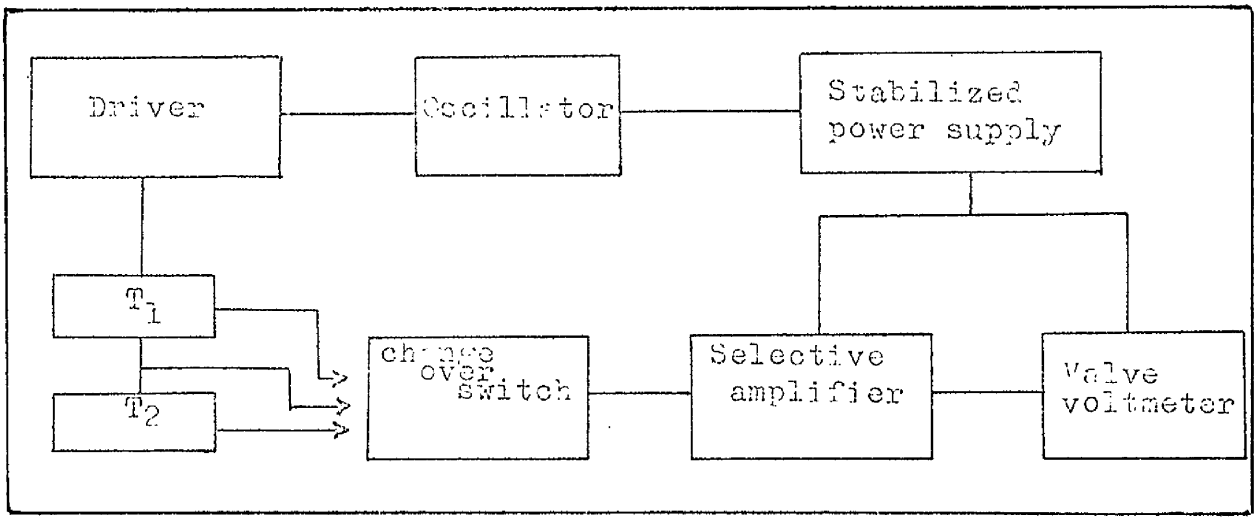

Fig.11. Block diagram of the tan δ meter.

The electromagnetic transducer was driven at 20 cps by the Muirhead decade oscillator (D - 890 - A). The AC outputs of T_1 and T_2 were amplified to 1 volt (full scale of volt meter) by regulating the respective DC inputs to the two strain gauges.

By turning the change over switch to position 3 tan δ was read directly on the voltmeter.

(iii) Instrument calibration

For the strain gauge T_1,

$F = e_1/f_1 v_1$ gms..... (5) where F is the dynamic force in gms; e_1 is the Ac output from the gauge and v_1 is the DC input to the gauge. f_1 is the force calibration factor for the gauge T_1 and is defined as the AC voltage output per volt DC input per gram force.

Similarly, for the gauge T_2;

$$\Delta l = \frac{e_2}{f_2 v_2} \text{ cm} \quad \ldots\ldots (6)$$ where Δl is the dynamic displacement in cm, e_2 is the AC output from the gauge T_2, v_2 is the DC

input to the gauge. f_2 is the displacement calibration factor for the gauge T_2 and is defined as the AC voltage output per volt DC input per unit displacement.

If the length ℓ in cms and the area of cross section A in cm^2 of the specimen are known, then the dynamic tensile modulus E' will be equal to

$$E' = \frac{F}{\Delta \ell} \frac{\ell}{A} \quad gms/cm^2 \qquad \ldots\ldots\ldots (7)$$

The area of cross section A in equation (7) can be substituted by $\frac{m}{\rho}$ where m is the mass/unit length and ρ is density of the specimen.

Since the AC output voltages e_1 and e_2 are adjusted to unity for measuring tan δ from equations 5, 6 and 7.

$$E' = \frac{f_2}{f_1} \cdot \frac{\rho}{M} 1 \frac{V_2}{V_1} \quad gms/cm^2 \qquad \ldots\ldots\ldots (8)$$

It will be noticed that in the determination of both tan δ and E', absolute values of the output voltages of the two gauges are not necessary. Relative values of these quantities are sufficient for the calculations.

However, the accuracy of determination of the value of E' depends on the accuracy of measurement of the input DC voltages v_1 and v_2. In the instrument described here input DC voltages are read to 0.05 of a volt and this is found to be satisfactory for the determination of dynamic tensile modulus. The calibration factors f_1 and f_2 for the gauges T_1 and T_2 were determined by using a fine coiled spring of known displacement/gm load. The spring (in this instance 0.0128 cm/gm load)

was mounted between the gauges under a sufficient static strain to keep it taut. It was then subjected to longitudinal vibrations at 20 cps under a small dynamic strain amplitude of 0.02 mm. The input DC voltages v_1 and v_2 required to produce unit AC output voltage from gauges T_1 and T_2 respectively were determined. They were $v_1 = 4.8$ and $v_2 = 0.5$ when $e_1 = e_2 = 1$.

From equations 5 and 6

$$\frac{f_2}{f_1} = \frac{F}{\Delta \ell} \cdot \frac{v_1}{v_2} \quad \text{gm/cm}. \qquad \ldots\ldots\ldots (9)$$

substituting for F, Δl, v_1 and v_2

$$\frac{f_2}{f_1} = 7.5 \cdot 10^2 \quad \text{gm/cm}.$$

By using the spring between the two gauges the phase difference between the output voltages e_1 and e_2 should ideally be zero. On the tan δ meter described here, tan δ for the spring was less than 0.0025 for measurements made below 0.02 mm of dynamic amplitude of vibration. However, above 0.02 mm up to 0.045 mm of dynamic amplitude, due to inherent characteristics of the gauge construction the error in tanδ increases from 0.0025 to 0.01. Therefore, small corrections for tan δ values is necessary for experiments conducted above 0.02mm of dynamic amplitude.

The load at yield point for a swg 50 Karma resistance wire is reported to be about 28 gms.

However, the response of the two gauges to loading is linear up to 30 gms, and this is considered to be the maximum load that can be applied to the gauges. The displacement of each gauge for 20 gms load measured through a microscope was found to be 0.27 mm.

The Pye scale lamp galvanometer was also used for measuring the DC output voltage of each gauge per volt DC input per gm load. The gauges produce 4 μv/volt input/gm load. The load on the specimen at any time during the experiment is conveniently measured on the galvanometer, by reading the DC output of the force gauge T_1 for a unit DC input.

The dynamic amplitude of vibration of the transducer was found to increase linearly from 0 to a maximum of 0.045 mm by increasing the oscillator output from 0 to 40 volts.

The output signal of gauge T_2 was checked for sine wave characteristics on an oscilloscope. No distortion in the signal was noticed when the amplitude of vibration was increased from 0 to 0.045 mm.

In the tan δ meter the restriction on the choice of frequency of vibration is set by the resonance frequencies of the strain gauge units and transducer. On the present instrument the resonance frequencies of the strain guage units (T_1 and T_2) and transducer was 80 cps and 500 cps, respectively. Therefore, a frequency vibration of 20 cps was found satisfactory in the present investigations.

(iv) Experimental procedure.

The investigations on dynamic tensile properties, unless otherwise mentioned, were carried out mostly on 2 cm length filaments taken from tyre cords. The ends of the filament were mounted on two small glass hooks with epoxy resin and left to set in an oven at about 60° for 30 minutes. The mounted filaments were later conditioned for 10 to 12 hours at $20^{\circ}C$ and 65% RH in a conditioned room.

The length of the specimen was measured on a travelling microscope reading to 10 microns. The mass/unit length of the specimen was calculated by weighing a bunch of 2 cm filaments (approximately 50) on a micro balance at $20^{\circ}C$ and 65% RH. The density of the specimens were measured in a density gradient tube at $20^{\circ}C$ and 0% RH.

The effect of static strain and dynamic strain was investigated on nylon 66, Dacron and viscose rayon in a conditioned room at $20^{\circ}C$ and 65% RH.

The glass hooks carrying the specimen were mounted on to glass hooks N and G (Fig.8) between the gauges T_1 and T_2 on the apparatus.

Static strain was applied in steps from 1, 2, 3....6% of the specimen length. At each strain the specimen was allowed at least 1 hour for relaxation before the start of the dynamic experiments.

For the measurements of E' and tan δ the specimen was subjected to

longitudinal vibration of 0.02 mm dynamic amplitude and these measurements at any one temperature need less than one minute. The force gauge T_1 in the apparatus described above is not sensitive enough to record the dynamic tensile modulus of rayon (1.5 denier) at 1% static strain.

Since the amplitude of vibration that is possible on this instrument is only up to 0.045 mm, three lengths of filaments 1, 2 and 3 cm were used to study the effect of dynamic strain over a range of 0.03% to 0.45%, when the static strain on nylon and Dacron was 2% and on rayon 3%.

To study the effect of RH at 20°C the apparatus was covered with a bell jar and made leak proof by using silicone grease between the metal plate H (Fig.8) and the bottom of the bell jar. Salt solutions in petri dishes were used to maintain RH from 30% to 95% inside the bell jar. The humidity inside the system was recorded using a thermocouple hygrometer. Since the system was leak proof it was possible to attain equilibrium conditions at any humidity within 30-40 minutes.

For dry conditions P_2O_5 was used inside the jar and measurements of E' and tan δ were taken after 12-18 hours. However, no recording device was used to assess dry condition.

To study the effect of temperature and humidity on dynamic tensile properties of fibres, a Gallenkamp conditioning oven was adapted. The original metal door of the conditioning oven was replaced by a Formica

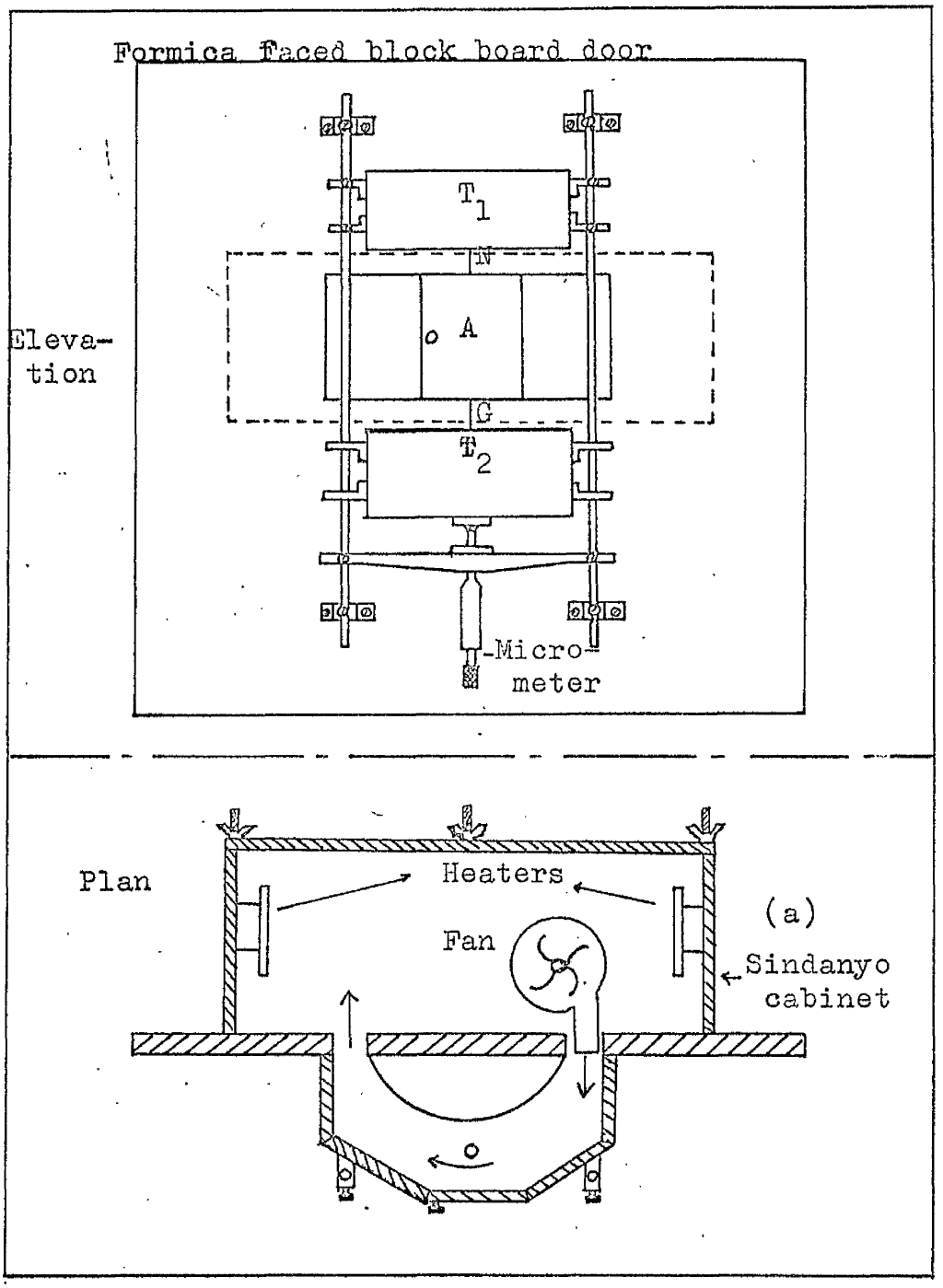

Fig.12. Modifications on Gallenkamp door to aecommodate tanδ meter.

faced block board door. On the out-side of the door a fibre enclosure A, and the units T_1 and T_2 were mounted as indicated in Fig.12. Similar to the arrangement in Fig.8 unit T_2 supported by the two vertical rods rests on the micrometer stud 3-4 cms below A, and unit T_1 is secured to the vertical rods 3-4 cms above the fibre enclosure A. Glass rods N and G from units T_1 and T_2 respectively are drawn through 1/8" holes provided in the centre of the enclosure and the specimen is mounted inside the enclosure between the rods N and G . The access to the specimen is through a small door in front of the enclosure A. Precautions were taken to see that the rods N and G are absolutely in line with each other by aligning the units T_1 and T_2 as required using the adjustable screws. (Fig.12). In order to minimise the escape of steam through the $\frac{1}{8}$" holes at high temperature and humidity the holes were reduced in size using split card board pieces leaving just enough room for the glass rods to move freely without touching the sides.Room air was blown into unit T_1 to avoid condensation of steam rising from the enclosure A during the experiment.

The fibre enclosure A is a cabinet made of Tuflon. The inside of the cabinet is built in the form of a U-shaped tunnel. (Fig.12a) terminating at the back of the door in an inlet and an outlet opening. A fan is fitted near the inlet opening inside the conditioning oven to circulate the conditioned air from the oven through the fibre enclosure. Since the enclosure is exposed to room conditions outside the door, it was heat

insulated to avoid condensation of moisture inside the Tuflon cabinet. The temperature and the humidity inside the cabinet were recorded using a thermometer and a thermocouple hygrometer, respectively.

The Gallenkamp conditioning oven is an insulated copper chamber designed to maintain 0 to 100% RH and any desired temperature from ambient up to a maximum of 100°C. The conditioning oven is provided with a motor driven fan for circulation of air inside the chamber. Wet and dry bulb thermometers are also provided, which thermostatically control the input of heat and moisture into the oven and maintain the required temperature and humidity.

Since the highest temperature attainable in the Gallenkamp conditioning oven is only 100°C, for experiments up to 150°C in dry condition, a dry oven was used. The dry oven was a cabinet (17" x 10" x 10") made of heat resistant Sindanyo board. It was fitted to the inside of the door behind the fibre enclosure A. (Fig.12a). The temperature in the oven was regulated by a variable transformer feeding two 200 watt heaters. Dry condition inside the oven was obtained by using P_2O_5, but no recording device was used to assess dry condition. Circulation of hot dry air through the fibre enclosure was maintained by a fan. Access to the dry oven was through the back panel which was fitted to the cabinet on winged nuts. During the temperature and humidity experiments the back panel of the dry oven was left open inside the Gallenkamp conditioning oven, and during dry temperature experiments, only the dry oven was used independent of the Gallenkamp oven.

3. Heat Setting and Dynamic Mechanical Properties of Some Synthetic Fibres.

(i) Introduction

In the present investigation the effect of heat setting on dynamic mechanical properties were studied on nylon 66 (type 900), Terylene and Acrilan 16.

(ii) Methods of heat treatment of nylon 66 type 900, Acrilan 16 and Terylene.

Heat setting was carried out on nylon 66 (type 900) under three different conditions :

(1) Under 10% extension set at 150°C for 1 hour,.

(2) Under 10% extension set in boiling water at 10°C for 1 hour.

(3) Set at 150°C for 1 hour under zero tension.

And Acrilan 16 was heat set under the following conditions.

(1) Under 10% extension set at 130° and 150°C in an oven for 1 hour.

(2) Under 10% extension set in boiling water at 10°C for 1 hour.

(3) Set at 150°C for 1 hour under zero tension.

Terylene was, however, set under zero load and under 200 mg/denier load at 180° for 1 hour.

For applying the required extension on the filaments a frame with fixed and movable jaws as shown in Fig.13, was used.

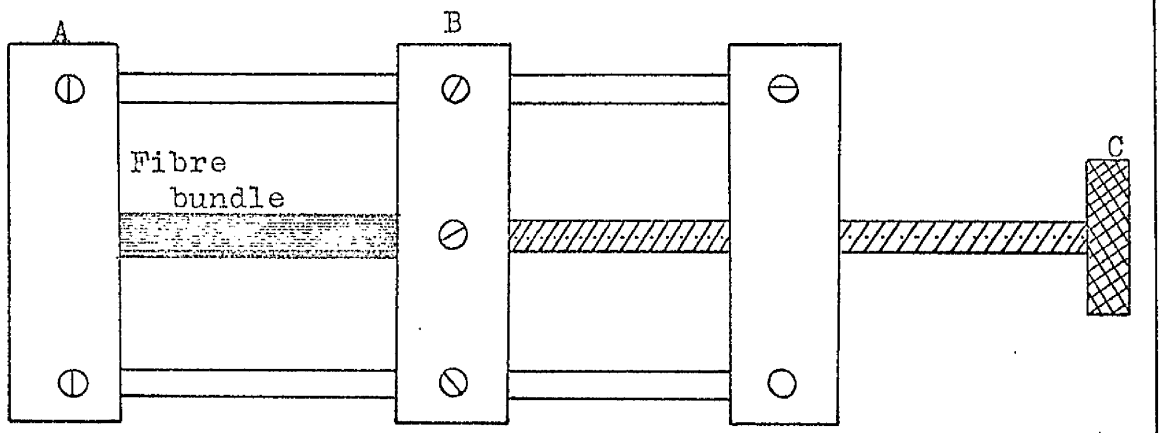

Fig.13. Stretching frame.

A parallel bundle of filaments gripped by the fixed jaw A and the movable jaw B were extended to the required extension by moving the jaw away from A to the required distance by means of the screw C.

4. Mechanical and Other Physical Properties of Some Synthetic Fibres.

(i) Introduction

Tensile properties, physical density and birefringence of some of the fibres were measured using well established techniques. These experiments were carried out, in order to examine the correlation between mechanical, physical and optical properties of some synthetic fibres, especially after heat setting.

(ii) Tensile tests on Acrilan 16 normal and heat set, nylon 66 types A, B, C and type 900 normal and heat set, Dacron and rayon.

Tensile tests were carried out on some samples at 20°C and 65% RH on the TM-M Instron at a constant rate of traverse. The specimens 1 cm long were mounted on cardboard with epoxy resin which was allowed to set at 80°C for about 30 minutes. The cardboard was provided with 1 cm

windows for easy mounting of the specimen.

All samples were allowed approximately 20 seconds to break and 10 to 15 tests were carried out for each sample.

(iii) Measurement of physical density of Acrilan 16 normal and heat set, nylon 66 nypes A, B, C and BH_1 and type 900 normal and heat set, Terylene normal and heat set, Dacron, rayon and polyblend types BH_2, BH_3, and BH_4.

The densities of some of the samples were measured using a density gradient column similar to the one described by Jones [81]. The low and the high density liquids were prepared by mixing pure liquids of carbon tetrachloride and xylene and the density of each mixture was measured by means of hydrometers. Glass floats of known density were used to check the calibration of the column so prepared, a theoretical calibration being obtained using the formula,

$$P_h = e^{-Ah/v} \qquad \ldots\ldots\ldots\ldots\ldots\ldots (10)$$

where P_h is the proportion of low density liquid in the column and v is the initial volume of low density liquid in the mixing chamber.

All measurements were made at 20°C under dry condition and dry condition in the density column was obtained by using P_2O_5. To free the samples from any moisture, they were boiled in xylene for a few minutes before introducing them into the column. Readings were taken after equilibrium condition was attained.

(iv) Measurement of optical birefringence of nylon 66 types A, B, C, BH_1 and type 900 normal and heat set, Terylene normal and heat set, Dacron and Polyblend types BH_2, BH_3 and BH_4.

Birefringence of some of the nylon 66 and Terylene fibres were measured using Mercers method.

As described by Quynn and Steele[82] if Mercers method is to be used the following requirements must be met.

(1) obliquely cutting into wedge-like stumps a continuous yarn containing large number of filaments.

(2) counting the interference lines in the area of the oblique cross section (i.e. on the surface of the wedge) of fine denier fibres.

(3) measuring the last fraction of the wave length lag (not the total lag) by a suitable technique (e.g. by using a quarter-of-the wave length plate and a rotatable analyser).

In the present investigation oblique cross sections of fibres of length 0.3 to 0.5 mm were obtained by threading the filament yarn into a piece of cork and cutting the cork into thin slices of 0.3 to 0.5 mm at approximately 45° to the yarn axis using a sharp razor blade. The fibre sections were then carefully removed from the cork slice on to a slide and mounted in liquid paraffin. The mounting liquid chosen must not, however, swell the fibre.

Birefringence measurements were made on a polarizing microscope using sodium light. The vibration plane of polarizer was oriented into the 90°C position and that of the analyser into 0 degree position. The vibration plane of the quarter-of-the-wave-length plate was set parallel to the polarizer. For measurements, one fibre lying with the oblique area upwards, was picked out at a time and the interference rings were counted with crossed polaroids with the fibre stump set at 45°. The last wave length lag was measured by turning the analyser so as to make both interference rings that are nearest the fibre centre melt into each other. The angle of compensation found thus is α . Finally the fibre diameter d was measured with great accuracy on the microscope.

The birefringence was then obtained using the formula.

$$\text{Birefringence} = \frac{(\alpha + 180.\ n)\lambda}{d} \qquad \ldots\ldots\ldots\ldots\ldots\ldots (11)$$

where d the diameter of the fibre is expressed in $m\mu$ or A°, and λ is the wave length of mono-chromatic light expressed in the same units, and n is the number of interference rings.

CHAPTER IV. RESULTS AND DISCUSSION

RESULTS AND DISCUSSION

1. The Dynamic Bending Modulus

Meredith and Hsu[40] made a rigorous analysis of the theory of vibration of viscoelastic bars and applied the theory to fibres, to obtain the standard expression for the dynamic bending modulus in terms of measurable experimental quantities. They have shown that the dynamic bending modulus is,

$$\epsilon' E'_b = 1.295 \pi^3 \varrho^2 l^4 f_o^2 / m \quad \ldots\ldots\ldots (12)$$

where ϱ is the density (g/cm^3), l is the specimen length (cm) f_o is the resonant frequency (cycles / sec) in the fundamental mode of vibration, m is the mass per unit length (g/cm) and ϵ' is a shape factor given by

$$\epsilon' = 4 \pi I / A^2 \quad \ldots\ldots\ldots (13)$$

where I is the moment of inertia of a cross section about an axis perpendicular to the plane of bending and A is the area of cross-section.

For a fibre of circular cross section the shape factor is unity and for fibres of non-circular cross section the shape factor differs from unity.

In the present investigation it was found that most fibres (which are not circular in cross-section) resonate at two different frequencies on two principal axes that are not mutually perpendicular.

If the resonant frequencies are too close to each other (as in specimens which are very nearly circular e.g. nylon) it is not possible to resolve the band width accurately. In such circumstances fibres that are completely circular or decidedly elliptical have to be carefully chosen for dynamic bending experiments.

Okajima and Suzuki[23], however, seem to have been successful in resolving four different resonance frequencies in four different directions perpendicular to each other in a plane in single filaments of commercial viscose rayon. They used a rotatable clamp attached with a test filament and driven to vibration by a transducer. From their observations they have concluded that the arithmetic mean of the maximum and the minimum values of the resonance frequencies is to be used to calculate the absolute value of dynamic bending modulus and discuss the theoretical reasons for doing so.

In the present investigation an electrostatic method has been used for exciting the test specimen to resonance, and the test specimens were as fine as 15 to 20 μ. In this method since there is no control over the plane of bending of the test specimen, the resonance frequencies for fibres of non-circular cross-section could not be resolved in directions mutually perpendicular in a plane. The non-circular fibre was found to resonate at two different frequencies on two principal axes that were not mutually perpendicular. The values of resonant frequencies

thus observed are represented in the results for some fibres. The values of dynamic bending modulus calculated in this work for specimens of non-circular cross section using the expression (12) could therefore, only be regarded as representing an approximate magnitude of the modulus and not the absolute value.

However, if one assumes that the shape factor of the fibre does not change on heating, the relative value of the bending modulus defined as $\epsilon' E'_b / \epsilon' E'_{b20}$ (where the shape factor cancels out) serves as a useful parameter in studying the effect of temperature on relative dynamic bending modulus.

2. Dynamic bending properties and temperature at 0% RH.

The results of the effect of temperature on the dynamic bending properties over a range of -70° to 180°C at frequeeffect of temperature on dynamic)0 cps of several dry fibres in vacuo obtained in the present investigation have been graphically represented in Figs. 14 to 22. Some of the data for individual runs and mean values of tan δ and relative bending modulus for each type of fibre have been tabulated in Tables 1 to 1X in the hope that it may be useful for any future calculation.

The densities quoted, unless otherwise mentioned, are assumed densities of dry fibres obtained from literature: wool[83], silk[84], Fibrolane[85], ramie[86], Fortisan[85], acetate[87], Tricel[85]. The densities of the rest of the fibres used in this investigation were determined under

dry conditions at 20°C using a density gradient tube.

It is apparent from the results presented here, and from the work of other research workers discussed in the literature review that limited information obtained from dynamic measurements alone, is quite inadequate for a detailed interpretation of the observed effects at a molecular level. In the limited time available for a research project of the type presented in this thesis, one cannot be too ambitious to plan elaborate experiments to obtain a fuller understanding of the observed phenomenon in dynamic experiments. A compromise has to be sought and it is believed that the results presented in this thesis give a first hand information on the behaviour of textile fibres and fibres from tyre cords to dynamic stresses and strains under various conditions of temperature and/or humidity. It will be noticed from the literature review that very little similar information is available on fibres, although much useful information is available from the work of Ward et al and Woodward et al on rod like polymers. The discussion in this chapter will be divided into four sections dealing with;

(1) Protein fibres

(2) Cellulosic and regenerated cellulosic fibres

(3) Modified regenerated cellulosic fibres

(4) Synthetic fibres

and the results will be discussed in comparision with the information available to date from the work reported by other research workers.

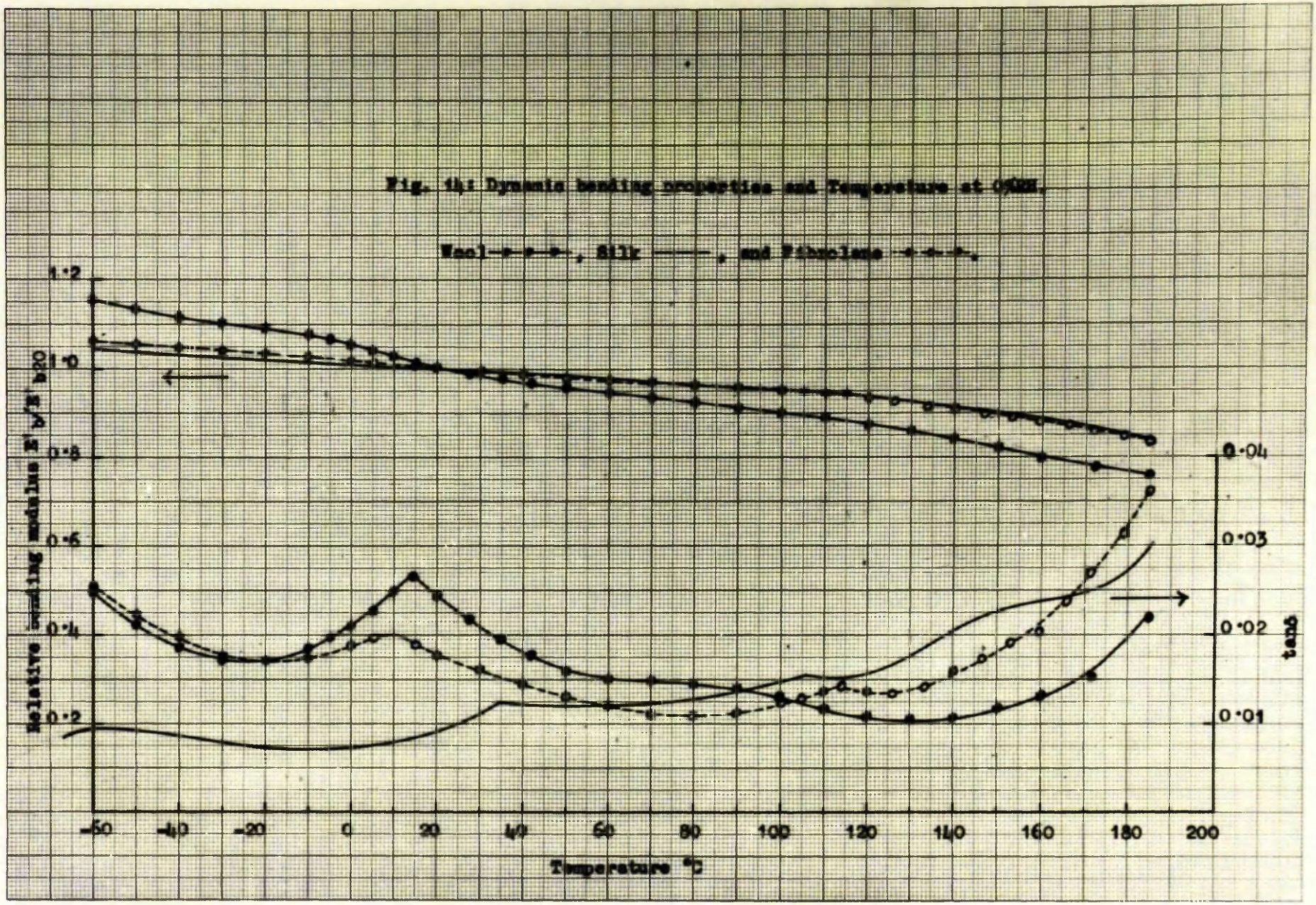
Fig. 14: Dynamic bending properties and Temperature at 0%RH.
Wool -•-•-•-, Silk ——, and Fibroïne -•-•-•-.
Relative moduli E'/E' 20
1·2
1·0
0·8
0·6
0·4
0·2
0·04
0·03
0·02
0·01
tan δ
-50
-40
-20
0
20
40
60
80
100
120
140
160
180
200
Temperature °C

(i) Protein fibres - Wool : Silk : and Fibrolane.

Fig. 14 indicates graphically the effect of temperature in the range -60°C to + 190°C on the relative bending modulus and loss tangent of dry wool, silk and Fibrolane fibres in vacuo. Tables 1, 11 and 111 show some of these findings tabulated.

All the three protein fibres in the range of temperature investigated show multiple transitions e.g. for wool a shoulder around +90°C and a distinct maximum in the loss tangent curve at about + 14°C: for silk a shoulder around +150°C, and three small loss tangent peaks at about 106°C, 35°C and -60°C; and for Fibrolane a small loss tangent peak at about 114°C and a distinct loss tangent peak around 10°C. The rising loss tangent curve for wool and Fibrolane from -20° to -60°C does perhaps indicate a loss maximum below the range of temperature investigated in these experiments.

The relative bending modulus curves for Fibrolane and silk over the range of temperature investigated are similar and seem less sensitive compared with the multiple transitions exhibited on the loss tangent curves. The relative bending modulus curve for wool, however, is different from that of silk and Fibrolane. The change in modulus above and below 20°C is much steeper for wool and also there is evidence of a sharp fall in modulus from -10° to 20°C, which can be associated with the loss peak around 14°C.

Consistent with the high degree of crystallinity (about 80 %) reported for silk[88] the value of $\epsilon' E'_{b20}$ for silk is found to be 10.8. 10^{10} dynes/cm^2, whereas for wool and Fibrolane the value of $\epsilon' E'_{b20}$ is found to be 5.3 . 10^{10} dynes/cm^2.

In general, it may be said that inspite of the structural complexity of wool with a helical structure for α- Keratin[89] with twenty or more amino acids; the silk with a comparatively simpler chemical constitution than wool and with fully extended poly peptide chains which do not assume coiled configuration, although in crystalline regions may lie in closely packed pleated sheets[90], and Fibrolane with a simpler chemical constitution than wool and silk, and consisting of β crystallites and comparatively random amorphous domain[91], all the three protein fibres investigated show similar multiple transition behaviour. The transition temperatures for wool and Fibrolane lie closer together, whereas, in the highly crystalline silk the transition temperatures seems to occur at higher temperatures.

At this stage it may be sufficient to say, that the high temperature transitions observed in the three protein fibres are probably due to the freeing of larger segments in the side groups and the low temperature transitions may be due to motion of smaller segments in the side groups and/or motion of segments in the main chains of the polymer.

It may be useful to note from Tables 1 and 11 the consistent nature

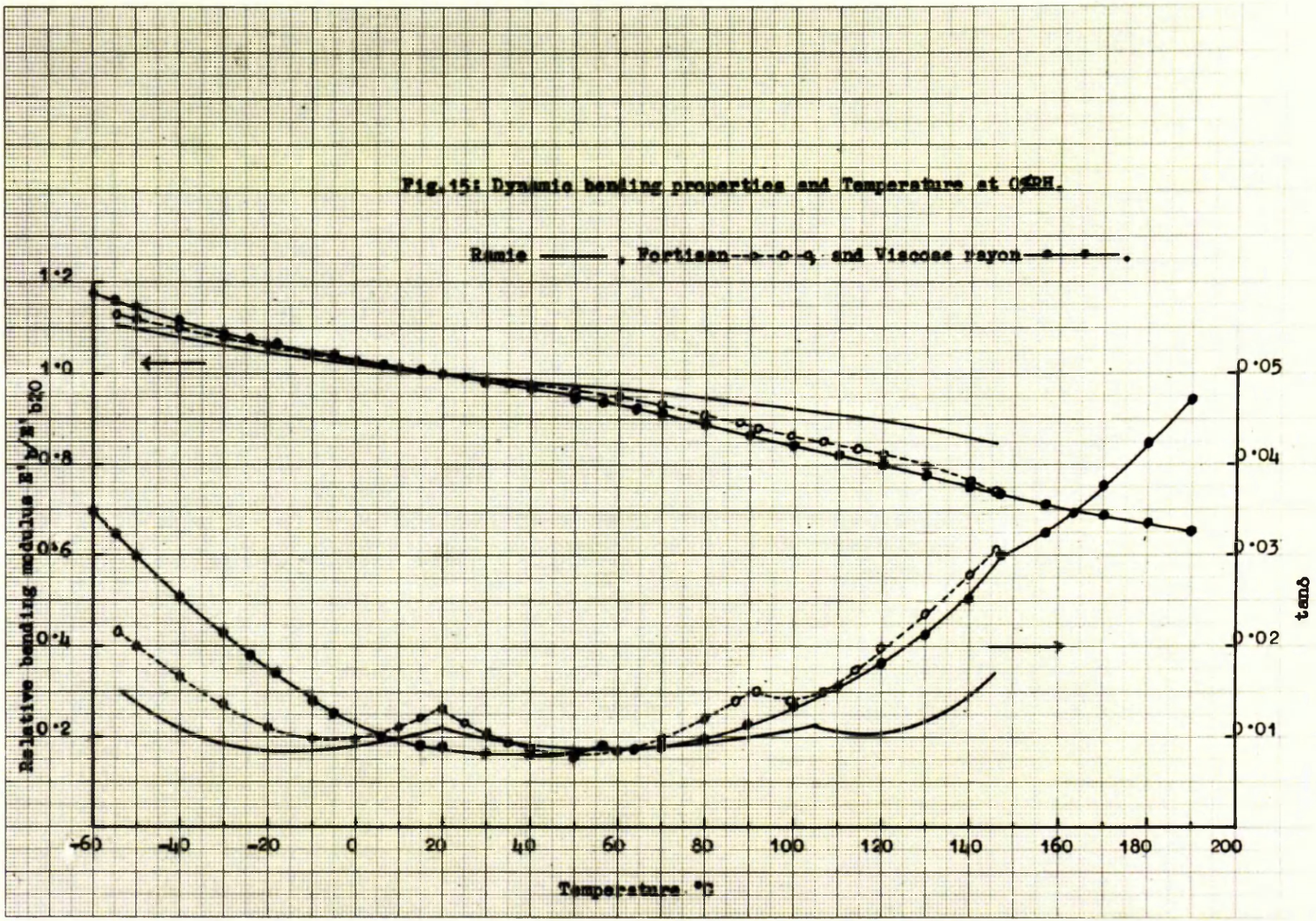
Fig. 15: Dynamic bending properties and Temperature at 0% RH.
Ramie ——— , Fortisan --▸--o--◂ and Viscose rayon —•—•—
Relative bending modulus E'/E'20
tanδ
1·2
1·0
0·8
0·6
0·4
0·2
0·05
0·04
0·03
0·02
0·01
-60
-40
-20
0
20
40
60
80
100
120
140
160
180
200
Temperature °C

of these transition temperatures exhibited in loss tangent values even in natural fibres like wool and silk.

(ii) Cellusosic and regenerated cellulosic fibres.

Ramie, Fortisan and Viscose.

In Fig.15, the effect of temperature in the range -60° to 190°C on the relative bending modulus and loss tangent of dry ramie, Fortisan and viscose rayon fibres in vacuo are represented graphically. Some of the data of individual runs have also been tabulated in Tables IV, V and VI respectively.

The cellulosic fibre ramie and the regenerated cellulosic fibres Fortisan and viscose rayon show two small loss peaks in the range of temperature investigated, e.g. for ramie a peak around 105°C and another at 20°C: for Fortisan around 92° and at 20°; for viscose rayon however, one around 148°C and another around 58°C.

The high value of bending modulus($\epsilon' E'_{b\ 20}$) for ramie and Fortisan e.g. 24 to 79 . 10^{10} dynes/cm^2 for ramie and 52 . 10^{10} dynes/cm^2 for Fortisan, reflect the fact that these materials are stiff and have a high degree of crystallinity. For ramie and Fortisan the reported values of degree of crystallinity are 70% and 50% respectively determined by the x-ray method [92] and 95% and 83% respectively determined by the acid hydrolysis method[93]. For the textile viscose rayon, however, the value of $\epsilon' E'_{b\ 20}$ = 9.3 . 10^{10} dynes/cm^2 and the reported values of degree of

crystallinity are 30% and 68% by x-ray[92] and acid Hydrolysis[93] methods, respectively.

From Fig.15 it will be noticed that the relative bending modulus is more temperature dependent for Fortisan and viscose rayon than for ramie.

Meredith and Hsu[40] report two weak loss peaks for viscose rayon at 90°C and at -20°C. They attribute the high temperature peak to breaking of hydrogen bonds and the motion is thought to be impeded by the stiff nature and bulky structure of cellulose chain molecules. Tokita[56] however, reports a dispersion at 80°C for dry viscose rayon monofilaments and this dispersion was found to shift to a lower temperature when the moisture content was increased showing thereby that OH groups are associated with this phenomenon. Dunell and Price[55] have observed a well-defined maximum in energy loss around -55°C. By taking the maximum slope of the log E' or log E'' v s. T^{-1} curve (where E' and E'' are the dynamic storage and loss modulus respectively and T is the absolute temperature) in the temperature region -20° and -60°C for viscose rayon, Dunell and Price have estimated the values of the averaged activation energy for the relaxation processes involved applying the relation:

$$E_{act} = \frac{2.3R}{2} \times \frac{d \log E'}{d(1/T)}$$

or

$$E_{act} = 2.3R \frac{d \log \eta'}{d (1/T)}$$

Values estimated in this way are reported to be 400 cal/mole and 1100

cal/mole, respectively. These activation energy values are low compared with Mark's estimate of the molar cohesion energy of cellulose per 5 Å. of chain of 6200 cal/mole based on the assumption of a cordination number of four for each chain[94]. This leads them to suggest that the flow, or relaxation, unit responsible for the transition at -55°C in viscose rayon, is either a single glucose residue in an amorphous region where the effective co-ordination number is much less than four, or a $-CH_2OH$ side chain whose flow motion does not involve the breaking of a hydrogen bond.

In a recent letter Wahba[95] reports to have observed a transition at about 24°C for dry as well as wet cellophane in his studies on variation of refractive indices with temperature.

From the results of ramie, Fortisan and viscose rayon, presented in this thesis it is, as yet, difficult to conclude why low stretch viscose rayon which is known to have a lower optical orientation factor (0.54) compared with that of Fortisan (high stretch viscose rayon 0.88) or of ramie (0.97) should exhibit transition at higher temperatures. Crystallites which may probably vary in size in differently stretched rayons[96] and their restraint to segmental motions in the remaining non-crystalline regions needs to be studied in detail for a fuller understanding of the different transition behaviour in Fortisan and viscose rayon.

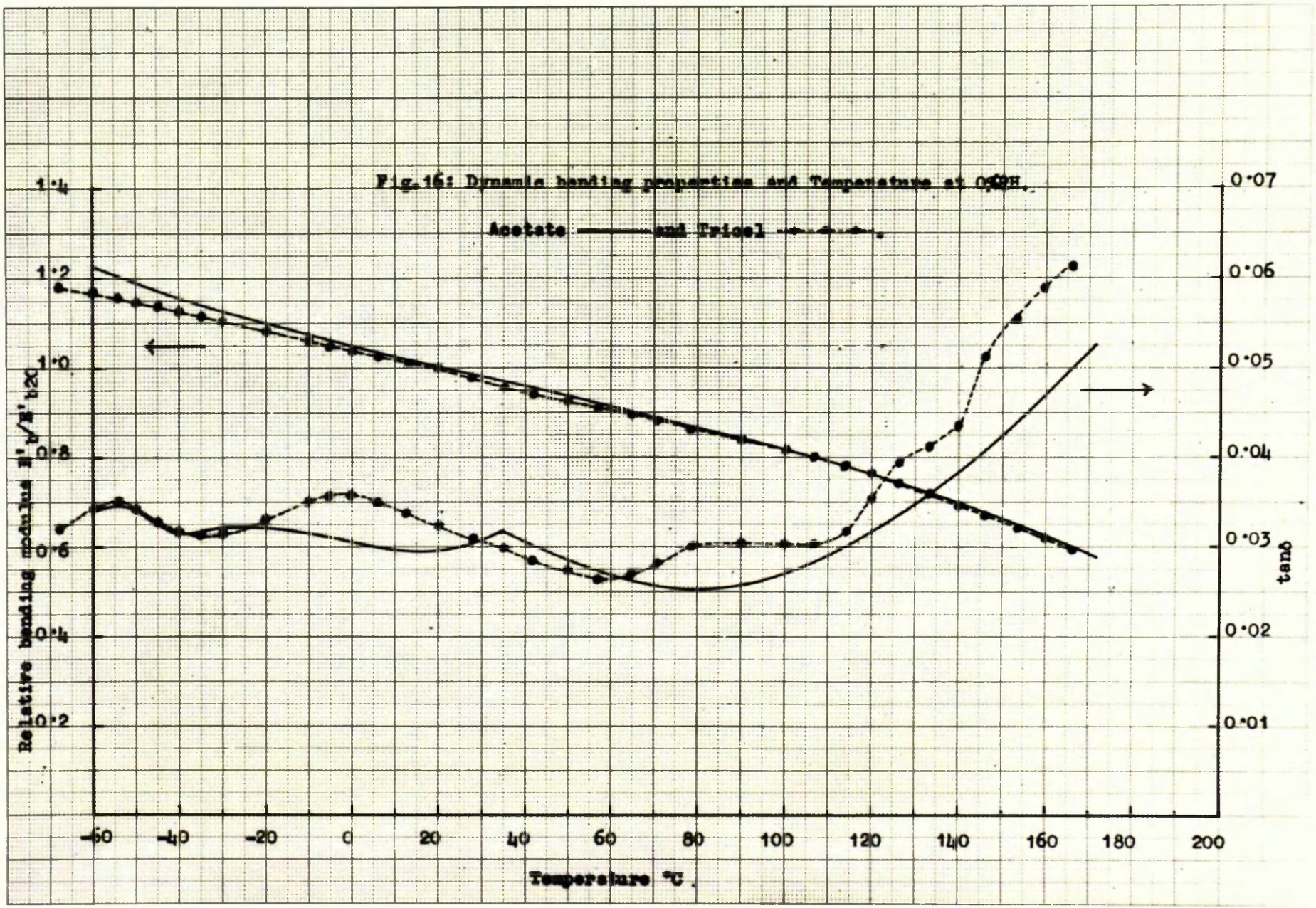
Fig. 16: Dynamic bending properties and Temperature at 0%RH.
Acetate ——— and Tricel - - - - -.
Relative bending modulus E'b/E'b20
tanδ
Temperature °C.
1·4
1·2
1·0
0·8
0·6
0·4
0·2
0·07
0·06
0·05
0·04
0·03
0·02
0·01
-60
-40
-20
0
20
40
60
80
100
120
140
160
180
200

(iii) Modified regenerated cellulosic fibres.

Acetate and Tricel.

The effect of temperature in the range -60° to +170°C on the relative bending modulus and loss tangent of dry cellulose acetate and triacetate in vacuo are graphically represented in Fig.16. Tables V11 and V111 show the data for individual runs.

It is apparent from Fig.16, that secondary acetate and Tricel exhibit multiple transition phenomenon characterised by, (1) two small loss peaks one around 35°C and another around -55°C and in addition a shoulder around -20°C for secondary acetate, and (2) two distinct loss peaks around -53°C and 0°C and in addition three shoulders around 80°C, 115°C and 150°C for Tricel.

The relative bending modulus curves for the two fibres over the temperative range are essentially similar. Once again the smooth featureless drop in the bending modulus with temperature probably supports the view that the dissipation factor is more sensitive to molecular motion than the dynamic modulus.

The value of bending modulus at 20°C $\epsilon' E'_{b20}$ for acetate ($7.3.10^{10}$ dyn./cm^2) is slightly higher than the value for Tricel (4.8 to $6.9.10^{10}$ dyn./cm^2).

From dilatometric studies on cellulose acetate and triacetate Mandelkern and Flory[97] report transitions at 60°C and 120°C for the former

and 30°C and 105°C for the latter. In similar experiments, Nakamura[58] also reports to have observed transitions corresponding to those reported by Mandelkern and Flory[97]. From dilatometric measurements Russel and Van Kerpel[57], however, observed transitions at 55°C and 115°C in secondary acetate and at 40°C, 120°C and 155°C in cellulose triacetate.

From dynamic experiments at audio frequencies Nakamura[58] observed a damping peak at 120°C for cellulose acetate and at 60°C and 180°C for cellulose triacetate, while Russel and Van Kerpel[57] observed damping peaks at -38°C, 130°C (shoulder) and 195°C for acetate and at -48°C, 100°C (shoulder) and 175°C for cellulose triacetate. Although there is a considerable spread in the results reported by various workers, they generally believe that the low temperature transitions in the -40° to -60°C region are associated with the mobility of acetate groups, while the high temperature transitions in the 175° to 195°C region are associated with the movement of groups of atoms in the anhydroglucose chain.

Recently, from dilatometric measurements Daane[98] et al reported to have observed four glass transitions in cellulose 2.5 acetate below 130°C, at about 15°, 50°, 90°, and 114°C with probable errors of about $\pm$ 3°C. They believe that the presence of multiple glass transitions suggest a variety of molecular mechanisms. The lowest transition temperature would be that at which the number of configurations approaches a minimum value. As temperature increases through succeeding transition ranges,

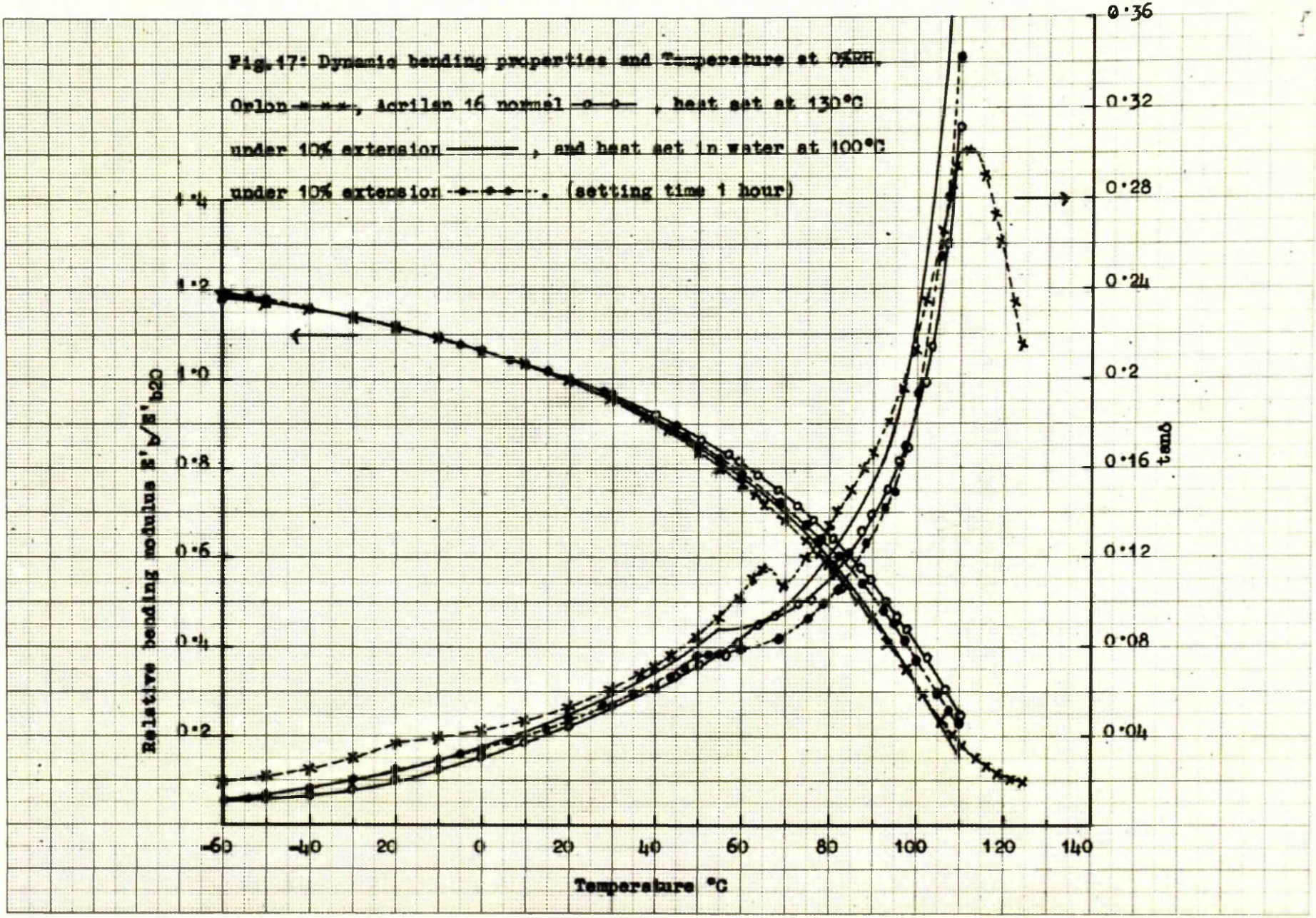
Fig.17: Dynamic bending properties and Temperature at 0%RH.
Orlon -x-x-x-, Acrilan 16 normal -o-o-, heat set at 130°C
under 10% extension ———, and heat set in water at 100°C
under 10% extension -•-•-•-. (setting time 1 hour)
Relative bending modulus E'b/E'b20
tanδ
Temperature °C
1·4
1·2
1·0
0·8
0·6
0·4
0·2
0·36
0·32
0·28
0·24
0·2
0·16
0·12
0·08
0·04
-60
-40
20
0
20
40
60
80
100
120
140

the number of configurations and the free volume increases in a co-operative manner. Further they add, consideration of molecular structure shows that one could ascribe one transition to main chain motions and other transitions to the motion of the acetate groups (separately or co-operatively).

The above mentioned arguments put forward by several research workers to the observed multiple transition phenomenon in secondary and tertiary acetate rayons, however logical they may be, are purely speculative and by no means conclusive. In such polycrystalline material, multiple transitions probably represent the varying degrees of order between the non-crystalline phase and the crystalline phase. From the observed dynamic bending properties of acetate and Tricel fibres in the present investigation, one may only say that the presence of a greater number of bulky acetyl groups in the latter apparently shifts the peaks in the loss tangent curve to lower temperatures and yet both fibres exhibit the same modulus temperature relationship in the range investigated.

iv. Polyacrylonitrile fibres.

Acrilan 16 normal and heat set, and Orlon.

In Fig.17 the effect of temperature in the range -70° to 120°C, on the relative bending modulus and loss tangent of dry fibres of Orlon, Acrilan 16, Acrilan 16 set in boiling water at 100°C for 1 hour under 10% extension and Acrilan 16 heat set at 130°C for 1 hour under 10% extension,

in vacuo have been graphically illustrated. As before, Tables IX show the data for individual runs.

It is apparent that Orlon exhibits a distinct main transition around 112°C (Fig.17) and a minor one around 65°C. There is also some evidence of a shoulder around -20°C. Unlike natural fibres and rayons, in synthetic fibres there is a sharp drop in the modulus associated with glass transition temperature. In Orlon it will be noticed that in raising the temperature from 20° to 120°C the modulus drops from 10^{10} to 10^{9} dynes/cm^2. Therefore, the loss peak at 112°C for Orlon can be ascribed to glass transition peak involving the motion of large segments. The two resonance frequencies at 20°C for the two principal axes of vibration for Orlon are given in Table IX_D. The value of ϵ 'E'$_{b20}$ calculated using the expression (12) and the resonance frequencies is thus found to vary between 12.4. 10^{10} and 22.16. 10^{10} dynes/cm^2.

Meredith and Hsu[40] observed similar behaviour in Orlon and report a main and a minor loss tangent peak, at 120°C and 75°C respectively. They ascribe the loss tangent peak at 120°C to motion of hydrogen bonds which may be expected between the CN groups of one chain molecule, and the CH group of an adjacent molecule. The minor loss tangent peak however, is thought to be due to the motion of segments involving rotation of main chain molecules in the non-crystalline region which are not hydrogen bonded.

This interpretation is not totally convincing because of the poor x-ray diffraction pattern, the crystal structure of poly acrylonitrile has not yet been definitely determined. There seems to be differing opinion among research workers in the field of x-ray and infra-red studies regarding the determination of the structure of poly acrylonitrile [99,100] [101,102,103,104]. Tadokoro[104] et al, from infra-red spectral studies on poly acrylonitrile and dauterated poly acrylonitrile conclusively exclude the possibility of hydrogen bonding between CN and CH groups. Under these circumstances, the above interpretation of the observed mechanical dispersions in acrylonitrile fibres at a molecular level is open to criticism.

It is interesting to note the dynamic mechanical behaviour of Acrilan 16 (Fig.17). Acrilan 16 is reported[105] to be produced from a polymer composed principally of acrylonitrile. A small amount of other substances (not reported) is supposed to be present in the polymer which contributes to the good processibility and dyeability of the fibre. Acrilan 16 does not melt, but is reported to decompose before melting. This probably is the reason why it has not been possible to establish a major loss tangent peak around 90° to $110^{\circ}C$, even though the tan δ continues to rise sharply at temperatures above $100^{\circ}C$. In dynamic bending experiments the Acrilan 16 fibres were getting bent above $110^{\circ}C$ and hence, it was not possible to resolve the loss tangent values above this temperature.

Similar to Orlon, although not a minor peak, at least a shoulder is visible for Acrilan 16 around 65°C. Apparently, there is no associated inflection in the relative bending modulus curve around this temperature. This is probably due to the fact that the drop in modulus with temperature (above room temperature) is very high for the acrylonitrile fibres and any small inflection in modulus curve associated with minor segmental motions is not noticeable.

Heat setting of Acrilan 16 in boiling water at 100°C or at 130°C in an oven under 10% extension does seem to have some effect on the dynamic mechanical properties. A slight shift in both loss tangent and relative bending modulus curves towards lower temperature is noticeable in both the heat treatments.

This effect apparently is more for the dry heat set fibre than for the fibre set in boiling water. However, the shoulder at 65°C for normal Acrilan 16 shifts down to 55°C for the dry heat set fibre compared with the shift to 50°C for the fibre set in boiling water. It may be useful to mention that stretching Acrilan 16 to 10% and heat setting it for 1 hour in the oven at 150°C instead of 130°C results in complete relaxation of the stress in the fibres which acquire crimp, and hence develop bulk. Heat setting Acrilan 16 fibres in general seems to decrease the dynamic bending modulus at 20°C (Table IX).

From the load extension curves and physical density values indicated

Fig.18: Dynamic bending properties and Temperature at 0%RH.

Polypropylene types A ———, B -•-•-•-, and C -o-o-o- .

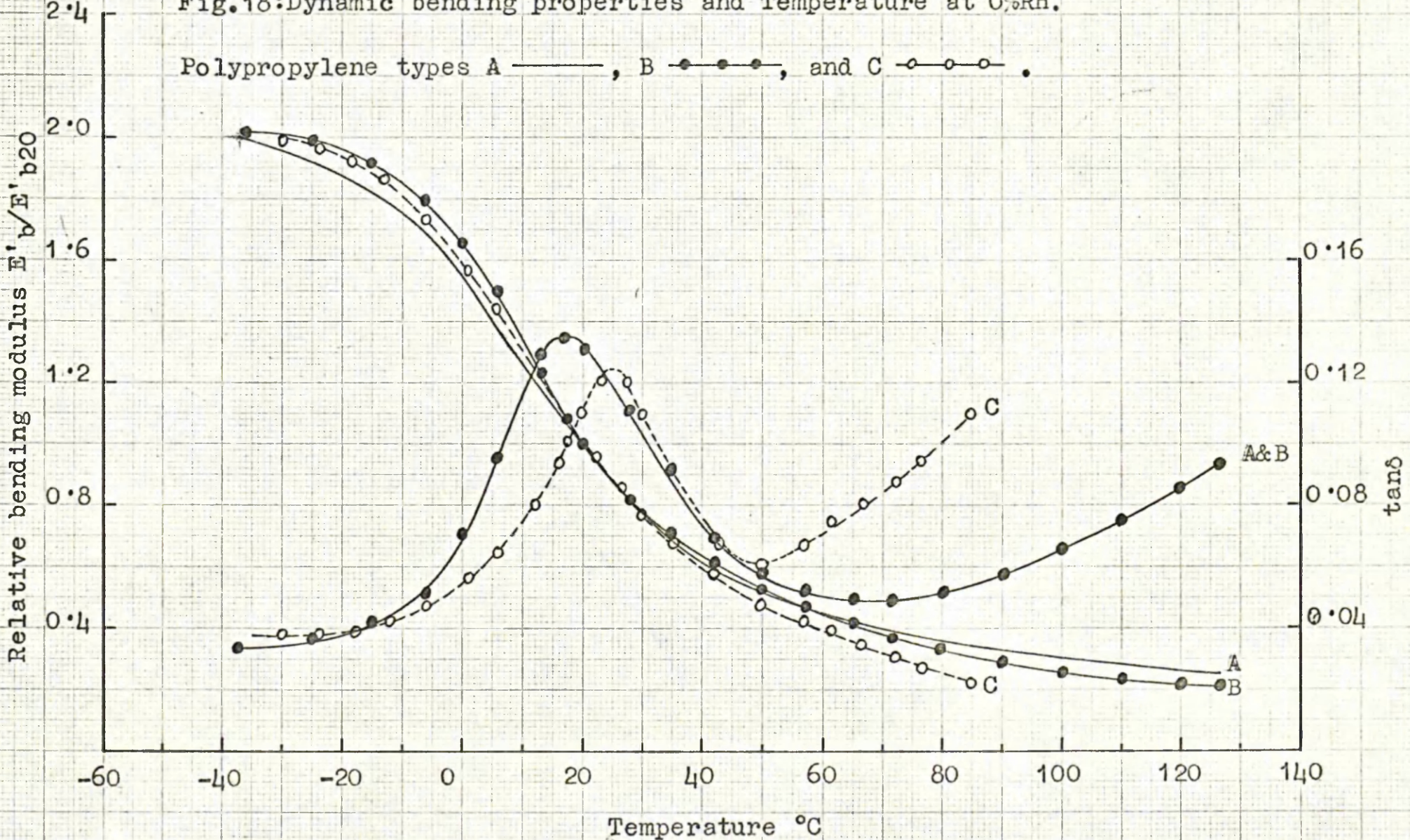

in Fig.40 and Table XVII respectively, it will be seen that the initial modulus (also Table XVIII), the stress at yield point and the density values for heat set Acrilan 16 are in general higher compared with normal Acrilan 16. The density value of Acrilan 16 heat set at 150°C under 10% extension is lower than that set at the same temperature under zero tension. The breaking load and the breaking extension of heat set Acrilan 16 seem dependent on the condition of heat setting.

The effect of heat setting of Acrilan 16 on the dynamic bending properties as observed in the present investigations are contrary to which is expected. This effect cannot, however, be attributed to possible degradation due to heat treatment since the observed changes in tensile behaviour do not exhibit this effect.

(v) Polyolefin fibres.

Polypropylene types A, B and C.

The effect of temperature in the range -40°C to 130°C on the relative bending modulus and loss tangent of three dry polypropylene fibres A,B and C in vacuo have been illustrated graphically in Fig.18 Table X shows the data for individual runs. These fibres were conditioned under a small load of 2 mg/denier for 2 hours in vacuo over P_2O_5 at 140°C.

From the density and birefringence values shown in Table XVII it may be said that polypropylene A and B have apparently the same % crystallinity and orientation, where as polypropylene C has a slightly lower

crystallinity and higher orientation.

This may also be seen from the dynamic bending results: in the range of temperature covered only one peak in the loss tangent curve at about 17°C for polypropylene A and B and 25°C for polypropylene C with an associated rapid decrease in the relative bending modulus is observed. The value of $\epsilon' E'_{b}20$ at 20°C for polypropylene A 3.9. 10^{10} dyn/cm^2 is, however, lower than that observed for polypropylene B, 4.9 .10^{10} dyn/cm^2. Below room temperature upto about -40°C dynamic bending modulus for sample B remains higher than for sample A. The value of dynamic bending modulus $\epsilon' E'_{b20}$ at 20°C for polypropylene C is 5.48 .10^{10} dynes/cm^2. The observed differences in the dynamic mechanical behaviour of the three samples may be due to differences in tacticities, which however, cannot be concluded from the above results.

The dynamic mechanical properties of amorphous and crystalline polypropylene over the range -196°C and 162°C range at 100-2200 cps have been investigated by Sauer et al[39]. They report to have observed at least three transitions located at -33°C, 27°C and 162°C for a sample with room temperature crystallinity of 75-80%. Other dynamic mechanical studies of this polymer have also been reported by Baccareda and Butta[106], Wilbourn[10], Muus, McCrum and McGrew[107], Stichter and Mandell[108] and McDonald and Ward[109].

Nuclear magnetic resonance measurements have been extensively made

on polypropylene by several workers.[108,109,110,111,112,113,39,1]. There appears to be general agreement with regard to the general features of the nuclear magnetic resonance spectra. The curves all show two steep portions, one around -173°C and the other around 27°C where a composite signal begins to appear. It has been concluded that there is good correlation between the temperature of the dynamic mechanical transition and that of the line narrowing in the nuclear magnetic resonance experiments. The glass transition peak around 27°C has been generally accepted as due to segmental motions in the amorphous regions involving long sections of chains. The rise in the damping and the sharp fall in modulus near 162°C for the crystalline polypropylene has been attributed to the increase in chain mobility accompanying the processes of crystalline melting.

The dynamic mechanical data presented here suggest that in the temperature range covered there is good agreement in the location of the glass transition peak and the rising damping curve thereafter compared with those reported by other workers. The differences in behaviour observed for samples A,B and C as mentioned earlier are probably due to differences in tacticity between samples and this however, is not conclusive from the data presented here.

(xi) Polyamide fibres.

Nylon 66 types 200, 300, 600, A,B,C, and BH_1.

The dynamic bending results of several types of nylon 66 fibres and one of rayon fibre taken from tyre cord yarns and one of nylon 66 fibre from type 200 textile yarn are indicated in Figs.19 and 20. All nylon 66 fibres were conditioned at 170°C for 10 minutes in vacuo over P_2O_5 and under a small load of 2 mg/denier. The rayon fibres, however, were also conditioned under similar conditions but at 200°C. The results of individual runs are indicated in Tables XI and XII. nylon 66 fibres although they are considered to be circular, are not quite so, as exhibited by the two resonance frequency values at 20°C corresponding to two principal axes of bending (not mutually perpendicular) given in the tables. The two resonance frequencies, if too close together interferewith the determination of the band width, especially, at the transition region where the band width is large. Therefore, fibres before heat conditioning were carefully selected and tested at room temperature for the two frequencies, to choose only those whose differences in resonance frequencies in the two principal planes of bending are either sufficiently large or nil. This difficulty, of course does not arise in rayon fibres which are decidedly non-circular in cross-section, and the difference between the two resonance frequencies of the two principal planes of bending is invariably large (Table XII_E).

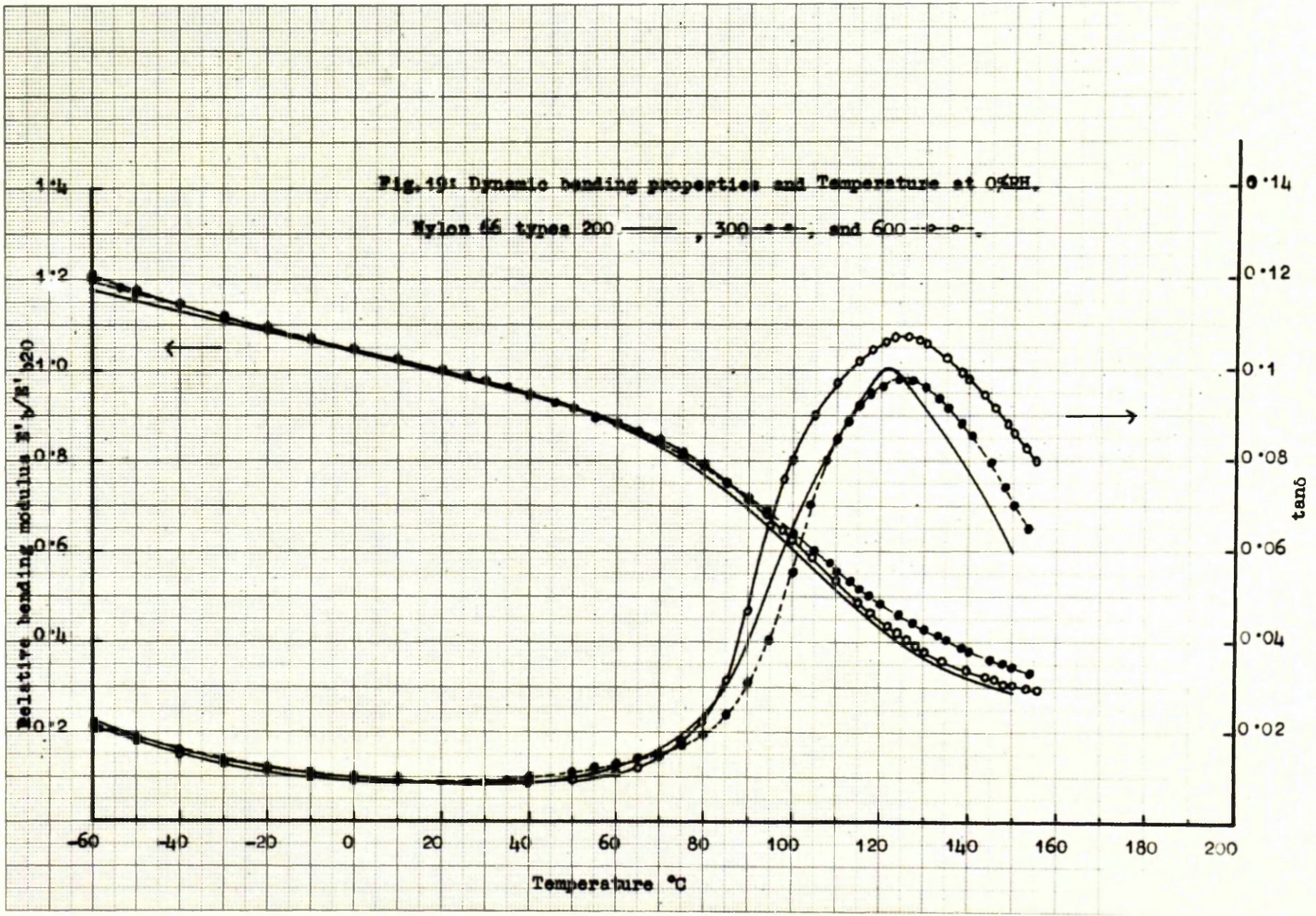
Fig.19: Dynamic bending properties and Temperature at 0%RH.
Nylon 66 types 200 ——— , 300 — • — , and 600 — ▷ — ○ —.
Relative bending modulus E'b/E'b20
tanδ
Temperature °C
1·4
1·2
1·0
0·8
0·6
0·4
0·2
0·14
0·12
0·1
0·08
0·06
0·04
0·02
-60
-40
-20
0
20
40
60
80
100
120
140
160
180
200

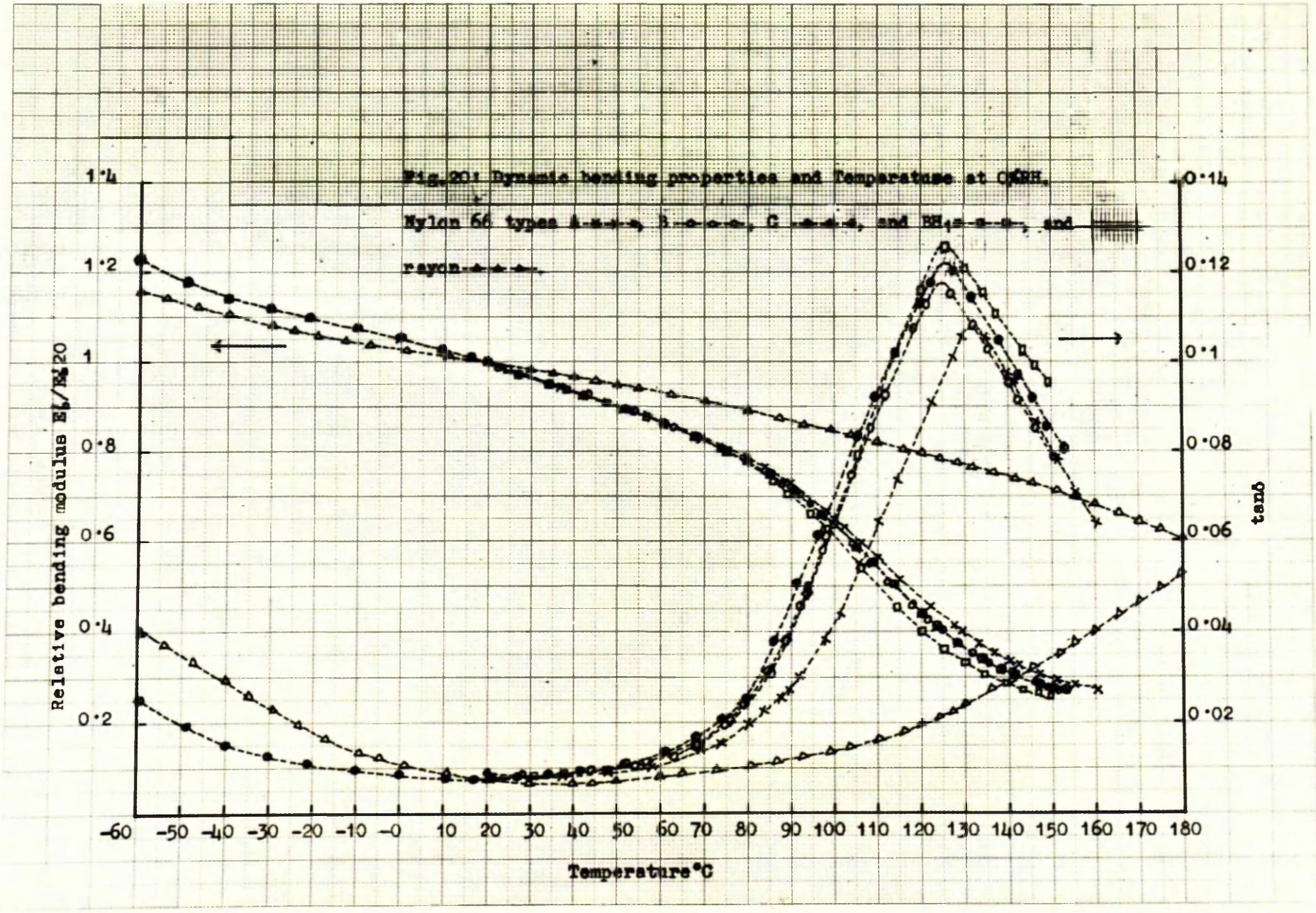
Fig. 20: Dynamic bending properties and Temperature at 0%RH,
Nylon 66 types A -x-x-x-, B -o-o-o-, C -•-•-•-, and BH₁ -□-□-□-, and
rayon -▲-▲-▲-.
Relative bending modulus E/E120
tanδ
1·4
1·2
1
0·8
0·6
0·4
0·2
0·14
0·12
0·1
0·08
0·06
0·04
0·02
-60 -50 -40 -30 -20 -10 -0 10 20 30 40 50 60 70 80 90 100 110 120 130 140 150 160 170 180
Temperature °C

From the tanδ and the relative bending modulus vs. temperature plots in Figs.19 and 20, it will be noticed for the several types of dry nylon 66 fibres in the range of temperature -70°C to +160°C investigated, only one transition around 120° to 135°C is observed. This observation is in agreement with the observations of Woodward[29] et al. However, the glass, transition temperature for nylon 66 rod like polyamide specimen reported by Woodward et al is only in the region of 80°C compared with that reported in this work for fibres 120° to 135°C. This difference is obviously due to the high orientation and probably also high degree of crystallinity of nylon 66 fibres. This is indicated by the birefringence and density values determined for some of the samples (Table XVII).

Referring to Fig.19, the difference in the dynamic mechanical behaviour of fibres from textile yarn nylon 66 type 200 and from tyre cords nylon 66 types 300 and 600 is clearly seen. The loss peaks for the fibres from tyre cords are dispersed over a much larger range of temperature with the loss peak occuring around 126°C compared with the loss peak at 122°C dispersed over a much smaller range of temperature for the fibre from textile yarn. Associated with the loss peak the sharp fall in modulus occurs at a lower temperature for nylon 66 type 200 than for the other two fibres. The value of relative bending modulus at 20°C for nylon 66 types 200 is also lower than for nylon 66

types 300 and 600. (Tables XI). Although no additional information than what has already been given is available for these three types nylon 66 fibres, it may be justifiable to presume that the differences in behaviour in dynamic bending properties, observed for these fibres are not only due to the difference in the crystallinity and orientation, between tyre cord fibres and textile fibres but also due to difference in the molecular weight of the three samples. A higher molecular weight material with longer polymer chains would cause more hinderance to segmental motion than a lower molecular weight material. Such a hinderance would be depicted by the broad dispersed nature of the mechanical damping peak.

The mechanical damping behaviour of fibres from tyre cords of nylon 66 types A, B, C and BH_1 (Fig.20) over the glass transition range are different compared with those of nylon 66 types 300 and 600. The former exhibit much sharper transition peaks, types B, C, and BH_1 around 125°C and type A at about 132°C. Inspite of this difference in the damping behaviour the drop in bending modulus with increasing temperature is similar between type A and type 600. For type 300 the drop in the bending modulus occurs at a slightly higher temperature than rest of the fibres, whereas for types B, C, and BH_1 the drop in the bending modulus occurs at a slightly lower temperature than for types A and 600. The modulus temperature relationship is one of the important factors in tyre cords. It may be readily seen by comparing the modulus temperature

relationship of various types of nylon 66 with rayon, why 'flat spots' occur in tyres reinforced with nylon cords and not with rayon cords. Comparing the optical birefringence and physical density values of nylon 66 types A, B, C, and BH_1 (Table XVII) with the dynamic mechanical data there appears to be a good correlation between the degree of crystallinity and/or orientation with the glass transition peak observed for these fibres. Nylon 66 type A, which has a high density value of 1.15 $g./cm^3$ compared with other types nylon 66 fibres, as expected, shows a different mechanical behaviour, also Fig.43. It has high initial modulus and breaking strength but a low extension (Table XVIII). However, good tyre cord yarns should possess high strength, combined with high breaking extensibility and rather low moduli of elasticity; the ability to withstand repeated flexing and compression without large reductions in strength and the ability to be deformed without substantial loss of properties in the manufacture of compact cords for rubber-reinforcement. Therefore, higher glass transition temperature, in fibres used in tyre cords is desirable providing the working range of modulus is also shifted to a higher temperature i.e., the sharp drop in modulus associated with the glass transition temperature should occur at a higher temperature. However, when the performance of a tyre cord is considered in general with respect to the end use to which it is put (e.g. Tractor, Aeroplane and car tyres etc)., many desirable properties have to be studies(as mentioned above) of which dynamic mechanical properties is but one.

Fig.21: Dynamic bending properties and Temperature at 0%RH.

Terylene normal —o—o—o—, heat set at 180°C under 200mg. load/denier —•—•—•—, and heat set at 180°C under zero tension —▫—▫—▫—. (setting time 1 hour)

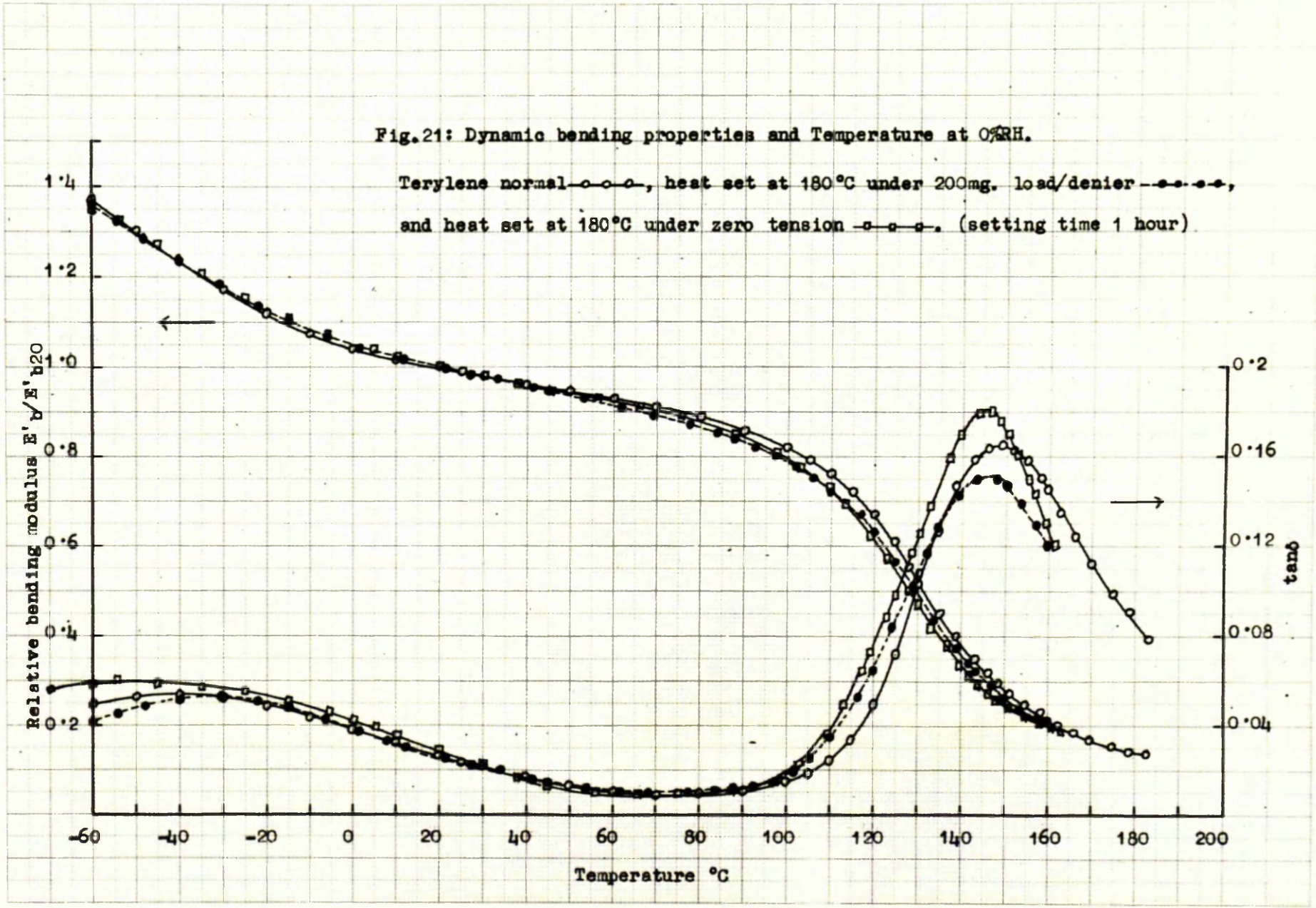

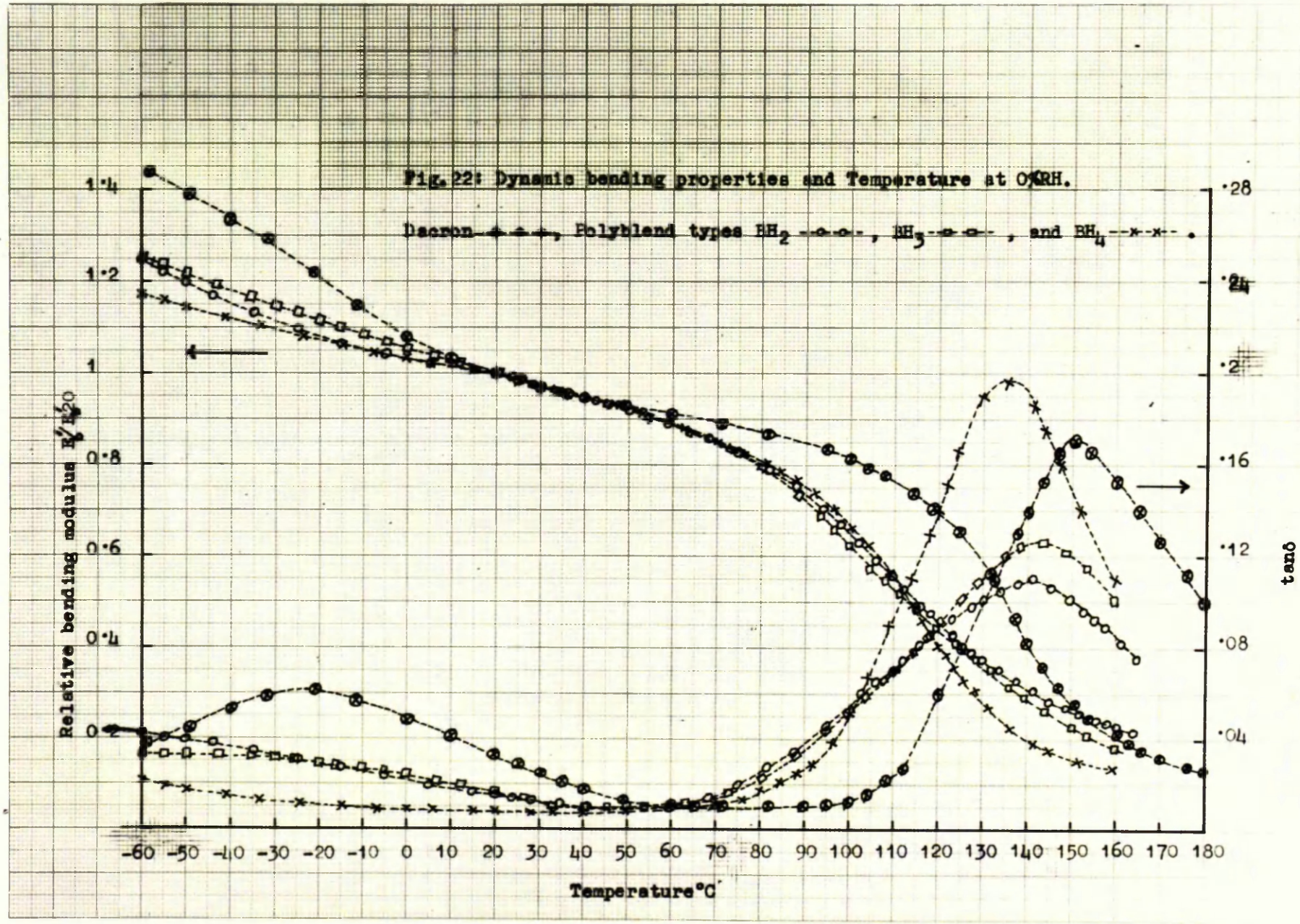
Fig. 22: Dynamic bending properties and Temperature at 0%RH.
Dacron
Polyblend types BH2, BH3, and BH4
Relative bending modulus E'/E'20
tanδ
Temperature°C
1·4
1·2
1
0·8
0·6
0·4
0·2
0
·28
·24
·2
·16
·12
·08
·04
-60 -50 -40 -30 -20 -10 0 10 20 30 40 50 60 70 80 90 100 110 120 130 140 150 160 170 180

(vii) Polyester fibres.

Terylene normal and heat set, and Dacron.

The effect of temperature in the range of -60°C to 180°C on the dynamic bending properties of dry fibres of Terylene normal and heat set, and Dacron are indicated in Fig. 21 and 22. The results of individual runs are indicated in Tables XIII and XIV.

Terylene and Dacron exhibit two mechanical dispersions and associated drop in modulus in the region of 150°C and -20°C to -40°C. These observations are consistent with those reported by other workers which has been reviewed in the literature survey (chapter 11).
However, it is interesting to note that Dacron fibre from tyre cord and Terylene fibre from textile yarn which have optical birefringence values of 0.1854 and 0.1828, respectively and density values 1.383 and 1.373 g/cm^3 (Table XVII) both exhibit similar glass transition peaks at 150°C. But the secondary transition peak for Dacron has a higher value and occurs at a higher temperature (-20°C) compared with that of Terylene (-40°C). The dynamic bending moduli at 20°C for both Dacron and Terylene fibres are $\epsilon' E'_{b20} = 10.8 \cdot 10^{10}$ dyn/cm.

Heat setting Terylene fibres under 200 mg load/denier, and zero load, for 1 hour in the dry oven at 180°C, apparently increases crystallinity as shown by density values 1.393g/cm^3, and as expected the orientation of the fibre heat set under 200 mg load/Denier, increases as shown by the

birefringence values which increase from 0.1828 to 0.209. Whereas in the fibre heat set under zero load disorientation occurs, as shown by the birefringence value which decreases from 0.1828 to 0.173. The glass transition peak for both heat set fibres occurs at about the same temperature 147°C compared with 150°C for the normal Terylene. However, the loss peak value is lower for the fibre heat set under load and is higher for the fibre heat set under zero load compared with the loss peak value of the normal fibre. The secondary dispersion for the fibres heat set under load and zero load occurs at -30°C and -50°C compared with -40°C for normal Terylene. As before, the secondary loss peak value for the fibre heat set under zero load is higher than for normal Terylene but is unaffected for the fibre heat set under load. The dynamic bending modulus at 20°C, for the fibres heat set under load and zero load are $\epsilon'E'_{b20} = 10.86 .10^{10}$ dyn/cm^2 and 8.2 10^{10}dyn/cm^2 respectively.

(viii) Rayon fibre.

The dynamic bending properties of dry Rayon fibre from tyre cords over a range of temperature -60°C to 180°C are represented in Fig. 20. The results are also shown in Table XII_E.

It will be noted that because of the non-circular cross-sectional shape of rayon, two resonance frequencies have been noted at 20°C Table XII_E, corresponding to two principal planes of bending. The values of dynamic bending modulus in the two planes of bending for dry fibres of rayon from tyre cords at 20°C, $\epsilon'E'_{b20}$ range from 26.9 $.10^{10}$ to 36.2 dynes/cm^2

It is interesting to note that no inflections or peaks in the tan δ curve were observed for these fibres as compared with those observed for Fortisan and Viscose rayon (Fig.15). The value of tan δ in the range of temperature investigated is lower for rayon than for Fortisan and viscose rayon. The drop in modulus with increasing the temperature from 20°C to 180°C is considerably smaller than the drop in moduli observed in nylon 66 and Dacron in the same range of temperature.

(ix) Polyblend fibres. Types BH_2, BH_3 and BH_4.

The dynamic bending properties of dry polyblend fibres in the range of -60 to 170°C are graphically represented in Fig.22. The results of individual runs are also indicated in Tables XIV. Since the chemical constituents of these fibres have not yet been made known, the results represented here are only meant as a guide to the dynamic mechanical properties of these newer fibres for tyre cords compared with those of nylon 66, Dacron and rayon. The optical birefringence and density values for these fibres are given in Table XVII. Both samples BH_2 and BH_3 exhibit a distinct glass transition region around 140° to 145°C and loss peak value for BH_2 is slightly lower than that of BH_3, and are comparable with those encountered in nylon 66. However, the loss peak for sample BH_4 occurs around 135°C and the peak value is higher compared with the rest of the fibres from tyre cords.

A low temperature transition for samples BH_2 and BH_3 is apparent

Dynamic tensile properties, static and dynamic strain at 20°C and 65%RH.

NYLON66 SAMPLE A Fig. 23a

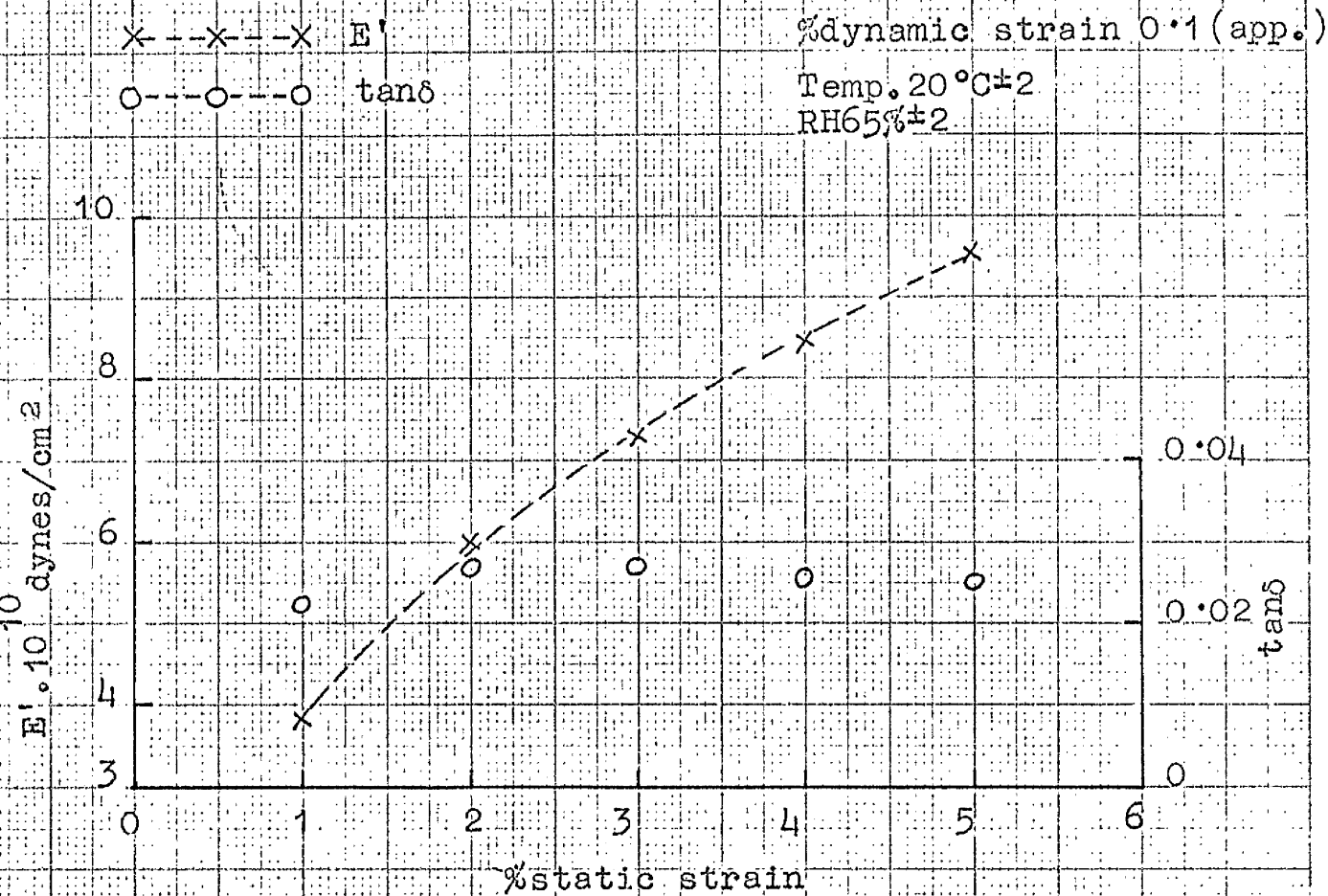

Fig. 23b

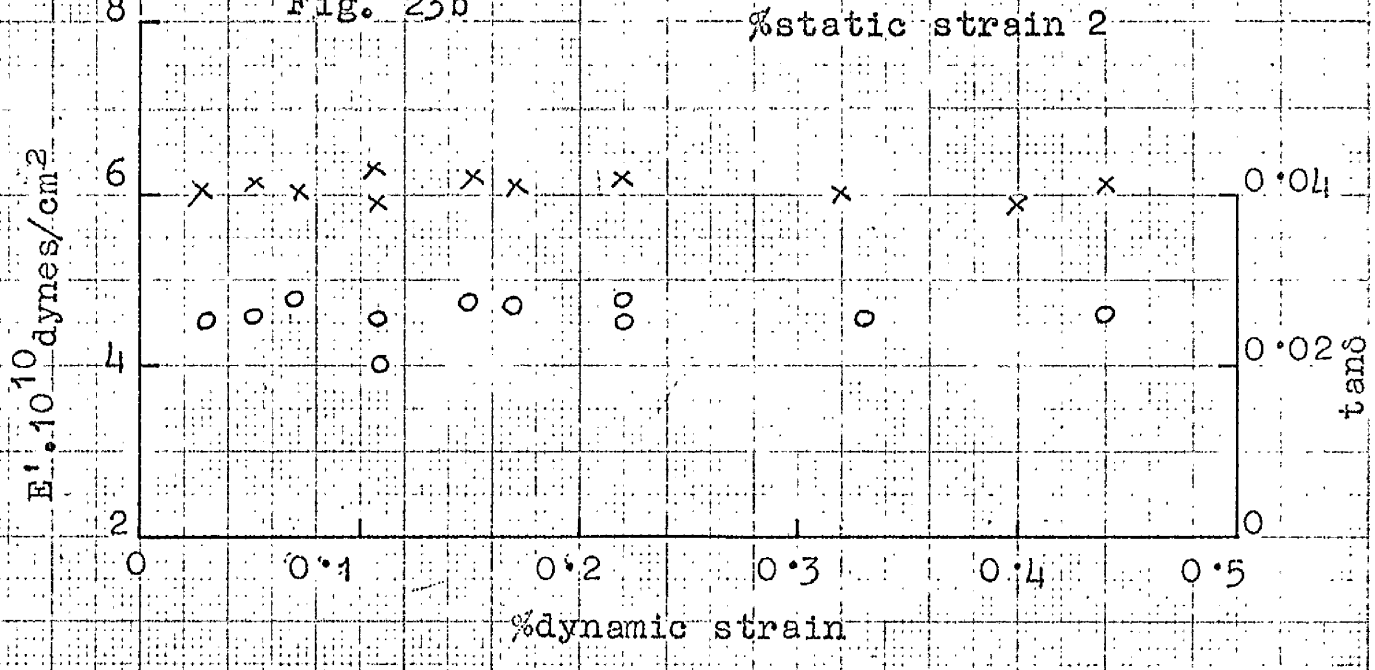

Dynamic tensile properties, static and dynamic strain at 20°C and 65%RH.

DACRON Fig. 24a

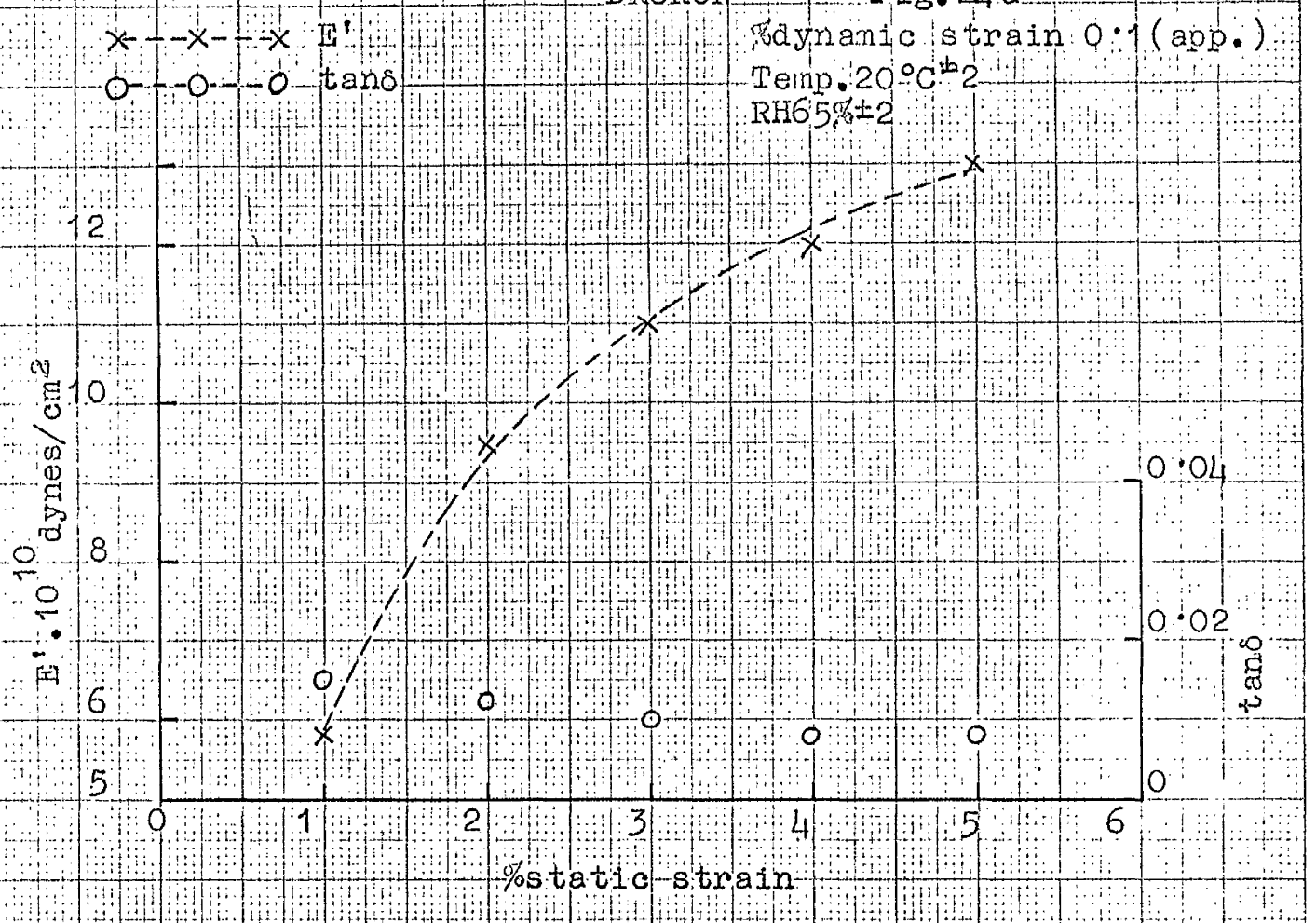

Fig. 24b %static strain 2

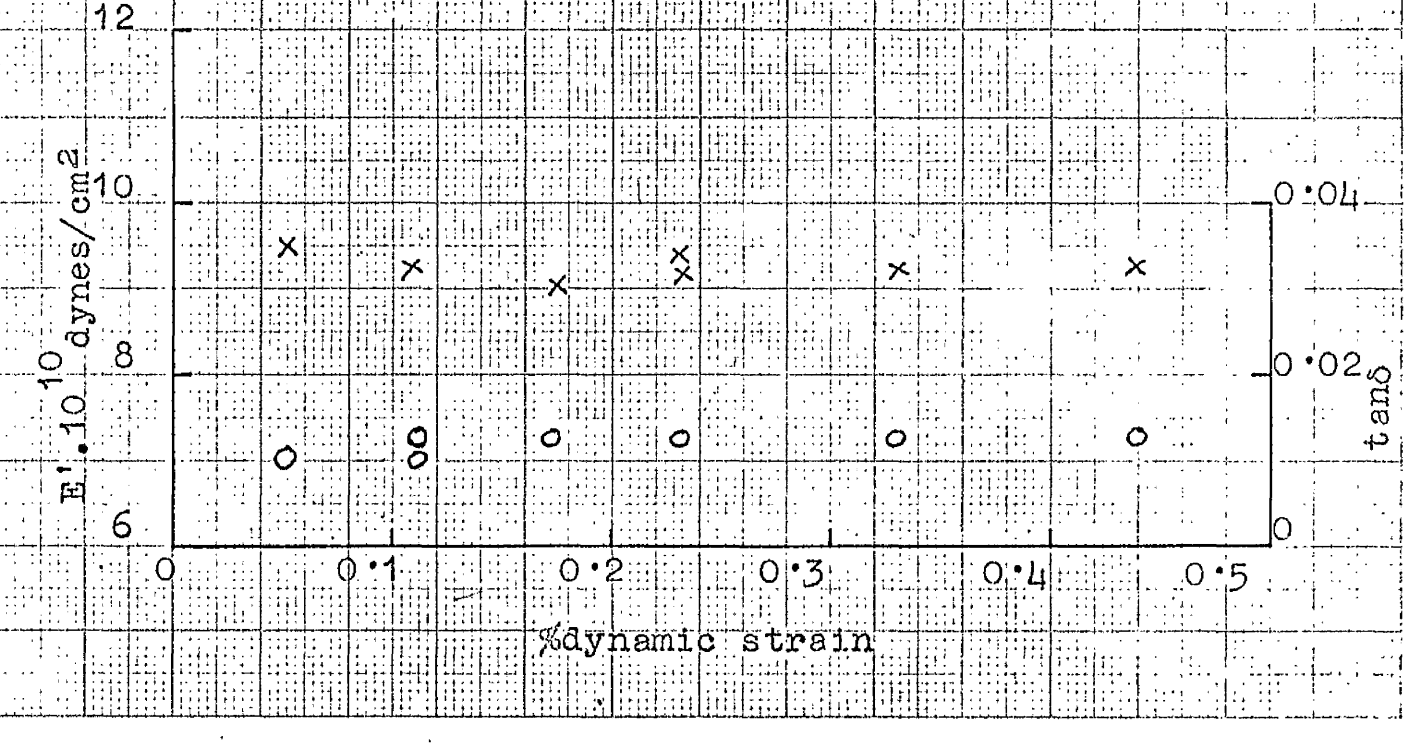

Dynamic tensile properties, static and dynamic strain at 20°C and 65%RH.

RAYON

Fig.25a

×--×--× E'

o--o--o tanδ

%dynamic strain 0·1 (app.)

Temp. 20 °C±2

RH65%±2

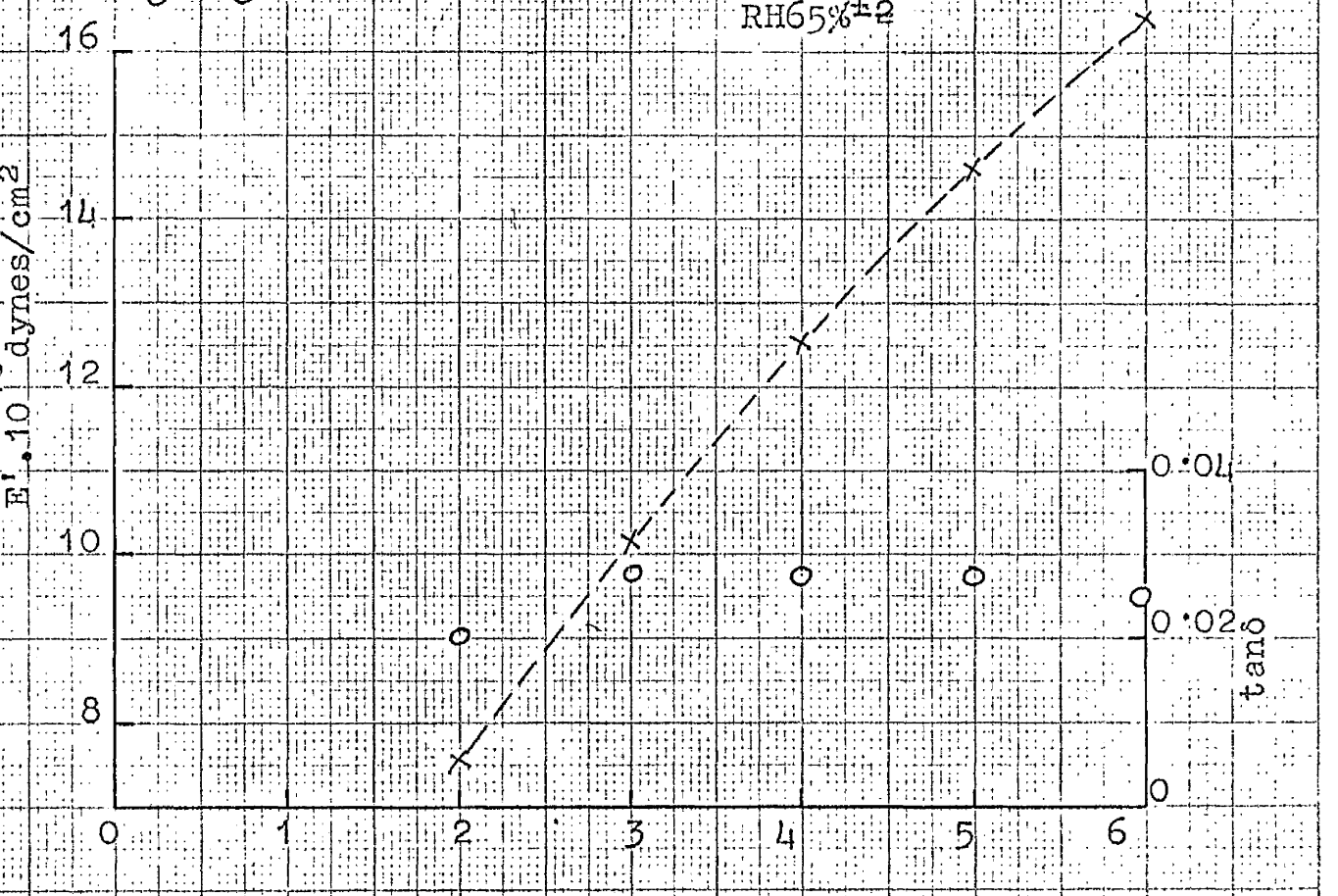

Fig.25b

%static strain 3%

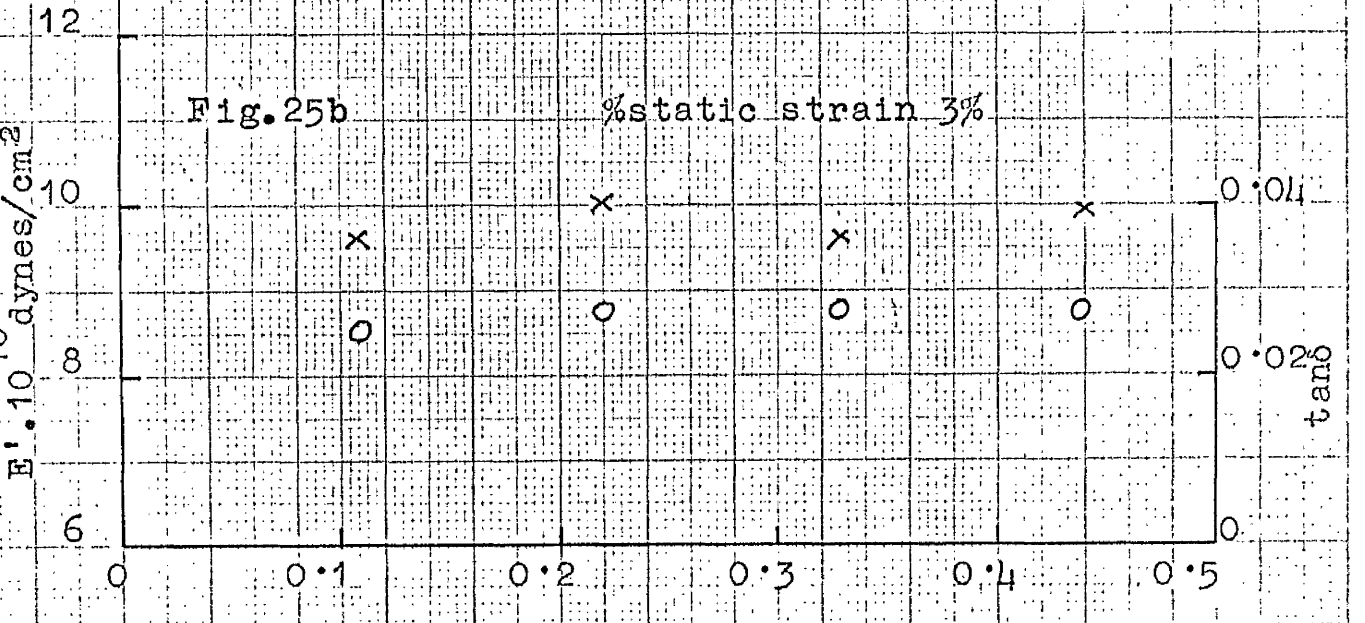

around -60° to -70°C and -30°C, respectively, with an associated drop in the moduli. A low temperature transition for sample BH_4 is probable below -70°C. The values of dynamic bending moduli at 20°C for samples BH_2 and BH_3 which are 7.2 $.10^{10}$ and 7.6 $.10^{10}$ dyn/cm^2, respectively are in-between the modulus values observed for nylon 66 and Dacron. The interesting point to note here is, that although the transition temperature and the moduli of samples BH_2 and BH_3 are higher compared with nylon the relative fall in the dynamic bending modulus in the temperature range 20°C to 150°C is about the same as that for nylon. Therefore, for the two polyblend samples BH_2 and BH_3 the working modulus range over the temperature scale has not increased with the shift in the transition peak. Taking into account the optical, physical, and dynamic mechanical properties of the samples BH_2 and BH_3 one may conclude the samples are probably a polyamide, polyester blend; whereas these properties for the sample BH_4 are much nearer those of nylon 66.

3. Effect of Static and Dynamic Strain on Dynamic Tensile Properties. Nylon 66 type A, Dacron and Rayon.

The results on the effect of static and dynamic strain on dynamic tensile properties are represented graphically in Figs.23, 24 and 25, for the samples nylon 66 type A, Dacron and rayon. It will be noted that with an increase in static strain from 1 to 5% in nylon and Dacron and 2 to 6% in Rayon at 20°C at 65%RH and under a dynamic strain amplitude of approximately 0.1% the loss tangent for all the three fibres remains

constant, but the dynamic tensile modulus increases sharply at low static strains and tends to reach a limiting value. It is therefore, apparent that energy loss also increases with increase in static strain. The sharp increase in dynamic tensile modulus with static strain is attributed to the unfolding of the structure in the non-crystalline regions resulting in increased orientation which reaches a limiting value at higher strains.

However, for these fibres dynamic tensile modulus and tan δ are found to be independent of the dynamic strain amplitude in the range between 0.1% to 0.5% Figs. 23b, 24b, and 25b.

4. Dynamic Tensile properties and Relative humidity.

Nylon 66 types A, B and C, nylon 6, Dacron, Acrilan 16, and rayon.

The effect of varying the relative humidity from zero to 95% at 20°C, on the dynamic tensile modulus and tan δ of nylon 66 types A, B and C, nylon 6, Dacron, Acrilan 16, and rayon are indicated in Figs. 26, 27 and 28. It will be noted that in nylon 6 fibres a distinct dispersion occurs at about 85% RH, whereas in nylon 66 fibres (types A, B and C) a dispersion is apparent above 90 or 95% RH. All the nylon fibres show a decrease in the dynamic tensile modulus with an increase in RH. The differences in behaviour noticeable between samples A, B, and C are attributed to the differences in the degree of crystallinity between the three types of fibres as shown by their density values (Table XVII). These findings are consistent with the observed differences in tensile (Fig. 4

Fig.26: Dynamic tensile properties and Humidity at 20°C.

nylon 6 ——— , nylon 66 types A -o-o-o , B —x—x—, and C -o-o-o-.

%static strain 2 and %dynamic strain 0·1(app).

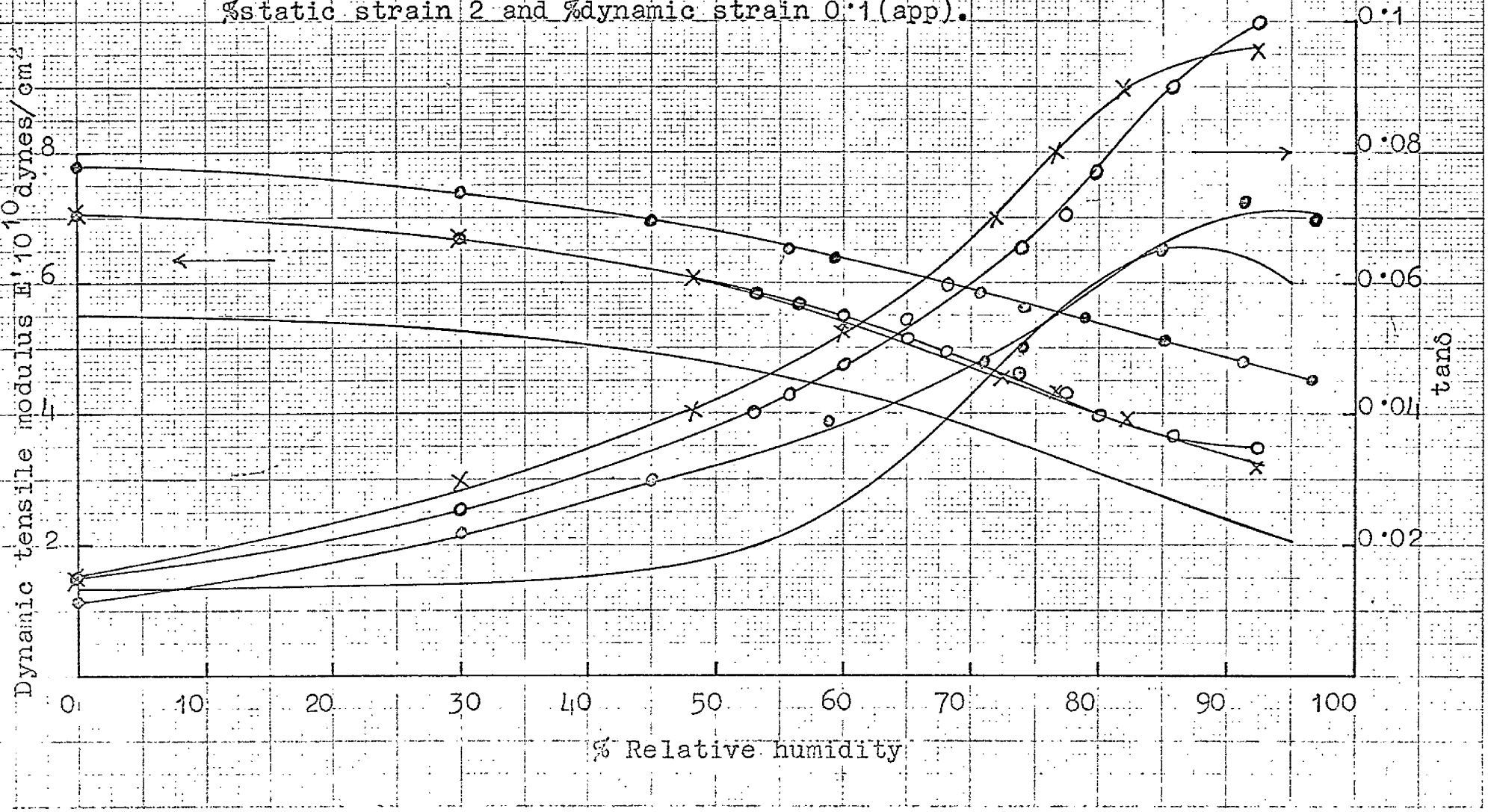

Fig. 27: Dynamic tensile properties and Humidity at 20°C.
Dacron ——— , Acrilan 16 -o-o-o- . %static strain 2 and
%dynamic strain 0·1(app).

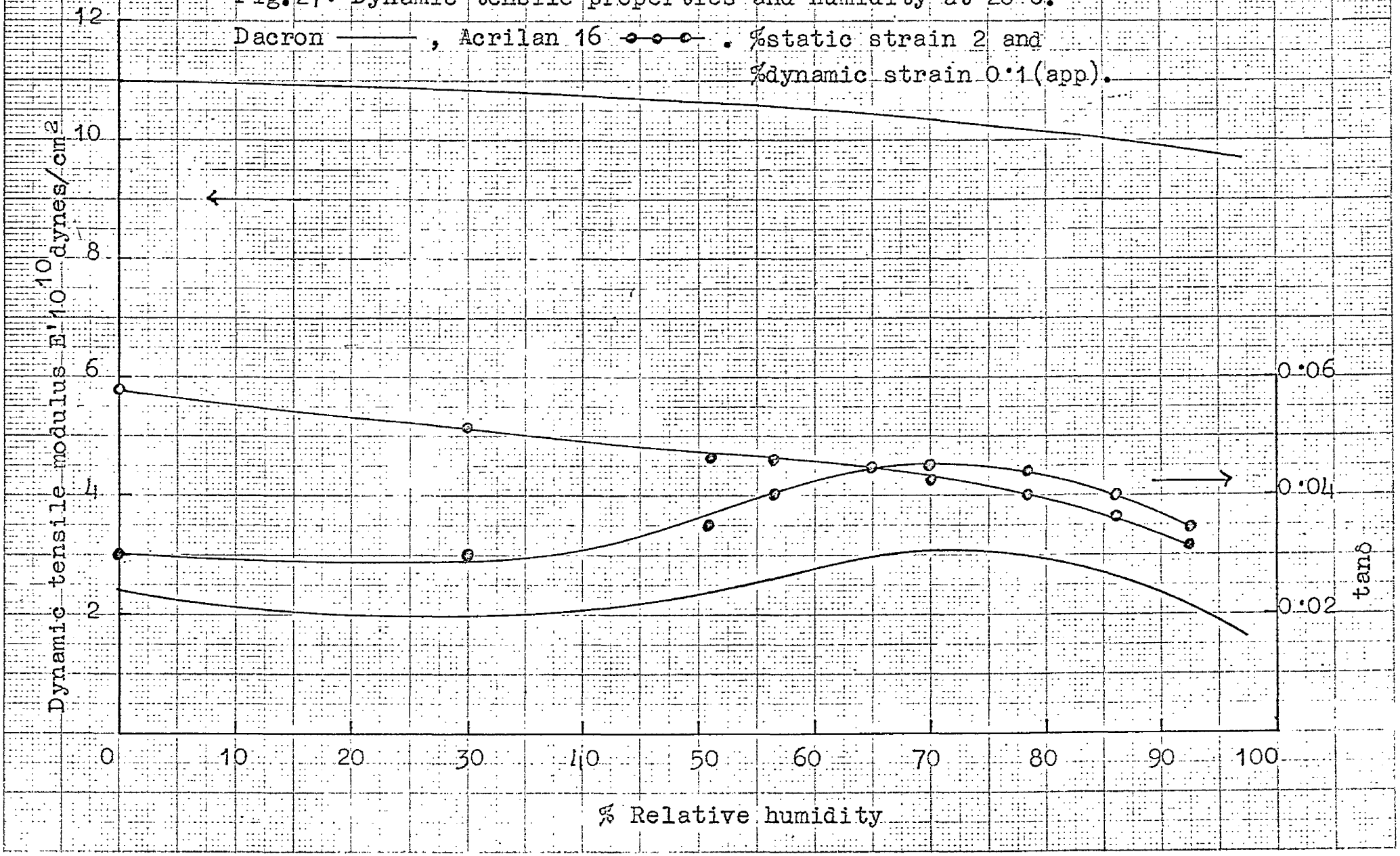

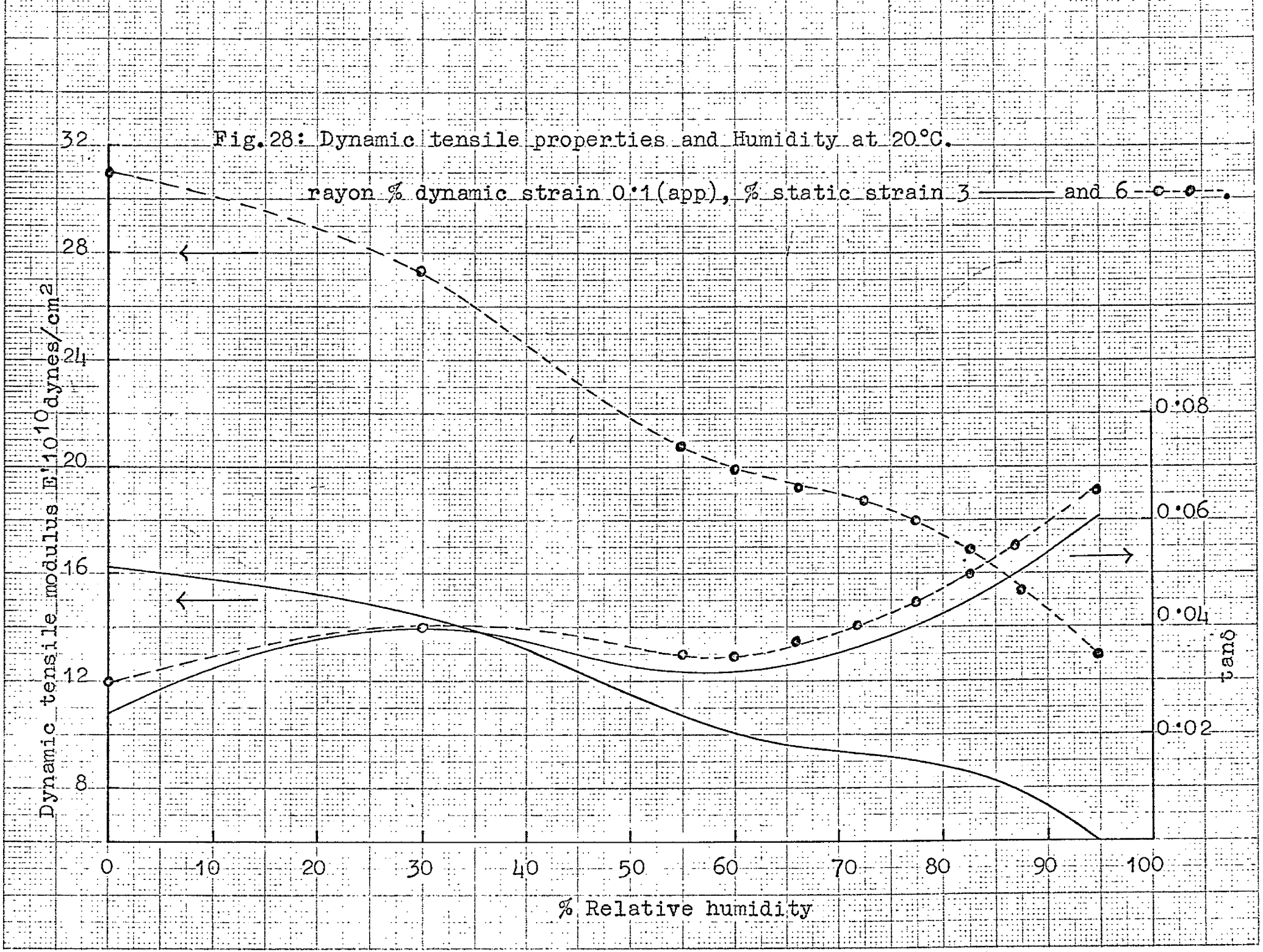
Fig. 28: Dynamic tensile properties and Humidity at 20°C.
rayon % dynamic strain 0·1 (app), % static strain 3 ——— and 6 - - o - - o - -
Dynamic tensile modulus E' 10^10 dynes/cm²
32
28
24
20
16
12
8
0·08
0·06
0·04
0·02
tanδ
0
10
20
30
40
50
60
70
80
90
100
% Relative humidity

and dynamic bending properties of nylon 66 fibres types A, B and C. The observations on nylon 66 presented here are in agreement with those reported by Quistwater and Dunell[74]. which has been reviewed in the literature survey.

Dacron and Acrilan 16, also show similar dispersion to nylon 66 and nylon 6 but around 70% or 75% and their dispersion peaks are, however, much smaller. Considering the differences in the moisture regain of these fibres (Table XIX) it appears that the presence of water decreases intermolecular cohesion and therefore, segmental mobility increases depending on the amount of moisture absorbed by the fibre.

The results on rayon fibre Fig.28 show that apparently two dispersion regions exist, one around 30% RH and another above 90% RH. A sharp change in the dynamic tensile modulus associated with these dispersions may also be noted. An increase in static strain from 3% to 6% on rayon fibres increases the tensile moduli over the range of RH investigated, but the dispersions on the loss tangent curve appear to move toward lower humidities. This is probably due to the fact that by increasing the static strain on the fibre, mechanical strain energy is imparted to the system and therefore, water molecules can now disrupt the intermolecular bonds more easily and increase segmental mobility at a lower regain. The two dispersions observed in rayon fibres by changing the relative humidity from 0 to 95% may be attributed to the

directly and indirectly absorbed water molecules in non-crystalline region. The directly absorbed water would initially free some segments in the molecular chain which acquire greater mobility as the process of moisture absorption continues.

5. Dynamic Tensile properties, Temperature and/or Relative Humidity. Nylon 66 types A, B, C, BH_1 and type 900 normal and heat set, Dacron, Acrilan 16, Rayon and Polyblend types BH_2, BH_3, and BH_4.

Figs.29 to 35 indicate the results of measurements of dynamic tensile properties of nylon 66 types A, B, and C and 900, Dacron, Acrilan 16 and rayon over a range of temperature 20°C to 95°C at 85%, 65% and 45%, and over a range of temperature 80° to 150°C at 0% RH. Single filaments from tyre cords of 2 cm length (except for Acrilan 16 and rayon) were used for the dynamic tensile experiments which were carried out at a constant frequency of 20 cps with the fibres subjected to 2% static strain and 0.1% dynamic strain.

At high temperatures the modulus of Acrilan is very low and therefore on the present apparatus dynamic tensile measurements could not be carried out on 8 denier single filament of Acrilan 16. However, with two filaments of 2 cm.length fixed to the apparatus parallel to each other and subjected to 2% static strain and 0.1% dynamic strain it was possible to cover a wide range of temperature and humidity. Since rayon fibres were of finer denier, two filaments of 2 cm length were fixed to

Fig.29: Dynamic tensile properties, Temperature and or Humidity.

nylon 66 type A. % static strain 2 and % dynamic strain 0·1(app).

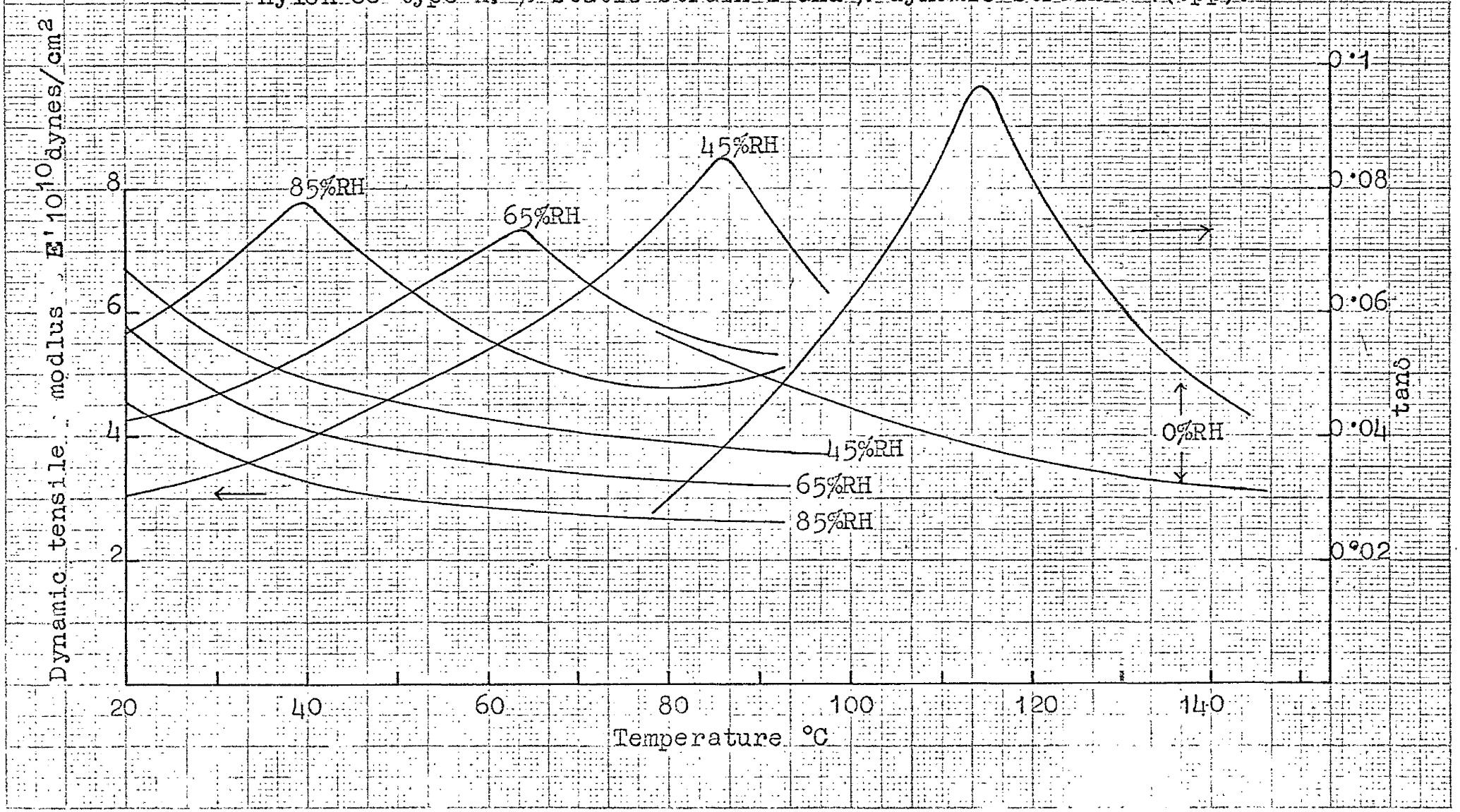

Fig.30: Dynamic tensile properties, Temperature and or Humidity.

nylon 66 type B. %static strain 2 and %dynamic strain 0·1(app).

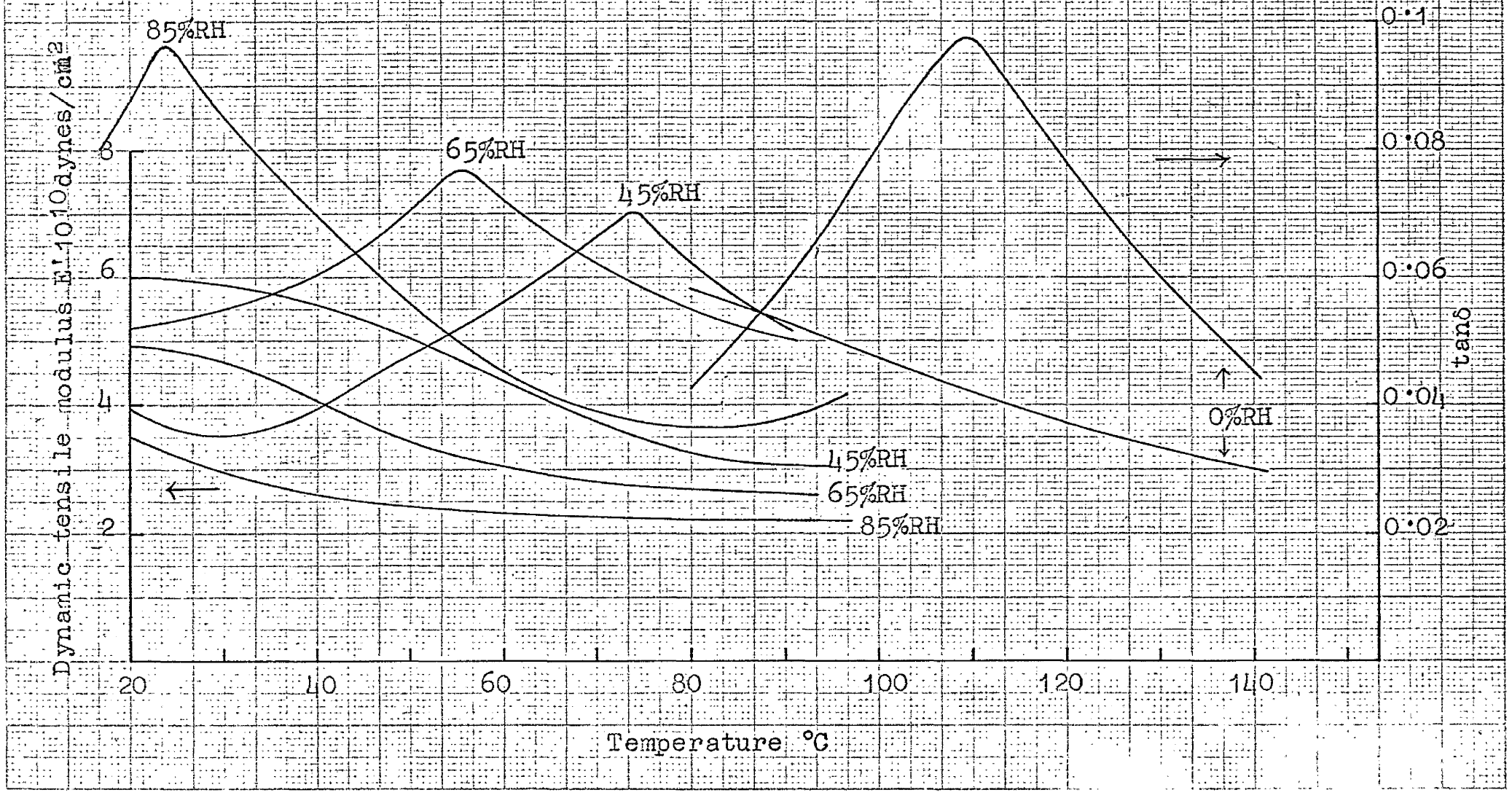

Fig. 31: Dynamic tensile properties, Temperature and or Humidity.

nylon 66 type C. % static strain 2 and %dynamic strain 0·1 (app).

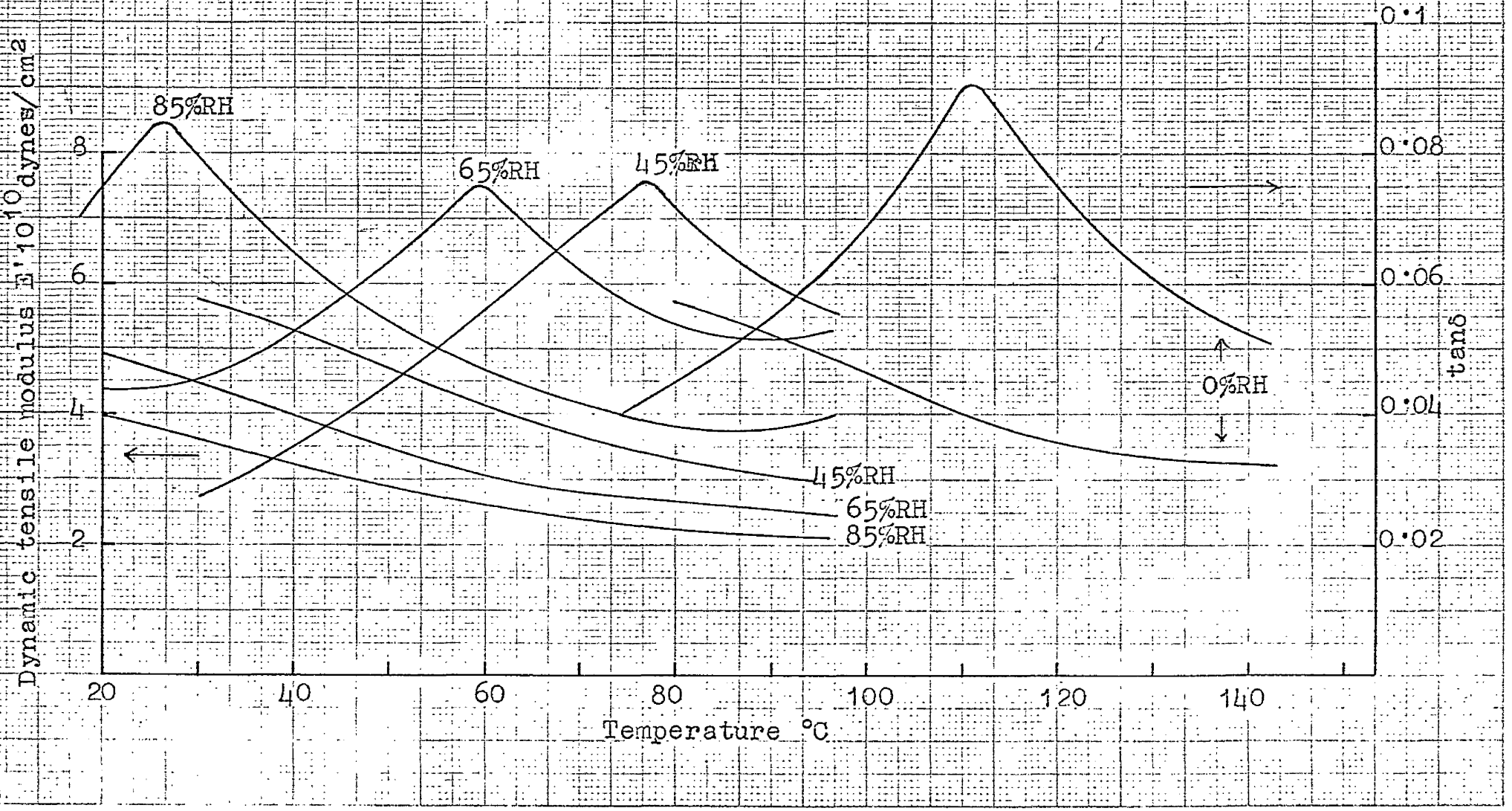

Fig.32: Dynamic tensile properties, Temperature and/or Humidity.

nylon 66 type 900. % dynamic strain 0·1 (app), % static strain 1 --o--o--o--,

2 -o-o-o- , and 4 --o--o--o--.

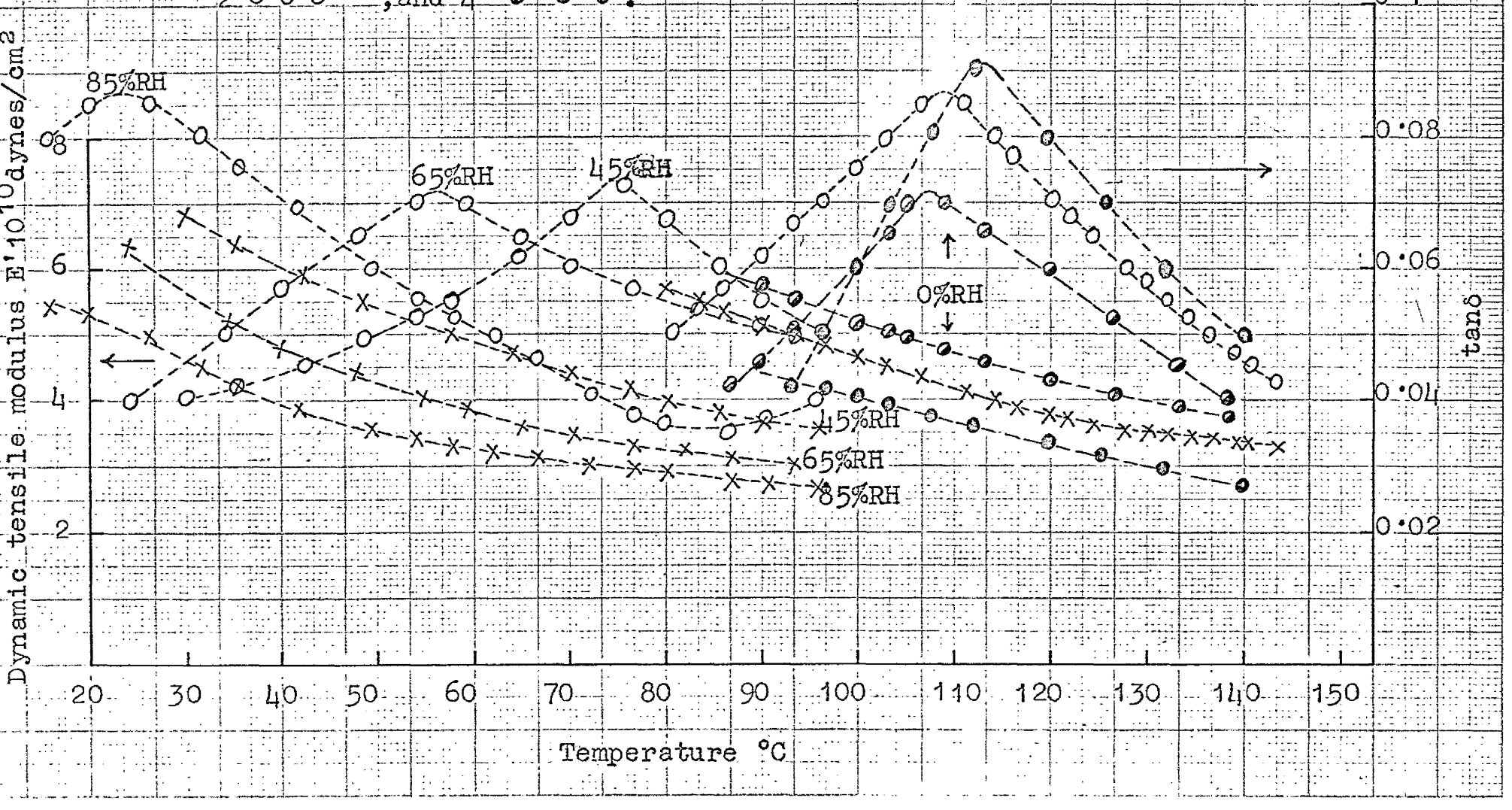

the apparatus parallel to each other as for Acrilan but were subjected to 3% static strain and 0.1% dynamic strain. On nylon 66 types A, B, and C, experiments were carried out on two fibres each, in order to establish the reproducibility of the experimental technique. It will be seen from Tables XV that reproducibility of the results using the experimental technique described earlier is good. On nylon 66 type 900 dynamic tensile properties at 0% RH over 80°C to 145°C, have also been studied under 1% and 4% static strains (Fig.32).

Referring to Figs.29 to 32 nylon 66 types A, B, C and type 900 show loss tangent peaks (glass transition) between 108° to 115°C at 0% RH. With increase in moisture content the glass transition peak shifts towards lower temperature and the height of the loss tangent peak is affected by the absorbed moisture which is dependent on the ambient conditions of temperature and relative humidity. This finding is consistent with those reported by Woodward[29] et al for rod like specimen of nylon 66. It is interesting to note that with the fibre A which has higher density than types B, C and type 900 the loss peaks at all humidities occur at a higher temperatures; This was also found to be true in the dynamic bending experiments at 0% RH.

The effect of density can also be noted in the tensile behaviour of these nylon 66 fibres shown in Figs.41 and 42. Nylon 66 type A exhibits a higher initial modulus and breaking stress and a low breaking extension compared with the other nylon 66 fibres.

The sensitivity of the position of the glass transition peak observed at about 108°C to 115°C to the water content of the nylon polymer may indicate a connection with the amide linkages in the non-crystalline region. Since dynamic tensile experiments at different relative humidity below 20°C were not carried out in the present instance, the β damping peak around -33°C for polyhexamethylene adipamide, samples containing water reported by Woodward et al[29] could not be studied. Woodward et al interpret that in polyamides the α peak (glass transition peak) is associated with segmental motions in amorphous regions as a consequence of the breaking up of hydrogen bonds (or polar forces of attraction) between chains, and the β peak (the secondary glass transition peak) in the specimen containihg water is associated with segmental motions in the amorphous regions involving the co-operation of methylene groups and non-hydrogen bonded amide links. Such an interpretation, although logical, assumes the existence of hydrogen bonded and non-hydrogen bonded amide linkages in the non-crystalline parts of polyamide polymer merely to explain the observed phenomenon in dynamic mechanical measurements. However, there seems to be no support for such an assumption from the infra-red and NMR studies reported by other workers.

From the work of Holliday[115] it may be recalled that the 3300 cm^{-1} bonded NH band changes only gradually in intensity and frequency as the temperature is raised from 100°C to 200°C and the changes become more

marked above 200°C although no break in NH band is observed. Trifan and Terenzi[116] have estimated that no more than one percent free NH groups is present in a series of nylons including even odd members. Miyake[117] has also investigated different types of nylons and has concluded from quantitative estimate of optical densities, that the amide groups form hydrogen bonds almost completely, irrespective of the number of methylene groups.

Recently Glick and Phillips[118] have studied the proton magnetic resonance spectra of variously treated nylon 66. They report that the broad line NMR spectra of all samples consisted of a superimposition of a broad and narrow component at all temperatures studied, -163°C to 137°C. Dried nylon and dried deuterated nylon afforded indentical NMR spectra. This identity has been interpreted as indicating a possible electrostatic rather than overlap description of hydrogen bonds in amorphous regiohs. Additives such as water, deuterium oxide, methanol, and deuterium methoxide, have been found to lower the temperature at which the narrow component line width further reduced. Such an effect, however, is consistent with other studies that indicated such additives were associated with hydrogen bonds in amorphous regions of the polymer. This effect, appeared to saturate at a concentration of additive equal to that of the amide functions in the amorphous regions. Contrary to their earlier studies, it has been reported that there is little difference if any between NMR spectra obtained with samples containing

proton additives and those with appropriately substituted deuterium additives.

Amidst such controversies it appears that from only dynamic bending and tensile data on nylon 66 over a range of temperature and humidity presented here, it would be futile to conclude and to attribute the observed transitions in nylon 66 to motions of specific molecular groups or segments.

Referring to Fig.32 it may be interesting to note the heights and the positions of the glass transition peak at 0% r.h. for nylon 66 type 900 at static strains 1%, 2% and 4% which occur at 112°, 109° and 107°C respectively, the heights of the peaks decreasing with increasing static strain. As expected the dynamic tensile moduli in the temperature range investigated are higher at higher static strains. The shift in the transition peak to slightly lower temperature with increasing static strain in the range investigated may be attributed to the higher mechanical energy imparted to the system with straining and therefore, less additional thermal energy is required to activate the segments to rotate.

Fig.33 indicates the effect of temperature and/or humidity on the dynamic tensile properties of Dacron. In the temperature range investigates, only one dispersion peak at about 145°C for the dry fibre was observed. In the present investigations dynamic tensile experiments at different humidities were not carried out above 95°C and below 20°C

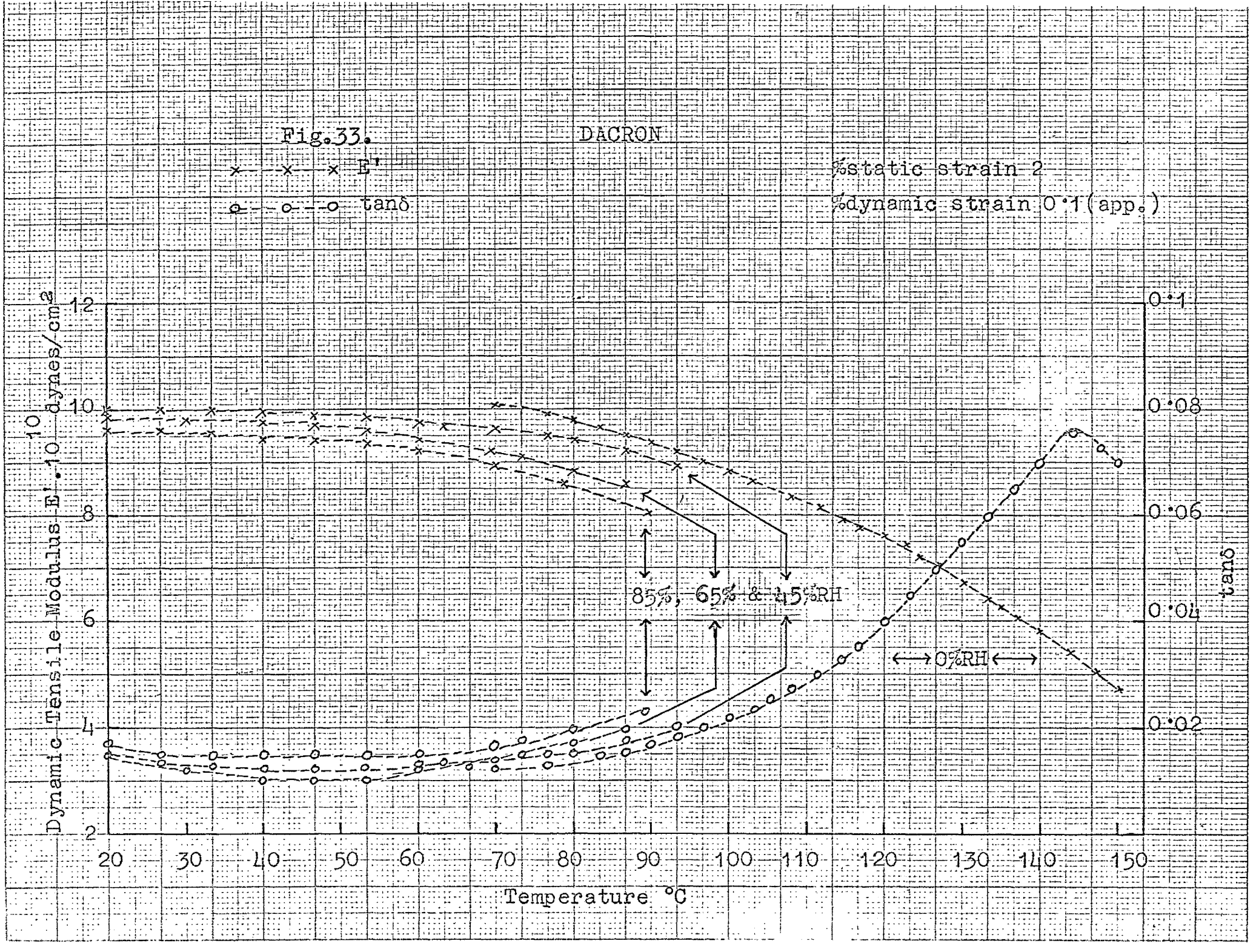
Fig.33.
DACRON
× — × — × E'
o — o — o tanδ
%static strain 2
%dynamic strain 0·1 (app.)
Dynamic Tensile Modulus E' · 10 dynes/cm²
tanδ
85%, 65% & 45%RH
0%RH
Temperature °C
2
4
6
8
10
12
0·02
0·04
0·06
0·08
0·1
20
30
40
50
60
70
80
90
100
110
120
130
140
150

and therefore, the effect of moisture content on the glass transition and secondary glass transition peaks could not be studied as studied by Kline and Sauer. However, from the dynamic tensile modulus and loss tangent values over a range of temperature at different humidities represented in Fig.33 one can conclude that the effect of moisture on the dynamic tensile properties of Dacron is comparatively less than that on nylon 66. At higher humidities if the experiments were carried out at higher temperatures the glass transition peak might occur at a slightly lower temperature than 145°C as reported by Kline and Sauer[33], From the extensive work of Ward[34] and others on the segmental motion of polytheylene terephthalate polymers using dynamic mechanical technique, nuclear magnetic resonance spectra, infra-red spectra and x-ray diffraction, reviewed in the literature earlier, the glass transition peaks of polyethylene terephthalate fibres observed in the present investigation in dynamic bending and tensile experiments may probably be attributed to considerable rotation of the glycol residue also involving paraphenylene linkages in the non-crystalline parts of the fibre. The low temperature secondary transition peak observed in the dynamic bending experiments may be attributed to some very restricted rotation of the glycol residue. The position of these two dispersions in different polyethylene terephthalate fibres is, however, affected by the previous history of the material (e.g. heat treatment, orientation etc).

Fig.34: Dynamic tensile properties, Temperature and Humidity.

Acrilan 16. % static strain 2 and % dynamic strain 0·1 (app).

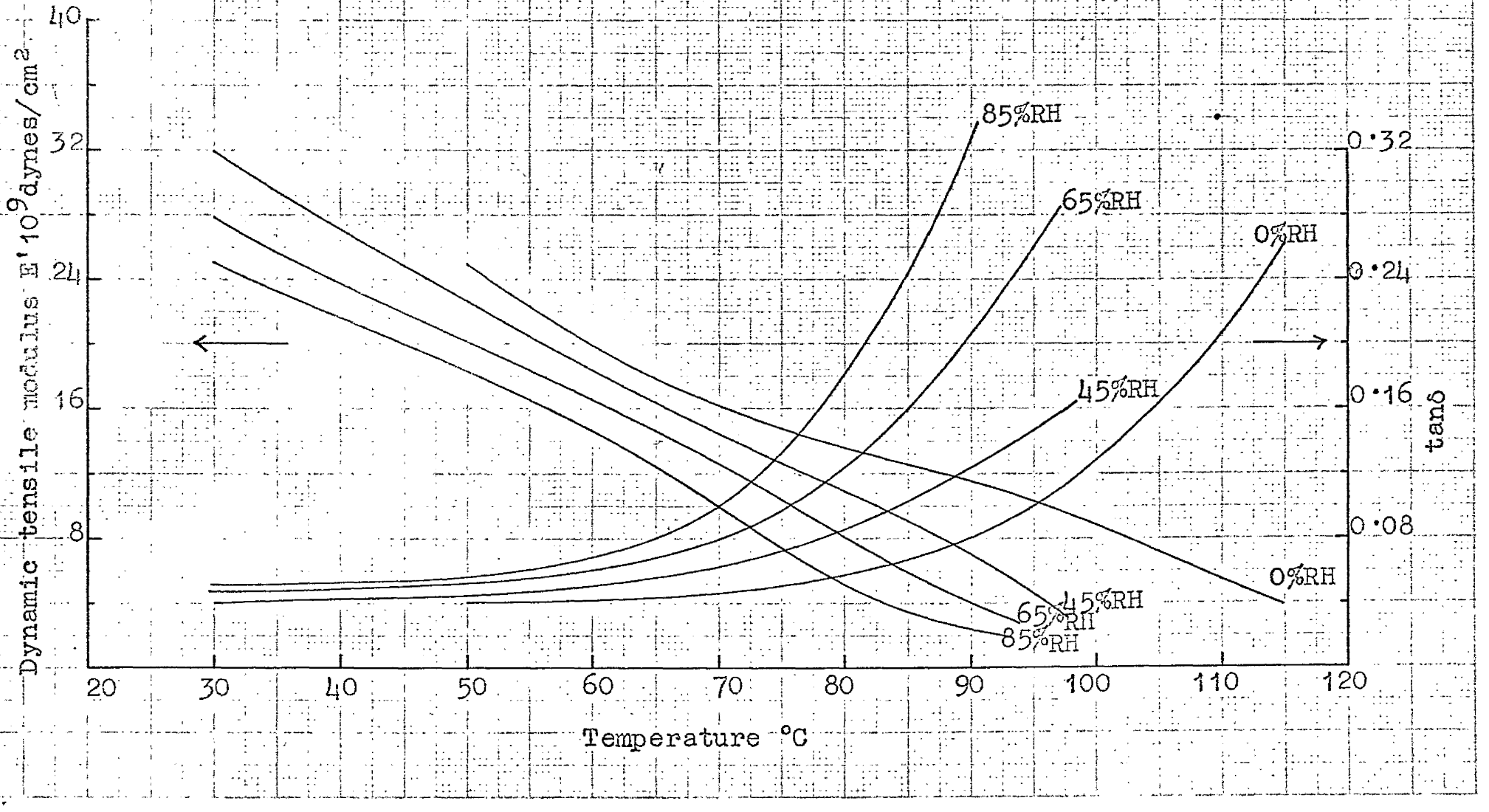

The differences in the temperature location of the glass transition peaks for dry fibres of nylon 66 and Dacron between dynamic bending and tensile experiments are attributable to the difference in frequency(about a decade) adopted in the two experimental techniques in the present investigations. From Nielson's[4] theoretically calculated values, and Yasaka Wada's[8] compiled data, it may be seen that for most common polymers a shift in the glass transition peak temperature of about 7° to 8°C occurs for a decade change in frequency.

Fig.34 indicates the effect of temperature and/or humidity, on the dynamic tensile properties of Acrilan 16. Consistent with the results of the dynamic bending experiments (Fig.17) it has not been possible to establish a major loss tangent peak around 90° to 110°C at 0% RH in the dynamic tensile experiments. However, it may be seen that tan δ continues to rise sharply (Fig.34) with a corresponding drop in modulus above 100°C exhibiting a rubbery behaviour at that temperature. It is also interesting to note that this rubbery response in Acrilan 16 occurs at lower temperatures with increase in moisture content. Comparing the moisture regain of Acrilan 16 with polyamide and polyester fibres (Table XIX) it becomes obvious that the presence of water decreases intermolecular cohesion and therefore, segmental mobility increases depending on the amount of moisture absorbed by the fibre. Since Acrilan fibres absorb comparatively more ~~amount of~~ water than polyester fibres and less amount of moisture than polyamide fibres, the effect of

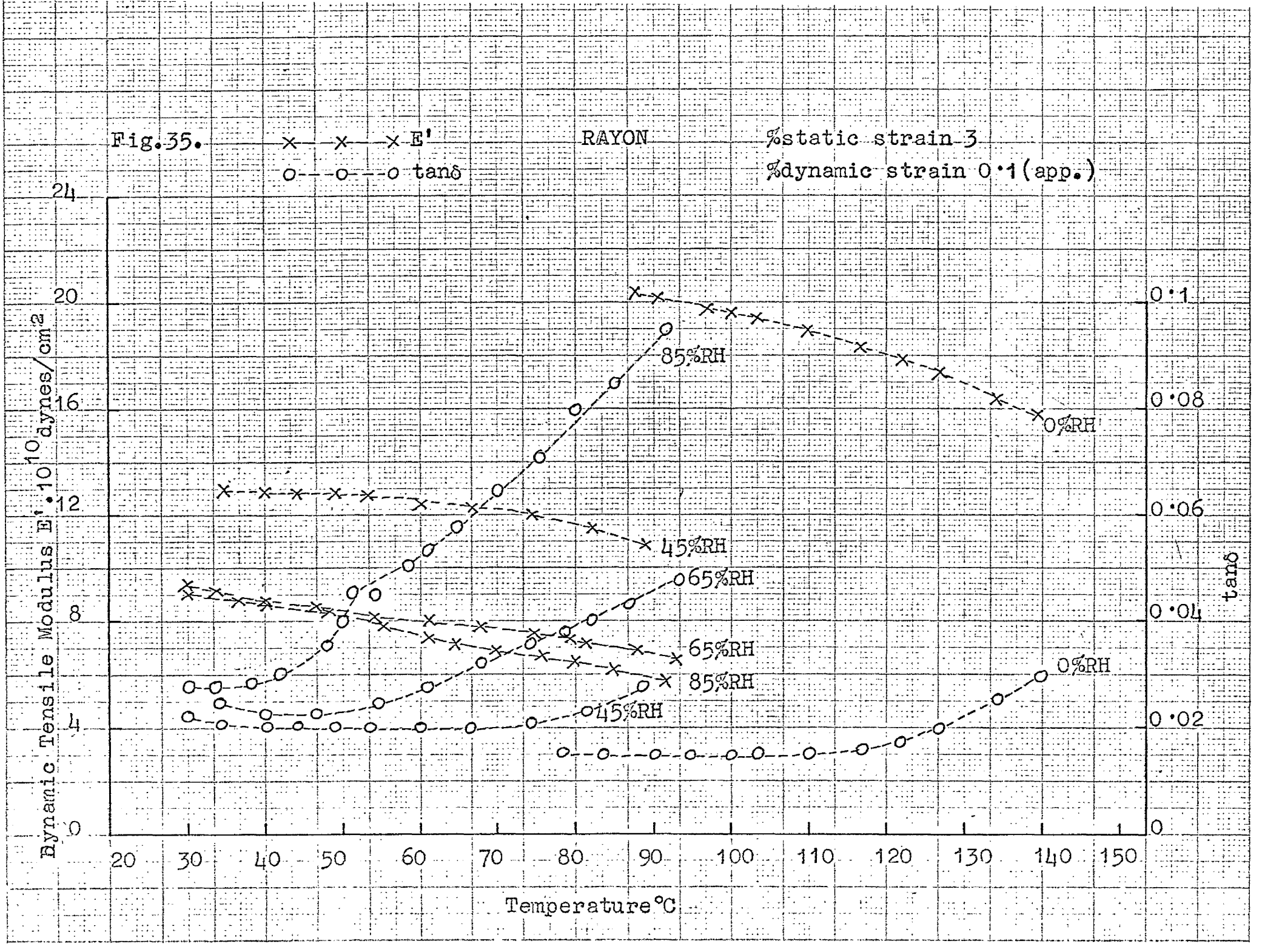
Fig.35.
× × × E'
o o o tanδ
RAYON
%static strain 3
%dynamic strain 0·1 (app.)
Dynamic Tensile Modulus E' ·10 dynes/cm²
tanδ
Temperature °C
85%RH
0%RH
45%RH
65%RH
65%RH
85%RH
45%RH
0%RH
24
20
16
12
8
4
0
0·1
0·08
0·06
0·04
0·02
0
20
30
40
50
60
70
80
90
100
110
120
130
140
150

moisture on the dynamic mechanical properties of Acrilan fibres lie between polyester and polyamide fibres.

Unlike in the dynamic bending experiments, here no shoulder in the loss tangent curve around 65°C is visible for Acrilan 16. Similar to the arguments presented earlier, from these results alone it is not possible to attribute the behaviour of Acrilan 16 fibres in the glass/rubber region to motions of specific molecular groups or segments. The sensitivity of the loss tangent and dynamic moduli values around 80° to 110°C to moisture content may indicate that segmental motion in the glass/rubber region involve the rotation of polar groups.

The results of the dynamic tensile properties of rayon fibres over a range of temperature at different humidities are represented in Fig.35. Although temperature has a comparatively smaller effect on the dynamic mechanical properties of dry rayon fibres than on dry nylon 66 and Dacron fibres, humidity has a more marked effect on rayon fibres. This finding is consistent with the high moisture regain in rayon fibres at any given conditions. It will be noted that no dispersion peaks were observed in the rayon fibre investigated in the present instance over the wide range of temperature and humidity. However, with increase in humidity the loss tangent values rise rather sharply at lower temperature compared with dry fibre. Associated with these rising tendencies of loss tangent values a drop in the dynamic tensile moduli may also be noted. A small shoulder at about 52°C at 85% r.h. is visible which is not observed at other humidities. These findings are consistent

Fig.36: Dynamic tensile properties and Temperature at 0%RH.

Nylon 66 type BH_1 -o-o-o-, and Polyblend types BH_2 —o—o—, BH_3 —o—o—o— and BH_4 —o—o—o—.

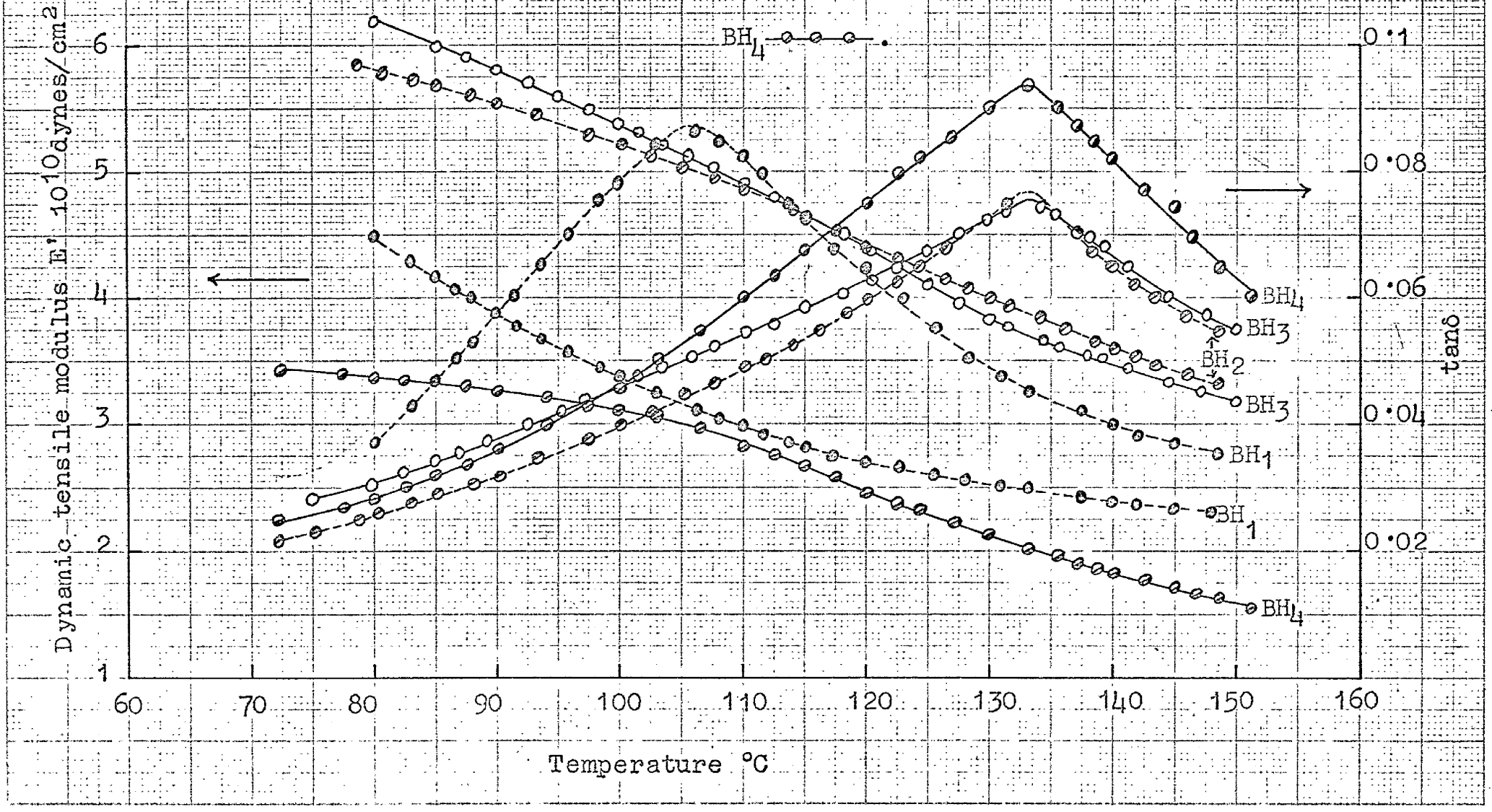

with those reported by Tokita[56] for rayon monofilaments except that Tokita observed a dispersion peak at 80°C for dry viscose rayon, which shifted to 65°C at 65% RH. The absence of dispersion peak may be due to differences in crystallinity, size of crystallites and/or orientation between the viscose rayon samples used by Tokita and the fibres from tyre cord rayon used in the present investigations.

It may be interesting to note the tensile behaviour of rayon fibres Fig.41 compared with nylon 66 and Dacron. Rayon fibres have a low breaking stress and low breaking extension. As mentioned earlier high breaking stress and high breaking extension is one of the desirable properties in tyre cords. However, the choice of tyre cords for tyres depends on the end use of the tyre itself.

The effect of temperature, in the range 70° to 150°C on the dynamic tensile properties of polyblend fibres types BH_2, BH_3 and BH_4 at 0% RH are indicated in Fig.36. The dynamic tensile properties of nylon 66 type BH_1 are also shown in the same figure for comparison. It will be noted that the effect of temperature on these fibres measured in dynamic bending experiments Fig.22 are in general agreement with those measured in dynamic tensile experiments. Slightly low temperatures registered for the transition peaks in dynamic tensile experiments are attributed as mentioned earlier to the differences in frequency (about a decade) adopted in the two experimental techniques. As observed in

Fig.37: Dynamic tensile properties, Temperature and/or Humidity.

nylon 66 type 900 heat set in an oven at 150°C under 10% extension (setting time 1 hour). %static strain 2 & %dynamic strain 0·1(app).

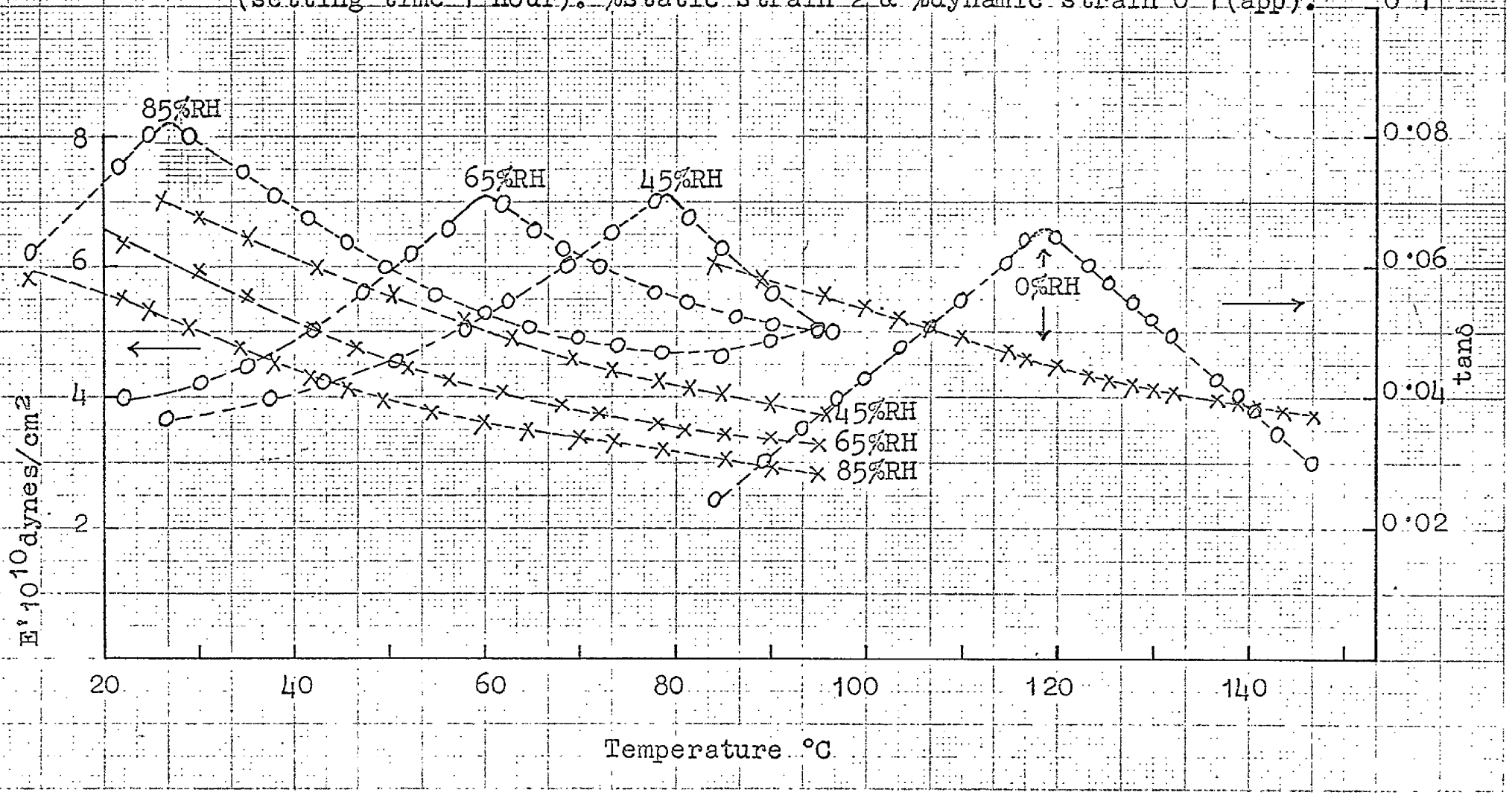

Fig.38: Dynamic tensile properties, Temperature and/or Humidity.

nylon 66 type 900 heat set in boiling water at 100 °C under 10% extension (setting time 1 hour). % static strain 2 and % dynamic strain 0·1 (app).

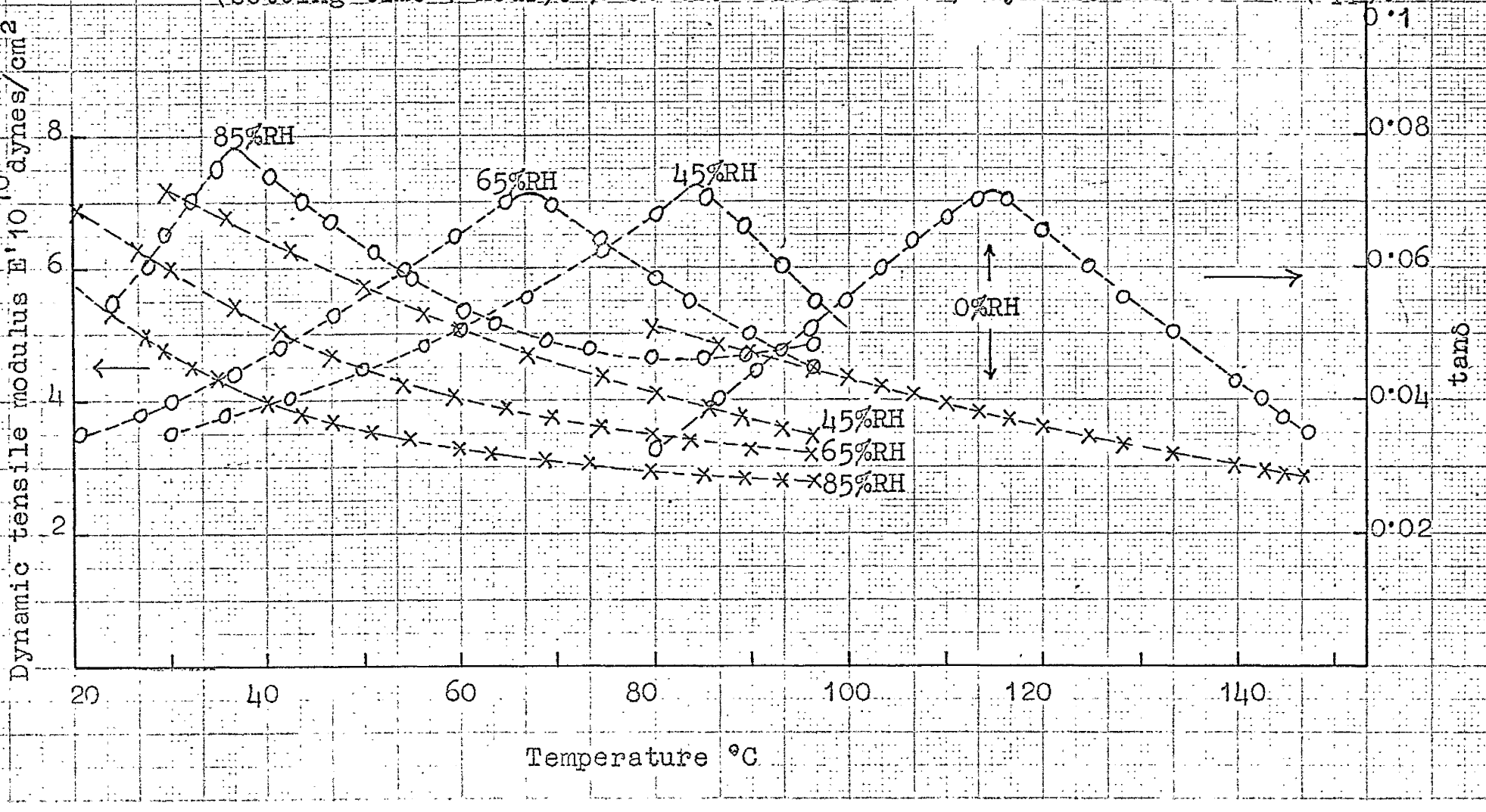

Fig.39: Dynamic tensile properties, Temperature and/or Humidity.

nylon 66 type 900 zero set at 150°C for 1 hour in an oven.

% static strain 2 and % dynamic strain 0·1(app).

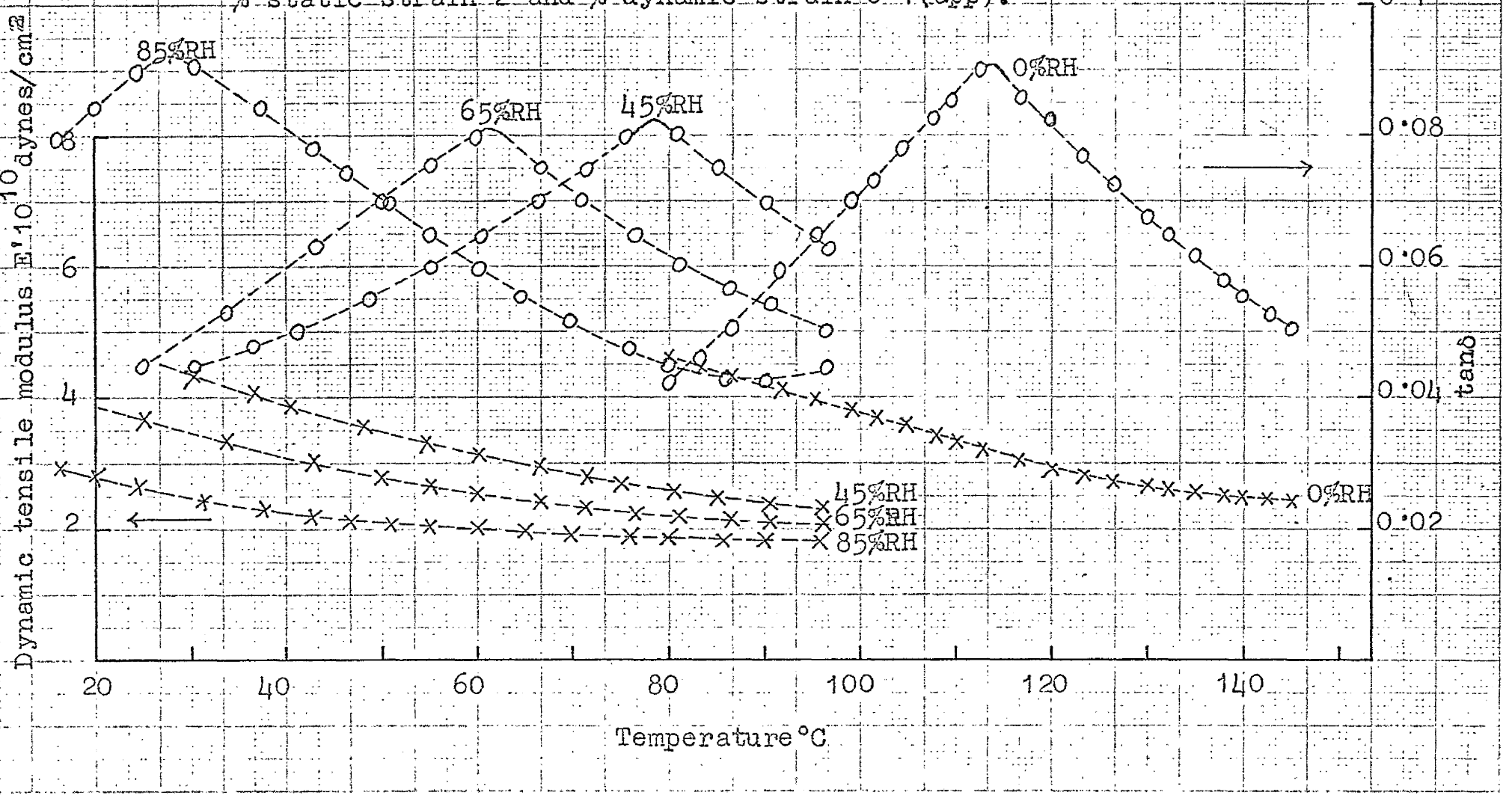

Fig.40: Tensile properties at 20 °C and 65%RH.

Acrilan 16 (setting time 1 hour)

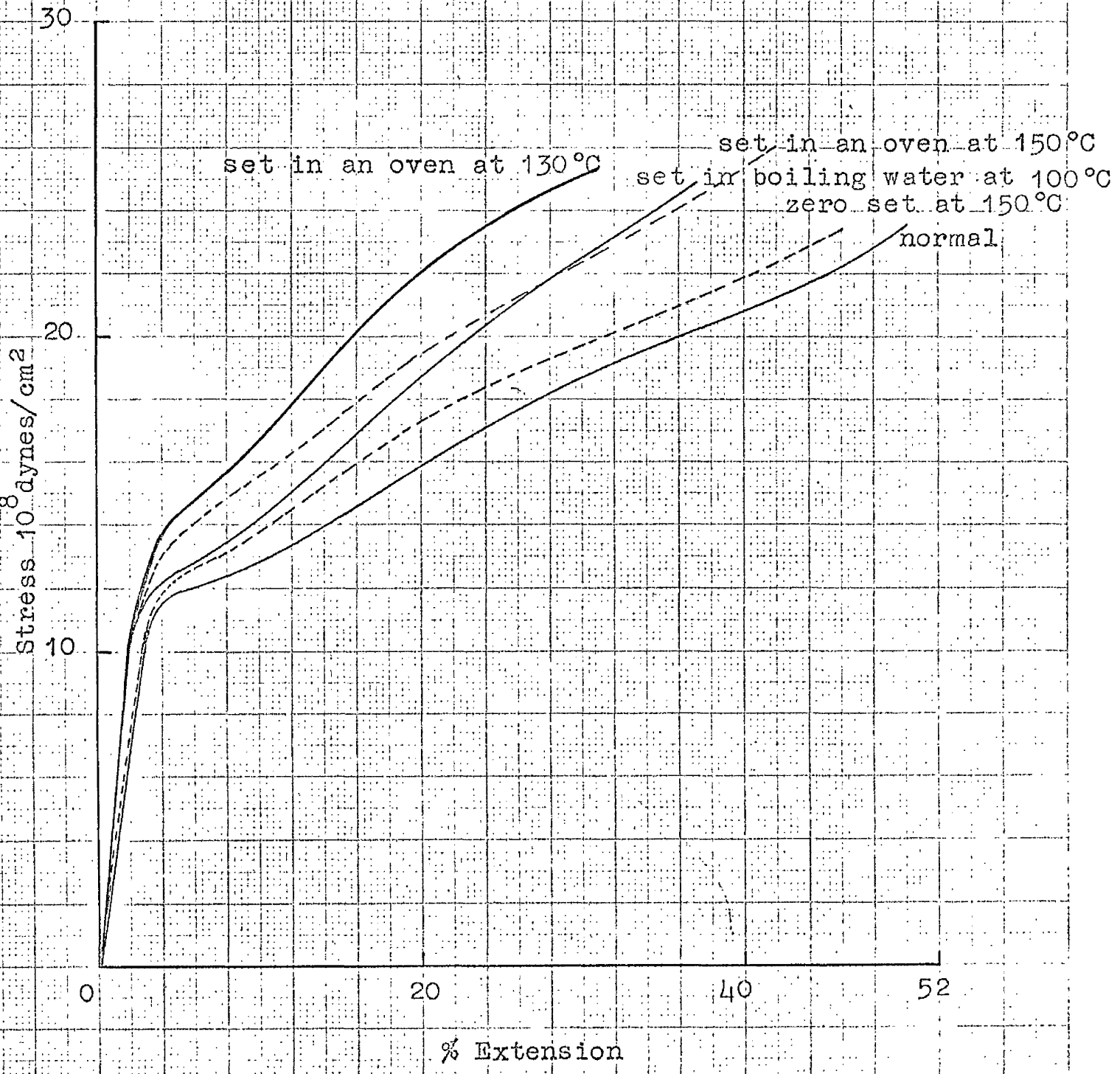

Fig.41: Tensile properties at 20°C and 65%RH.

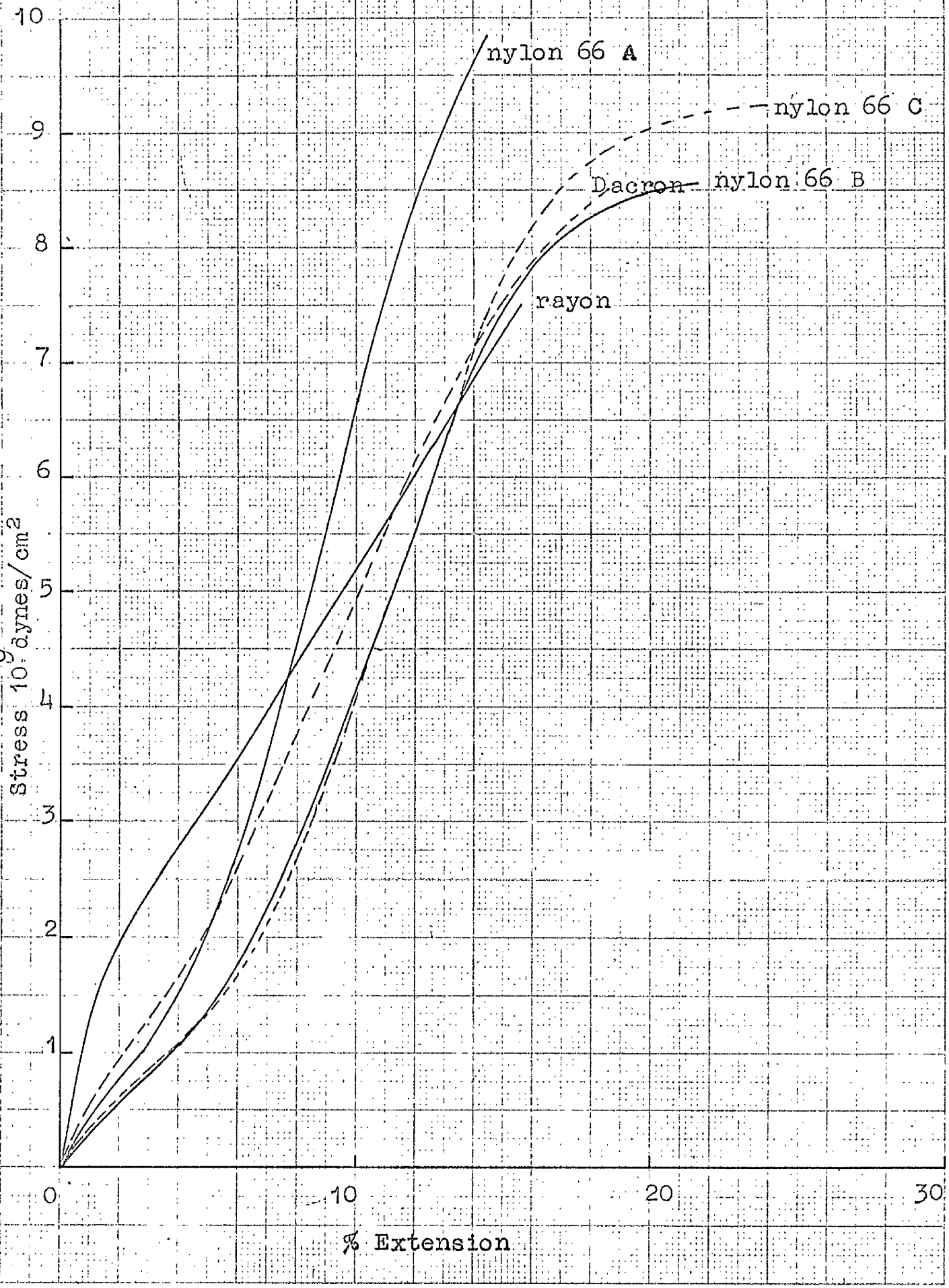

Fig.42: Tensile properties at 20°C and 65%RH.

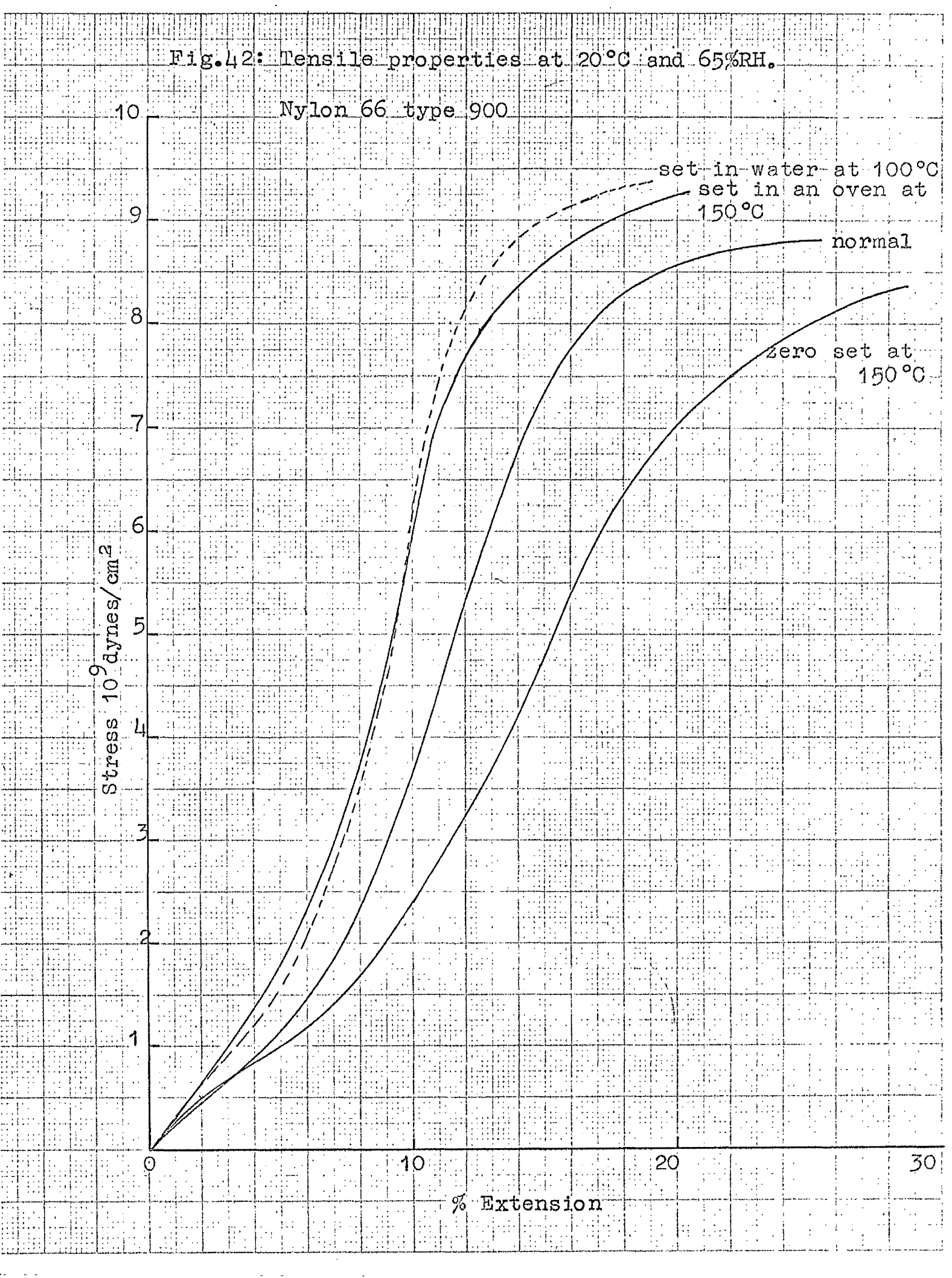

the dynamic bending experiments the dynamic tensile moduli for samples BH_2 and BH_3 are higher at all temperatures in the range investigated compared with corresponding values for the nylon sample BH_1 and the poly-blend sample BH_4.

6. Effect of Heat Setting on Dynamic Tensile Properties.

Nylon 66 Type 900.

The effect of heat setting on the dynamic tensile properties of nylon 66 type 900 are indicated in Figs.37, 38, and 39. Conditions of heat treatment of these fibres are shown in Table XVI and measured values of optical birefringence and physical density are shown in Table XVII. It will be noted from the birefringence values that disorientation occurs in fibres heat set at 150°C under zero tension, whereas orientation increases when the fibres are heat set either in the oven at 150°C or in boiling water at 100°C for one hour under 10% extension. The physical density, however, increases (therefore, the crystallinity increases) under all three conditions of heat setting. The effect of crystallinity and orientation is also reflected in the tensile behaviour of these fibres Fig.42. The fibres heat set for one hour at 150°C or in boiling water at 100°C under 10% extension show higher breaking stress and lower breaking extension, whereas fibres heat set at 150°C for one hour under zero tension show lower breaking stress and higher breaking extension compared with normal fibres. Fibres heat set under zero tension also show a lower initial modulus compared with fibres heat

set under extension but show a slightly higher initial modulus than normal fibre. This is due to fact that heat setting under zero tension has increased crystallinity and has reduced orientation compared with the normal fibre.

From Figs.37, 38 and 39 it is interesting to note that the temperature of the glass transition peak of nylon 66 type 900 at various humidities is affected by the condition of heat treatment. The transition temperatures at different humidities for both samples heat set at 150°C for 1 hour under 10% extension and under zero tension occur around similar temperatures (also shown in Tables XVIII) which are higher than those observed for normal nylon 66 type 900 fibre. The corresponding heights of the peak for the sample heat set under zero tension show an increase compared with normal fibre, whereas for the sample heat set under extension the peak heights decrease. Since the orientations of the two samples are different and the densities are nearly the same it may be concluded, as in Terylene Fig.21 in dynamic bending experiments, that increase in orientation apart from increasing the dynamic tensile modulus ovef the range of temperature investigated reduces energy losses in nylon 66 over the transition region.

The fibres heat set under 10% extensions in boiling water show still higher transition temperatures at different humidities (except at 0% RH) compared with fibres heat set in an oven at 150°C under extension and under no tension. It is interesting to note that the birefringence and

density values for the fibres heat set in ~~the~~ oven and in boiling water under 10% extension are about the same. Therefore, the increase in the transition temperature observed at all humidities in the range investigated for fibres heat set in boiling water is attributed to the larger size of crystallites that are possibly formed in nylon 66 in the presence of water. It is thought that although the overall crystallinity between the two heat set samples may be the same, the presence of water in one sample would increase molecular mobility of the chains to reorient easily and therefore form larger crystallites. Slightly lower transition temperature of 115°C at 0% RH for the fibre set under 10% extension in boiling water at 100°C, compared with 120°C for the fibre set under 10% extension in an oven at 150°C is probably due to the effect of unsetting in the former at temperature above 100°C.

TABLE I A.

WOOL: Dynamic bending properties and Temperature.

Fibre 1. Temperature $\theta^{\circ}C$	Resonant frequency f_o c/s.	tan δ	Relative bending Modulus $E'b/E'_{b20}$.
185	448.5	0.022	0.783
172	454	0.015	0.81
159.5	459.5	0.0124	0.822
146	465	0.0116	0.841
133	470.5	0.01	0.861
120	475.5	0.0098	0.88
106.5	480.25	0.0116	0.9
99	482.5	0.0128	0.91
92	484.5	0.0134	0.913
78	489.5	0.0138	0.932
64	493.75	0.014	0.948
50	498.5	0.0148	0.967
42	501	0.0176	0.98
35	503.5	0.019	0.99
27.5	504.5	0.0216	0.997
20	507	0.024	1
15	510	0.0258	1.015
9.5	513	0.0242	1.035
6	516.5	0.0224	1.045
-6	524.5	0.019	1.07
-18	528.5	0.0168	1.09
-24	532	0.0164	1.1
-30	534	0.0172	1.11
-42	539.5	0.0194	1.132
-54.5	544	0.023	1.153
-67	548.5	0.0274	1.173

Fibre dimensions.
Length = 0.549 cm.
Mass/Unit length = 22.7 $\mu g/cm$.
Density ϱ = 1.305 gm/cm^3

$\epsilon' E'_{b20} = 5.46 \cdot 10^{10}$ dynes/cm^2.

TABLE I B.

WOOL: Dynamic bending properties and Temperature.

Fibre 2.

Temperature ^{o}C	Resonant frequency f_o c/s.	tan δ	Relative bending Modulus $E'b/E'_{b20}$
185	306.5	0.022	0.725
172	312.75	0.015	0.755
159.5	317.5	0.013	0.778
146	322	0.0122	0.8
133	329	0.012	0.834
120	333.75	0.012	0.859
106.5	337.5	0.0124	0.878
99	339	0.0138	0.89
92	341	0.0144	0.897
78	344	0.015	0.913
64	347.25	0.0156	0.931
50	350.5	0.017	0.948
42	353	0.0184	0.96
35	355	0.0209	0.972
27.5	357.5	0.022	0.99
20	360	0.024	1
15	362	0.027	1.01
9.5	364.5	0.025	1.025
6	366	0.0236	1.039
-6	372	0.02	1.07
-18	375	0.0174	1.086
-24	377.5	0.0168	1.1
-30	379	0.0174	1.109
-42	383	0.0198	1.132
-54.5	386	0.023	1.152
-67	389	0.0274	1.173

Fibre dimensions: Length = 0.6 cm. Mass/unit length = 20.22 $\mu g/cm$.

Density = 1.305 gm/cm^3

$\epsilon' E'_{b20} = 5.117. 10^{10}$ dynes/cm^2.

TABLE IC.

WOOL: Dynamic bending properties and Temperature.

Mean values.

Temperature ϑ °C	tan δ	Relative bending Modulus $E'b/E'_{b20}$
185	0.022	0.76
172	0.0155	0.78
160	0.013	0.8
150	0.0115	0.82
140	0.0105	0.84
130	0.0105	0.86
120	0.0108	0.875
110	0.0118	0.89
100	0.013	0.9
90	0.014	0.915
80	0.0145	0.925
70	0.015	0.94
60	0.015	0.95
50	0.016	0.96
42	0.0175	0.97
35	0.0195	0.98
27.5	0.0218	0.99
20	0.0245	1
14	0.0265	1.02
10	0.025	1.03
5	0.0225	1.04
0	0.021	1.055
-5	0.0195	1.07
-10	0.0185	1.08
-20	0.017	1.09
-30	0.017	1.1
-40	0.0185	1.12
-50	0.021	1.135
-60	0.025	1.155

$\overline{\epsilon 'E'}_{b20} = 5.3.10^{10}$ dynes/cm^2.

TABLE II A.

SILK; Dynamic bending properties and Temperature.

Fibre 1.

Temperature °C	Resonant frequency f_o c/s.	tan δ	Relative bending Modulus E'_b/E'_{b20}
140	199	0.028	0.92
133	199.8	0.025	0.928
126	200.4	0.021	0.933
120	201	0.0194	0.939
114	201.9	0.0192	0.948
106.5	202.6	0.0185	0.955
92	203.6	0.017	0.964
78	204.6	0.0164	0.973
64	205.4	0.0157	0.98
50	206.2	0.0153	0.989
35	207.2	0.015	0.998
20	207.4	0.0114	1
6	208.7	0.0102	1.008
-8	209.2	0.01	1.017
-18	210	0.0095	1.025
-30	210.2	0.0088	1.026
-42	210.6	0.0094	1.03
-54.5	211.6	0.0093	1.04
-67	212.4	0.0085	1.048

Fibre dimensions:

Length = 0.5 cm. Mass/unit length = 1.43 μg/cm.

Density = 1.353 gm/cm^3.

$\in'E'_{b20}$ = 10.98. 10^{10} dynes/cm^2.

TABLE II B

SILK: Dynamic bending properties and Temperature

Fibre 2.

Temperature ^{o}C	Resonant frequency f_o c/s	tan δ	Relative bending modulus $E'b/E'_{b20}$
185	201	0.027	0.85
179	201.75	0.022	0.8567
172	202.75	0.0208	0.8654
159.5	205.2	0.0204	0.8857
143	206.5	0.019	0.8974
140	208	0.0157	0.9103
133	208.75	0.0143	0.9175
126	209.6	0.013	0.9243
120	210.25	0.0128	0.9303
114	211	0.0134	0.9367
106.5	211.5	0.0125	0.941
92	212.75	0.0104	0.9523
78	214	0.0092	0.9634
64	215	0.0086	0.9723
50	215.5	0.0086	0.9768
35	216.9	0.01	0.99
20	218	C.0074	1
6	219	0.0062	1.009
-6	220.15	0.0061	1.017
-18	221	0.0064	1.025
-30	221.75	0.0076	1.035
-42	222.95	0.0084	1.046
-54.5	223.1	0.0083	1.047
-67	223.3	0.0076	1.047

Fibre dimensions:

Length = 0.5 cm.

Mass/Unit length = 1.57 μg/cm.

Density = 1.353 gm/cm^3

$\epsilon'E'_{b20}$ = 11.08. 10^{10} dynes/cm^2.

TABLE II C.

SILK: Dynamic bending properties and Temperature.

Fibre 3.

Temperature °C	Resonant frequency f_n o/s.	tan δ	Relative bending modulus $E'b/E'_{b20}$.
185	225.75	0.0216	0.83
179	227.75	0.01816	0.84
172	230	0.0174	0.855
159.5	233.5	0.0162	0.883
143	234	0.0154	0.885
140	236	0.012	0.9
133	237	0.011	0.91
126	238	0.0106	0.92
120	239.75	0.0106	0.93
114	240.5	0.0106	0.937
106.5	241.25	0.0108	0.94
92	242.5	0.0098	0.952
78	243.75	0.009	0.96
64	245	0.0086	0.971
50	245.75	0.0086	0.977
35	247.25	0.009	0.99
20	248.4	0.0051	1
6	249	0.005	1.002
-6	250	0.0052	1.013
-18	250.5	0.0058	1.018
-30	251	0.0069	1.02
-42	251.65	0.0085	1.022
-54.5	252.5	0.009	1.033
-67	255	0.0078	1.055

Fibre dimensions:

Length = 0.4 cm.

Mass/Unit length = 1.5 μg/cm.

Density = 1.353 gm/cc.

$\epsilon' E'_{b20} = 10.34 \ 10^{10}$ dynes/cm^2.

TABLE II D.

SILK: Dynamic bending properties and Temperature.

Mean values.

Temperature - °C	tan δ	Relative bending modulus $E'b/E'_{b20}$
185	0.03	0.84
180	0.0275	0.85
170	0.025	0.87
160	0.024	0.89
150	0.0225	0.9
140	0.0205	0.915
130	0.0175	0.935
120	0.0155	0.94
115	0.015	0.942
106	0.0155	0.95
100	0.0145	0.952
90	0.0135	0.96
80	0.013	0.965
70	0.0125	0.97
60	0.012	0.98
50	0.012	0.985
40	0.012	0.99
35	0.0125	0.992
30	0.011	0.995
25	0.01	0.998
20	0.009	1
10	0.008	1.005
0	0.0073	1.01
-10	0.007	1.015
-20	0.0073	1.02
-30	0.008	1.025
-40	0.0085	1.03
-50	0.0092	1.035
-60	0.0095	1.045

$\overline{\epsilon' E'}_{b20} = 10.8. \ 10^{10}$ dynes/cm^2.

TABLE III A

FIBROLANE: Dynamic bending properties and Temperature.

Fibre 1.

Temperature °C	Resonant frequency f_o c/s.	tan δ	Relative bending modulus. E'_b / E'_{b20}
185	203	0.04	0.83
179	207	0.036	0.845
172	210.6	0.032	0.863
166	214	0.028	0.875
159.5	217	0.0238	0.885
153	218.5	0.021	0.892
146	220.25	0.02	0.9
140	221.75	0.0186	0.905
133	223	0.0157	0.91
126	225.5	0.0118	0.918
120	227.75	0.012	0.928
114.5	229	0.0126	0.935
106.5	230.5	0.0117	0.941
92	233	0.01	0.95
78	235.5	0.0088	0.96
64	237.5	0.01	0.968
50	240	0.012	0.978
35	242.6	0.0144	0.99
20	245.5	0.017	1
5.5	247.5	0.0192	1.01
-6	250	0.0162	I.02
-18	252	0.016	1.037
-30	255.25	0.017	1.04
-42	258	0.0194	1.052
-54.5	260.5	0.0234	1.062
-67	262	0.028	1.07

Fibre dimensions:
Length = 0.508 cm
Mass/Unit length = 3.5 μg/cm.
Density = 1.29 gm/cc.

$\epsilon' E'_{b20} = 5.2\ 10^{10}$ dynes/cm^2

TABLE III B.

FIBROLANE: Dynamic bending properties and Temperature.

Fibre 2.

Temperature °C	Resonant frequency f_o c/s	tan δ	Relative bending modulus $E's/E'_{b20}$
185	233	01031	0.83
179	237	0.0248	0.8475
172	240.5	0.0204	0.867
166	243.5	0.0188	0.376
159.5	245.5	0.018	0.885
153	247.5	0.0174	0.892
146	250	0.016	0.9
140	252.5	0.0135	0.91
133	256	0.0132	0.922
126	258	0.014	0.93
120	260	0.0146	0.936
114.5	261	0.0148	0.94
106.5	262	0.014	0.945
92	264	0.0131	0.95
78	266.5	0.013	0.955
64	269.25	0.0131	0.97
50	272	0.0136	0.98
35	274.75	0.015	0.99
20	277.5	0.0173	1
5.5	280.5	0.0193	1.01
-6	283.2	0.0184	1.021
-18	286	0.0172	1.031
-30	288.5	0.0177	1.04
-42	291.5	0.022	1.051
-54.5	294.7	0.024	1.065
-67	299	0.028	1.078

Fibre dimensions:

Length = 0.485 cm.

Mass/Unit length = 3.87 µg/cm.

Density = 1.29 gm/cc.

$\epsilon' E'_{b20} = 5.83. 10^{10}$ dynes/cm^2.

TABLE III C

FIBROLANE: Dynamic bending properties and Temperature.

Fibre 3.

Temperature °C	Resonant frequency f_o c/s.	tan δ	Relative bending modulus E'_b/E'_{b20}
185	232	0.037	0.83
179	235	0.033	0.845
172	237.5	0.0282	0.852
166	240	0.0236	0.862
159.5	243	0.02	0.872
153	246	0.0198	0.885
146	248	0.0175	0.89
140	252	0.015	0.905
133	256.6	0.01365	0.922
126	257.5	0.0144	0.925
120	259.5	0.0152	0.932
114.5	260.5	0.0153	0.937
106.5	262	0.013	0.94
92	264.5	0.0119	0.95
78	267	0.0116	0.96
64	269.5	0.0125	0.968
50	272	0.0147	0.977
35	275	0.0169	0.987
20	278.5	0.0185	1
5.5	281.7	0.0199	1.01
-6	283.5	0.01905	1.02
-18	286.7	0.0183	1.032
-30	289.45	0.0183	1.04
-42	292.4	0.02	1.05
-54.5	295.5	0.0237	1.062
-67	298.9	0.0274	1.075

Fibre dimensions:

Length = 0.45 cm.

Mass/unit length = 3.47 μg/cm.

Density = 1.29 gm/cm^3

$\epsilon' E'_{b20}$ = 4.865. 10^{10} dynes/cm^2.

TABLE III D.

FIBROLANE: Dynamic bending properties and Temperature.

Temperature °C	tan δ	Relative bending Modulus $E'b/E'_{b20}$
185	0.036	0.84
179	0.0313	0.85
172	0.02686	0.86
166	0.0235	0.87
160	0.0206	0.88
153	0.0194	0.89
146	0.0179	0.9
140	0.0158	0.91
133	0.0142	0.92
126	0.0134	0.93
120	0.0139	0.935
114.5	0.0142	0.945
110	0.0135	0.945
105	0.013	0.95
100	0.0125	0.95
90	0.0115	0.96
80	0.011	0.965
70	0.0112	0.97
60	0.012	0.975
50	0.013	0.98
40	0.0145	0.99
30	0.016	0.995
20	0.0175	1
15	0.019	1.01
5	0.0195	1.015
0	0.019	1.02
-10	0.0175	1.03
-20	0.017	1.035
-30	0.0175	1.04
-40	0.0195	1.05
-50	0.022	1.055
-60	0.0255	1.06

$\overline{\epsilon' E'_{b20}} = 5.3. 10^{10}$ dynes/cm^2.

TABLE IV A.

RAMIE: Dynamic bending properties and Temperature;

Fibre 1.

Temperature ϑ °C	Resonant frequency f_o c/s.	$\tan\delta$	Relative bending modulus E'_b/E'_{b20}
146	191	0.019	0.87
133	194.35	0.0143	0.9
120	195.7	0.0118	0.91
106.5	197.5	0.012	0.93
92	199	0.0115	0.94
78	200.5	0.0095	0.96
64	202	0.0093	0.97
50	202.7	0.0093	0.98
35	204.15	0.0103	0.99
20	205.1	0.0117	1
6	205.5	0.011	1.01
-6	206.5	0.0095	1.015
-18	208	0.0088	1.03
-30	209	0.01	1.04
-42	210	0.0128	1.05
-54.5	212	0.0158	1.07

Fibre dimensions:
Length = 0.7 cm, Mass/unit length = 4 μg/cm.
Density ρ = 1.553 gm/cm^3
ϵ'E'$_{b20}$ = 24.1. 10^{10} dynes/cm^2

TABLE IV B.

RAMIE: Dynamic bending properties and Temperature.

Fibre 2.

Temperature ^{o}C	Resonant frequency f_c c/s	tan δ	Relative bend ind modulus E'_b/E'_{b20}
146	574	0.0125	0.785
133	585	0.01025	0.81
120	595	0.0085	0.84
106.5	603.2	0.00975	0.87
92	612	0.0105	0.89
78	620	0.0095	0.915
64	627	0.00925	0.94
50	633	0.00925	0.955
35	640	0.0105	0.975
20	648	0.01225	1
6	660	0.01225	1.03
-6	673.7	0.01	1.06
-18	681	0.009	1.1
-30	690	0.01	1.125
-42	697.5	0.01275	1.16
-54.5	706	0.01575	1.18

Fibre dimensions: Length = 0.528 cm
Mass/unit length = 4.06 μg/cm.
Density = 1.553 gm/cm^3
$\epsilon' E'_{b20}$ = 78.89. 10^{10} dynes/cm^2.

TABLE IV C.

RAMIE: Dynamic bending properties and Temperature.

Fibre 3.

Temperature °C	Resonant frequency f_o c/s.	tanδ	Relative bending modulus E'_b/E'_{b20}
146	338	0.019	0.89
133	342.3	0.01425	0.91
120	346.4	0.0105	0.935
106.5	348.65	0.01	0.95
92	350.7	0.00925	0.96
78	352.65	0.0085	0.97
64	354.3	0.00825	0.98
50	355.5	0.008	0.985
35	356.75	0.00825	0.99
20	358.25	0.00925	1
6	360.25	0.009	1.01
-6	361.5	0.008	1.015
-18	363.75	0.00775	1.03
-30	366	0.0085	1.04
-42	371	0.011	1.07
-54.5	376	0.014	1.1

Fibre dimensions: length = 0.622 cm. Mass/Unit length = 4.56 μg/cm.

Density = 1.553 gm/cm^3

$\epsilon E'_{b20}$ = 25.75. 10^{10} dynes/cm^2.

TABLE IV D.

Ramie: Dynamic bending properties and Temperature

Mean values.

Temperature °C	tanδ	Relative bending Modulus E'_b/E'_{b20}
146	0.017	0.85
140	0.0145	0.86
130	0.0118	0.88
120	0.0105	0.9
110	0.0105	0.91
105	0.0115	0.918
100	0.011	0.922
90	0.01	0.935
80	0.0095	0.94
70	0.009	0.96
60	0.0085	0.97
50	0.0088	0.975
40	0.009	0.98
30	0.01	0.99
20	0.011	1
10	0.01	1.01
0	0.009	1.02
-10	0.0085	1.03
-20	0.0085	1.045
-30	0.009	1.06
-40	0.011	1.08
-54	0.015	1.11

TABLE V A.

FORTISAN: Dynamic bending properties and Temperature.

Fibre 1.

Temperature : °C	Resonant frequency f_o c/s.	tan δ	Relative bending modulus $E'b/E'_{b20}$
146	276.5	0.0295	0.724
133	283.5	0.0255	0.778
120	290	0.021	0.836
106.5	294.5	0.0163	0.84
92	298	0.016	0.86
78	304	0.012	0.894
64	309	0.00975	0.924
50	311.5	0.00875	0.939
35	315.5	0.01	0.963
20	321.5	0.015	1
6	325.5	0.0133	1.025
-6	329	0.013	1.047
-18	332.5	0.01375	1.07
-30	336	0.016	1.09
-42	340	0.019	1.12
-54.5	344	0.022	1.145

Fibre dimensions:

Length = 0.49 cm.

Mass/unit length = 1.11 µg/cm

Density = 1.52 gm/cm^3

$\epsilon' E'_{b20}$ = 49.82 10^{10} dynes/cm^2.

TABLE V B.

FORTISAN: Dynamic bending properties and Temperature.

Fibre 2.

Temperature °C	Resonant frequency f_o c/s.	tanδ	Relative bending modulus E'_b/E'_{b20}
146	234	0.031	0.745
133	240.5	0.026	0.79
120	246.5	0.02	0.83
106.5	252	0.0163	0.865
92	256	0.0165	0.89
78	260	0.0133	0.92
64	263.5	0.0105	0.945
50	266.5	0.009	0.97
35	268.5	0.0093	0.98
20	271	0.017	1
6	273.5	0.0155	1.02
-6	275.5	0.0153	1.035
-18	278	0.01675	1.055
-30	280.5	0.019	1.075
-42	283	0.022	1.09
-54.5	285	0.025	1.1

Fibre dimensions:

Length = 0.524 cm.

Mass/unit length = 1.1 μg/cm.

Density = 1.52 gm/cm^3

$\epsilon' E'_{b20}$ = 46.28. 10^{10} dynes/cm^2.

TABLE V C.

FORTISAN: Dynamic bending properties and Temperature.

Fibre 3.

Temperature $^{\circ}C$	Resonant frequency f_o c/s.	$\tan \delta$	Relative bending modulus $E'b/E'_{b20}$
146	290	0.033	0.745
133	295	0.027	0.775
120	304.5	0.021	0.83
106.5	309	0.0165	0.85
92	313	0.015	0.87
78	319.5	0.0123	0.91
64	325	0.0083	0.94
50	329	0.0075	0.97
35	332	0.0083	0.98
20	335	0.01075	1
6	338	0.0083	1.02
-6	341	0.008	1.04
-18	343	0.01	1.05
-30	345	0.012	1.06
-42	348	0.015	1.08
-54.5	351	0.02	1.1

Fibre dimensions:

Length = 0.5 cm.

Mass/unit length = 1.1 μg/cm.

Density = 1.52 gm/cm^3

$\epsilon' E'_{b20}$ = 58.64 $1o^{10}$ dynes/cm^2.

TABLE V D.

FORTISAN: Dynamic bending properties and Temperature.

Mean values.

Temperature °C	tan δ	Relative bending Modulus E'_b/E'_{b20}
146	0.0305	0.733
140	0.028	0.765
130	0.0235	0.8
120	0.02	0.82
114	0.0175	0.83
107	0.015	0.85
100	0.014	0.86
92	0.015	0.88
80	0.0125	0.91
70	0.01	0.93
60	0.0085	0.95
50	0.008	0.965
40	0.0085	0.98
30	0.0105	0.99
20	0.013	1
10	0.011	1.01
0	0.01	1.03
-10	0.01	1.045
-20	0.011	1.06
-30	0.014	1.08
-40	0.017	1.1
-50	0.02	1.12
-54.5	0.0215	1.13

$\overline{\epsilon' E'}_{b20} = 51.56.10^{10}$ dynes/cm^2.

TABLE VI A.

VISCOSE: Dynamic bending properties and Temperature.

Fibre 1.

Temperature $^{\circ}C$	Resonant frequency f_o c/s.	$\tan \delta$	Relative bending modulus E'_b / E'_{b20}
192	324	0.0468	0.65
185	327	0.0425	0.66
172	329	0.0357	0.67
159.5	334	0.0315	0.07
147	339	0.0285	0.72
140	346.7	0.0245	0.732
133	351.7	0.022	0.76
120	361.25	0.0175	0.805
106.5	367.5	0.014	0.83
92	375.4	0.011	0.87
78	381.5	0.009	0.9
70.5	385.5	0.0085	0.91
64	387.3	0.0083	0.925
56.5	388.8	0.0086	0.935
50	391	0.0075	0.942
35	396.75	0.008	0.97
27.5	400.5	0.0085	0.99
20	403	0.009	1
6	406.5	.0104	1.02
-6	410.75	0.013	1.04
-18	415	0.0175	1.06
-30	419.5	0.0225	1.08
-42	425	0.0275	1.111
-54.5	433.5	0.033	1.16
-67	440.7	0.039	1.2

Fibre dimensions:

Length = 0.474 cm.

Mass/Unit length = 6.66 μg/cm.

Density = 1.51 gm/cm^3

$\epsilon' E'_{b20}$ = 8.96 10^{10} dynes/cm^2.

TABLE VI B.

VISCOSE: Dynamic bending properties and Temperature.

Fibre 2.

Temperature ^{o}C	Resonant frequency f_o c/s.	$\tan\delta$	Relative bending Modulus E'_b/E'_{b20}
185	302	0.046	0.66
172	306	0.0417	0.67
159.5	310	0.0358	0.685
147	316.5	0.0318	0.712
140	323	0.025	0.75
133	326.5	0.022	0.76
120	335	0.018	0.8
106.5	341.8	0.0145	0.83
92	347.5	0.0115	0.86
78	353	0.0095	0.89
70.5	355.8	0.009	0.9
64	358.2	0.0088	0.915
56.5	359.5	0.009	0.92
50	363.2	0.0075	0.94
35	368	0.008	0.965
27.5	370.35	0.0085	0.985
20	374.4	0.009	1
6	377.5	0.01	1.02
-6	382.6	0.0125	1.042
-18	386	0.0165	1.06
-30	390.25	0.021	1.084
-42	395.5	0.026	1.111
-54.5	402	0.031	1.15
-67	409.5	0.037	1.2

Fibre dimensions:

Length = 0.5 cm.

Mass/Unit length = 6.66 μg/cm.

Density 1.51 gm/cm^3

$\epsilon' E'_{b20} = 9.55\ 10^{10}$ dynes/cm^2.

TABLE VI C

VISCOSE: Dynamic bending properties and Temperature.

Mean values.

Temperature °C	tan δ	Relative bending Modulus $E'b/E'_{b20}$
190	0.0465	0.65
180	0.0425	0.67
170	0.0375	0.685
163	0.0345	0.69
157	0.0325	0.71
147	0.03	0.73
140	0.025	0.75
130	0.0215	0.775
120	0.018	0.8
110	0.0155	0.82
100	0.013	0.84
90	0.0115	0.86
80	0.01	0.89
70	0.009	0.91
64	0.0085	0.925
56	0.009	0.94
50	0.0075	0.95
40	0.008	0.97
30	0.008	0.98
20	0.009	1
10	0.0095	1.01
0	0.0115	1.03
-10	0.014	1.05
-20	0.0175	1.07
-30	0.0215	1.09
-40	0.0255	1.11
-50	0.03	1.145
-60	0.035	1.18

$\overline{\epsilon' E'_{b20}} = 9.255. 10^{10}$ dynes/cm^2.

TABLE VII A

Acetate: Dynamic bending properties and Temperature.

Fibre 1.

Temperature. °C	Resonant frequency f_o c/s	tanδ	Relative bending modulus E'_b/E'_{b20}
172	226	0.05	0.62
159.5	234	0.0442	0.663
146	241.5	0.0376	0.701
133	248.5	0.0325	0.755
120	253.75	0.0298	0.78
106.5	259.5	0.027	0.81
92	265	0.025	0.85
78	270	0.0244	0.885
64	274.5	0.0252	0.915
50	279.3	0.0266	0.945
42	280	0.0275	0.95
35	284	0.0282	0.98
27.5	285.5	0.028	0.99
20	287.5	0.0279	1
6	293.5	0.0288	1.04
-6	300	0.0296	1.09
-18	301.5	0.0304	1.1
-30	306.5	0.0306	1.14
-42	310.5	0.0316	1.165
-48.5	312.5	0.032	1.18
-54.5	314.5	0.0326	1.2
-67	318.5	0.0308	1.23

Fibre dimensions:

Length = 0.521 cm.

Mass/Unit length = 6.15 µg/cm.

Density = 1.33 gm/cm^3

$\epsilon' E'_{b20}$ = 7.2 10^{10} dynes/cm^2.

TABLE VII B

ACETATE: Dynamic bending properties and Temperature.

Fibre 2.

Temperature °C	Resonant frequency f_r c/s.	tanδ	Relative bending modulus E'_b/E'_{b20}
172	177.5	0.0558	0.525
159.5	188.5	0.0526	0.59
146	197	0.047	0.648
133	204	0.0393	0.69
120	209	0.0346	0.73
106.5	214	0.0308	0.765
92	220	0.0278	0.81
78	226	0.025	0.85
64	231	0.026	0.89
50	235.5	0.0296	0.92
42	239	0.0318	0.95
35	242.5	0.035	0.98
27.5	243.5	0.0328	0.99
20	245.	0.0306	1
6	249	0.032	1.03
-6	254.5	0.0336	1.08
-18	256	0.034	1.09
-30	259.5	0.0346	1.12
-42	264.5	0.0266	1.165
-48.5	267	0.0375	1.19
-54.5	269.5	0.0384	1.21
-67	275.5	0.036	1.26

Fibre dimensions:

Length = 0.565 cm.

Mass/Unit length = 6.15 μg/cm

Density = 1.33 g./cm^3

$\epsilon' E'$ = 7.1 10^{10} dynes/cm^2

TABLE VII C

ACETATE: Dynamic bending properties and Temperature.

Fibre 3

Temperature °C	Resonant frequency f_o c/s.	tan δ	Relative bending modulus $E'b/E'_{b20}$
172	224.5	0.0536	0.58
159.5	235	0.048	0.645
146	244.5	0.04	0.7
133	252	0.0318	0.74
120	253.5	0.03	0.78
106.5	265	0.029	0.82
92	268.5	0.0278	0.84
78	273	0.0274	0.86
64	278.5	0.0283	0.905
50	282.5	0.0314	0.932
42	284.5	0.0338	0.94
35	287.5	0.035	0.97
27.5	289.4	0.0328	0.98
20	292.5	0.0306	1
6	296.75	0.031	0.03
-6	303	0.032	1.078
-18	307.5	0.0324	1.1
-30	312.5	0.0326	1.12
-42	318	0.0333	1.18
-48.5	320.5	0.034	1.2
-54.5	323	0.0344	1.22
-67	326.5	0.0314	1.24

Fibre dimensions:

Length = 0.525 cm. Mass/Unit length = 6.15 μg/cm.

Density = 1.33 g/cm^3

$\epsilon' E'_{b20}$ = 7.5 10^{10} dynes/cm^2

TABLE VII D.

ACETATE: Dynamic bending properties and Temperature.

Mean values.

Temperature °C	tan δ	Relative bending modulus $E'b/E'_{b20}$
172	0.0525	0.575
160	0.047	0.625
150	0.0425	0.665
140	0.0385	0.7
130	0.035	0.73
120	0.0315	0.76
110	0.029	0.79
100	0.027	0.82
90	0.0256	0.84
80	0.025	0.865
70	0.0256	0.89
60	0.027	0.915
50	0.0285	0.94
40	0.0305	0.96
35	0.032	0.97
25	0.03	0.99
20	0.0295	1
10	0.0295	1.025
0	0.0305	1.05
-10	0.0315	1.075
-20	0.032	1.1
-30	0.032	1.125
-40	0.031	1.155
-50	0.034	1.19
-60	0.034	1.225

$\overline{\epsilon' E'_{b20}} = 7.3 \cdot 10^{10}$ dynes/cm^2.

TABLE VIII A

TRICEL: Dynamic bending properties and Temperature.

Fibre 1.

Temperature °C	Resonant frequency f_o c/s	tan δ	Relative bending modulus E'_b/E'_{b20}
166	134	0.0615	0.63
159.5	136	0.059	0.65
153	138.5	0.056	0.675
146	141	0.0515	0.7
140	143	0.044	0.72
133	145.8	0.0415	0.75
126	147.5	0.04	0.767
120	149.5	0.036	0.787
114	151	0.032	0.804
106.5	152.5	0.031	0.82
92	155.5	0.031	0.85
85	156.7	0.031	0.865
73	158.	0.03	0.88
70.5	159	0.0285	0.89
64	160.5	0.027	0.91
57	161.5	0.0265	0.92
50	162.5	0.028	0.93
35	165.5	0.03	0.963
27.5	166.5	0.031	0.977
20	168.5	0.0325	1
6	170.3	0.035	1.021
-6	172.3	0.035	1.041
-18	174.3	0.034	1.07
-32	177	0.032	1.1
-42	180	0.0325	1.14
-54.5	181.2	0.036	1.16
-67	183.	0.033	1.18

Fibre dimensions:

Length = 0.475 cm.

Mass/Unit length = 2.04 μg/cm.

Density = 1.30 g/cm^3

$\epsilon' E'_{b20}$ = 4.832. 10^{10} dyn/cm^2.

TABLE VIII B.

TRICEL: Dynamic bending properties and Temperature.

Fibre 2.

Temperature $^{\circ}C$	Resonant frequency f_o c/s.	$\tan\delta$	Relative bending Modusus $E'b/E'_{b20}$
166	133	0.061	0.565
159.5	135	0.0585	0.625
153	137.5	0.055	0.637
146	141	0.051	0.667
140	144	0.0425	0.69
133	147.8	0.041	0.725
126	150	0.039	0.743
120	152.5	0.035	0.765
114	154.5	0.031	0.782
106.5	156.5	0.0305	0.802
92	160	0.0305	0.835
85	161.5	0.03	0.847
78	163	0.029	0.865
70.5	164.8	0.0275	0.88
64	166	0.0265	0.895
57	168	0.026	0.91
50	169.5	0.027	0.925
35	170.5	0.0295	0.946
27.5	174.5	0.031	0.973
20	177	0.032	1
6	181	0.035	1.021
-6	183.5	0.036	1.041
-18	185.8	0.033	1.072
-30	185.8	0.03	1.1
-42	188.2	0.0315	1.135
-54.5	190.7	0.034	1.16
-67	193	0.031	1.18

Fibre dimensions:
Length = 0.507 cm.

Mass/unit length = 2.04 μg/cm

Density = 1.30 gm/cm^3

$\epsilon'E'_{b20} = 6.9\ 10^{10}$

TABLE VIII C.

TRICEL: Dynamic bending properties and Temperature.

Mean Values.

Temperature °C	tan δ	Relative bending Modulus E'_b/E'_{b20}
166	0.0615	0.59
160	0.059	0.62
153	0.0555	0.64
146	0.051	0.67
140	0.0435	0.69
130	0.0405	0.73
120	0.0355	0.76
110	0.0305	0.79
100	0.03	0.82
90	0.03	0.84
80	0.03	0.86
70	0.028	0.89
60	0.0265	0.9
50	0.0275	0.93
40	0.029	0.945
30	0.0305	0.97
20	0.0325	1
10	0.034	1.02
0	0.036	1.04
-10	0.035	1.06
-20	0.033	1.08
-30	0.0315	1.1
-40	0.0315	1.13
-50	0.034	1.15
-55	0.035	1.16
-67	0.032	1.18

Table IX A.

ACRILAN 16: Dynamic bending properties and Temperature.

Normal Fibre.

Temperature °C	Resonant frequency f_o c/s.	tan δ	Relative bending Modulus E'_b/E'_{b20}
131.5	60.5	0.485	0.0475
129.5	67	0.51	0.058
110	137.5	0.312	0.245
106.5	154	0.26	0.308
103	172.5	0.24	0.385
102	171.5	0.198	0.38
98	184.5	0.168	0.44
95.5	190.5	0.163	0.47
93.5	195.5	0.148	0.495
89.5	206	0.136	0.55
87	211	0.132	0.578
84	216	0.12	0.605
80.5	222	0.117	0.638
76	229.5	0.1	0.68
73	234.5	0.098	0.712
68	240.5	0.094	0.75
63.5	246	0.0895	0.782
57	253	0.075	0.83
51	256.8	0.072	0.855
44.5	263	0.0685	0.895
40	266.5	0.062	0.92
33	271.1	0.0555	0.945
27.5	274.2	0.052	0.975
20	278	0.045	1
8	284	0.0352	1.04
-5	289	0.0277	1.08
-13	292.1	0.0238	1.1
-25.5	296.25	0.0185	1.14
-37	298.8	0.0154	1.16
-48	300.9	0.0118	1.17
-60	302.5	0.0112	1.18

Fibre Dimensions:
Length = 0.702 cm: Mass/Unit length 8.9 μg/cm.
Density = 1.1845 gm/cc.
$\epsilon E'_{b20} = 11.9\ 10^{10}$ dynes/cm^2

TABLE IX B.

ACRILAN 16: Dynamic bending properties and Temperature.

Heat Set at 130° for 1 hour under 10% extension.

Temperature °C	Resonant frequency f_o c/s.	$\tan\delta$	Relative bending Modulus E'_b/E'_{b20}
110	77	0.39	0.152
107.5	83	0.362	0.177
104	98.5	0.289	0.25
101	105.5	0.252	0.285
96	121	0.19	0.375
92	130	0.1615	0.43
87	142	0.141	0.52
82	150	0.1265	0.575
76	158	0.114	0.64
71	164	0.0975	0.69
63.5	172	0.09	0.755
55	177.8	0.86	0.81
49	181.8	0.077	0.85
42	186.7	0.07	0.89
35	190.5	0.063	0.93
26.5	195	0.055	0.975
20	197.4	0.05	1
17.5	198.4	0.044	1.01
5.5	202	0.04	1.03
-4	206.3	0.028	1.09
-19.5	209	0.024	1.12
-29.5	211	0.0208	1.14
-42	213	0.0141	1.16
-54.5	214.75	0.0117	1.18
-63	216	0.0925	1.2

Fibre dimensions:
Length = 0.725 cm: Mass/Unit length = 6.25 µg/cm.
Density = 1.187 gm/cc.

$\epsilon' E'_{b20} = 9.74 \cdot 10^{10}$ dynes/cm^2.

TABLE IX C

ACRILAN 16: Dynamic bending properties and Temperature.

Set in boiling water at 100°C for 1 hour under 10% extension.

Temperature °C	Resonant frequency f_o c/s	tan δ	Relative bending Modulus E'_b/E'_{b20}.
110	87.5	0.343	0.226
105.25	93	0.28	0.255
100	108.5	0.193	0.35
95	124.5	0.1465	0.466
88	135.8	0.1265	0.545
82.5	142.5	0.105	0.6
78.5	148	0.0965	0.648
75	151	0.093	0.672
69	156.5	0.083	0.722
60	162.6	0.079	0.78
55	166.4	0.077	0.82
52.5	167.65	0.0762	0.84
50	169.7	0.0765	0.85
44.5	173.5	0.0658	0.89
35	177.75	0.059	0.93
28	181.7	0.055	0.975
20	184	0.047	1
6.5	188.2	0.037	1.045
-5	191.4	0.0324	1.08
-20.5	194.8	0.0257	1.12
-29.5	196.7	0.0203	1.14
-43	198.9	0.014	1.16
-54	200.4	0.011	1.19
-63.5	201.7	0.01	1.2

Fibre dimensions.

Length = 0.8 cm. Mass/unit length = 9.16 μg/cm.

Density = 1.186 g./cm^3.

$\epsilon' E'_{b20} = 8.36 . 10^{10}$ dynes/cm^2.

TABLE IX D.

ORLON: Dynamic bending properties and Temperature.

Temperature ^{o}C	Resonant frequency f_o c/s.	$\tan\delta$	Relative bending Modulus $E'b/E'_{b20}$
124	84	0.214	0.0915
122.5	86.5	0.235	0.095
120.5	90.5	0.25	0.103
118.5	95	0.274	0.107
116.5	100.5	0.23	0.133
112	111	0.306	0.173
108	126	0.286	0.182
106	132	0.266	0.226
102	153	0.235	0.305
98	165	0.194	0.355
93	183	0.186	0,435
91	193	0.166	0.485
87	199	0.161	0.512
79.5	213.5	0.136	0.59
74.5	221	0.12	0.635
70.5	228	0.11	0.675
65.6	234.5	0.115	0.715
63	238.2	0.11	0.74
60	242.3	0.1	0.765
50	253	0.086	0.83
42.5	261	0.0766	0.885
37	265	0.066	0.91
29	272	0.0595	0.96
20	277.5	0.053	1
10	283	0.046	1.03
0	287	0.042	1.06
-10	291	0.04	1.09
-20	294	0.036	1.12
-30	296	0.03	1.14
-40	299	0.025	1.16
-50	301	0.022	1.175
-60	302.5	0.02	1.185

Fibre dimensions:
Length = 0.535 cm: Mass/unit length = 2.8 μg/cm.
Density = 1.17 gm/cm^3
Resonant frequency at 20^{o}C = 277.5 and 371 cps.
ϵ' E'_{b20} = 12.4.10 and 22.16 10^{10} dynes/cm^2.

TABLE X A.

POLYPROPYLENE A: Dynamic bending properties and Temperature.

Fibre 1.

Temperature ϑ^{o}C	Resonant frequency f_o c/s.	tanδ	Relative bending Modulus E'_b/E'_{b20}
126.5	137.2	0.094	0.24
120	143	0.086	0.26
106.5	152	0.071	0.295
92	162	0.058	0.335
78	172.5	0.049	0.38
70.5	179	0.048	0.41
64	187.5	0.05	0.45
57	194	0.053	0.48
50	198	0.059	0.52
42	213	0.071	0.58
35	227.5	0.1	0.66
27.5	250	0.11	0.8
20	280	0.131	1
18	285.5	0.134	1.04
13.5	303	0.128	1.17
6	326	0.1	1.36
0	365	0.07	1.56
-6	366	0.05	1.7
-18	383	0.04	1.87
-24	390	0.037	1.94
-37.5	399	0.036	2.04

Fibre dimensions:

Length = 0.503 cm: Mass/Unit length = 3.4 µg/cm.

Density = 0.92 g/cm^3

$\epsilon' E'_{b20}$ = $3.989.10^{10}$ dynes/cm^2.

TABLE X B

POLYPROPYLENE A: Dynamic bending properties and Temperature Fibre 2.

Temperature °C	Resonant frequency f_o c/s.	$\tan\delta$	Relative bending Modulus E'_b/E'_{b20}
126.5	137	0.094	0.24
120	143	0.086	0.26
110	148	0.075	0.28
106.5	151	0.0715	0.29
92	163.5	0.059	0.34
78	173	0.05	0.38
70,5	177	0.0485	0.4
64	181.5	0.05	0.42
57	187.8	0.053	0.45
50	198	0.0575	0.5
42	218.8	0.068	0.56
35	237.5	0.095	0.64
27.5	247.5	0.11	0.78
20	280	0.1305	1
18	288	0.134	1.06
13.5	309.5	0.128	1.18
6	322	0.095	1.36
0	348	0.07	1.54
-6	365	0.0525	1.7
-18	373	0.041	1.87
-24	390	0.038	1.94
-37.5	400	0.0365	2.06

Fibre dimensions: Length = 0.5 cm: Mass/unit length = 3.4 µg/cm.

Density = 0.92 g/cm^3

$\epsilon' E'_{b20}$ = $3.9.10^{10}$ dynes/cm^2.

TABLE X C

POLYPROPYLENE B: Dynamic bending properties and Temperature

Fibre 1.

Temperature °C	Resonant frequency f_o c/s.	tanδ	Relative bending Modulus $E'b/E'_{b20}$
120	154	0.086	0.2
114	160	0.078	0.21
106.5	165.6	0.072	0.23
99	176	0.065	0.26
90	185.5	0.058	0.29
75	212	0.05	0.345
70.5	216.8	0.048	0.395
60	234.3	0.05	0.46
45	266	0.064	0.595
42	272	0.07	0.62
39.5	284	0.074	0.68
35	292	0.09	0.72
27.5	314	0.11	0.83
20	345	0.13	1
13.5	393	0.13	1.3
6	432.5	0.096	1.57
-6	469.5	0.052	1.85
-12	478	0.044	1.93
-22	491	0.038	2.05
-28	503	0.036	2.14
-35	505	0.034	2.15

Fibre dimensions: Length = 0.543 cm: Mass/unit length = 5.6 μg/cm.

Density = 0.915 g./cm^3

$\epsilon'E'_{b20}$ = $4.934.10^{10}$ dynes/cm^2.

TABLE X D.

POLYPROPYLENE B: Dynamic bending properties and Temperature Fibre 2.

Temperature ^{o}C	Resonant frequency f_o c/s.	tan δ	Relative bending Modulus E'_b/E'_{b20}
120	198	0.086	0.22
114	207	0.078	0.24
101	215	0.066	0.26
92	227	0.058	0.29
78	261.5	0.052	0.38
66	278	0.05	0.435
60	286	0.05	0.46
49	307.5	0.06	0.53
45	319.5	0.064	0.57
39.5	336.5	0.074	0.637
35	357	0.09	0.72
29	379	0.106	0.805
24.5	400	0.12	0.9
20	422	0.132	1
10	490	0.116	1.34
-6	516.5	0.086	1.87
-16	595.5	0.04	2
-24	613	0.036	2.1
-30	620	0.034	2.15
-35	625	0.034	2.18

Fibre dimensions: Length = 0.47 cm: Mass/unit length = 6 μg/cm.

Density = 0.915 g./cm^3.

$\epsilon' E'_{b20}$ = 4.9. 10^{10} dynes/cm^2.

TABLE X E

POLYPROPYLENE A AND B: Dynamic bending properties and Temperature. Mean values.

Temperature - °C	tan δ	Relative bending Modulus E' b / E' b20.	
		A	B
126.5	0.094	0.24	0.21
120	0.086	0.26	0.22
110	0.075	0.28	0.23
100	0.066	0.3	0.26
90	0.058	0.33	0.3
80	0.052	0.36	0.33
70	0.048	0.4	0.38
60	0.05	0.45	0.45
50	0.058	0.52	0.53
40	0.074	0.62	0.64
30	0.103	0.78	0.78
20	0.13	1	1
10	0.116	1.26	1.34
0	0.07	1.55	1.66
-10	0.045	1.75	1.85
-20	0.038	1.87	1.96
-30	0.034	1.96	2.1
-37.5	0.0335	2.05	2.2

$\overline{\epsilon' E'}_{b20}A = 3.94. 10^{10}$ dynes/cm^2.

$\overline{\epsilon' E'}_{b20}B = 4.9. 10^{10}$ dynes/cm^2.

TABLE X F.

POLYPROPYLENE C: Dynamic bending properties and Temperature.

Temperature ^{o}C	Resonant frequency f_o c/s	$\tan\delta$	Relative bending Modulus E'_b/E'_{b20}
85	46	0.11	0.22
76.5	52	0.094	0.28
72	57	0.086	0.32
66.5	59.2	0.08	0.36
61	62.7	0.076	0.4
50	67.2	0.06	0.47
42.5	76.3	0.068	0.6
35	80.2	0.09	0.67
27.5	91	0.12	0.86
23	97	0.12	0.98
20	98	0.11	1
17.5	100	0.1	1.04
16	109.25	0.092	1.25
6	118.5	0.064	1.46
1	123	0.056	1.57
-6	133	0.047	1.74
-12.5	134.5	0.042	1.88
-18	136	0.039	1.92
-24	138	0.038	1.98

Fibre dimension: Length = 2.03: Mass/unit length = 77.8 μg/cm.

Density = 0.905 g./cm^3.

$\epsilon' E'_{b20}$ = $5.48.10^{10}$ dynes/cm^2.

TABLE XI A.

NYLON 66: Dynamic bending properties and Temperature.

Type 200.

Temperature °C	Resonant frequency f_o c/s.	tan δ.	Relative bending Modulus. E'_b/E'_{b20}.
150	135	0.0608	0.288
145.5	139.35	0.0695	0.306
139.5	143.85	0.0785	0.325
135	148	0.084	0.345
130	153.7	0.091	0.374
126	156.8	0.0975	0.386
122	160.9	0.1	0.408
116	171	0.095	0.46
111	179.4	0.085	0.508
105	186.2	0.0795	0.548
95.5	201.6	0.0595	0.64
88	213.1	0.0356	0.715
81	221.5	0.0253	0.775
76	225	0.0195	0.8
70	230	0.0156	0.835
63.5	233.5	0.0128	0.86
55	237.6	0.0101	0.89
46.5	241.1	0.009	0.92
38.5	244	0.009	0.94
30	246.9	0.009	0.96
23	247.7	0.009	0.99
20	252	0.009	1
6	258.6	0.009	1.03
-6	262	0.0108	1.06
-18	266	0.012	1.09
-30	269	0.0141	1.12
-42	272	0.0165	1.14
-54.5	276	0.02	1.17
-67	279	0.025	1.2

Fibre dimensions:

Length = 0.563 cm, Mass/unit length = 7 μg/cm.

Density = 1.14 g./cm^3.

$\epsilon' E'_{b20}$ = 4.85. 10^{10} dynes/cm^2.

TABLE XI B.

NYLON 66: Dynamic bending properties and temperature.

Type 300.

Temperature - ^{o}C	Resonant frequency f_c c/s.	tan δ	Relative bending Modulus E'_b/E'_{b20}
153	156	0.064	0.328
147	161.8	0.074	0.354
140.5	166.2	0.084	0.38
135.5	174.3	0.092	0.41
130.5	176.5	0.0965	0.42
127	180.9	0.098	0.44
124.5	186.7	0.0975	0.47
121	188.7	0.097	0.48
118	192.5	0.095	0.5
113	201.95	0.088	0.55
110.5	204.4	0.083	0.565
104	212.95	0.0695	0.612
98.5	220	0.0455	0.65
94	225.9	0.0408	0.69
89.5	231.6	0.032	0.72
82	240.6	0.0208	0.785
76	244.55	0.0176	0.81
69	249.85	0.0148	0.84
62.5	253.3	0.0142	0.862
55	257.1	0.012	0.895
45.5	261.7	0.01	0.925
38.5	264.75	0.009	0.95
28	269.5	0.0093	0.98
20	275.4	0.0095	1
6	279.3	0.0097	1.03
-5	283.4	0.0113	1.06
-23	289.25	0.0121	1.1
-34	294	0.015	1.14
-48	296.1	0.0178	1.16
-54	299	0.02	1.18
-63.5	303	0.023	1.23

Fibre dimensions: Length = 0.56 cm: Mass/unit length = 7 μg/cm.
Density = 1.14 g./cm^3.

$\epsilon' E'_{b20} = 6.1.10^{10}$ dynes/cm^2.

TABLE XI C.

NYLON 66: Dynamic bending properties and Temperature.

Type 600.

Temperature - °C	Resonant frequency f_r c/s.	tan δ	Relative bending Modulus E'_b/E'_{b20}.
155.5	137	0.08	0.29
149.5	139.6	0.086	0.3
146	144	0.092	0.32
140	147.5	0.098	0.335
135	153.25	0.101	0.36
131.5	156.4	0.102	0.376
127	161.25	0.107	0.4
124	165.7	0.107	0.42
117.5	174	0.104	0.465
111	184.6	0.098	0.52
104.5	196	0.089	0.59
100	201.5	0.0785	0.625
94	211.9	0.0615	0.69
90	214.9	0.0512	0.71
85	222.7	0.031	0.765
80.5	227.2	0.022	0.795
75	230.5	0.019	0.82
69	235.2	0.0136	0.85
63.5	238	0.0118	0.87
57	242.8	0.0102	0.91
43	247	0.00975	0.94
36	249	0.00965	0.955
30	251.8	0.0095	0.975
20	255	0.009	1
6	259	0.0085	1.03
-5	262.4	0.00875	1.06
-18	266.4	0.0124	1.095
-28	269.5	0.0134	1.11
-40	273.2	0.0146	1.15
-48.5	275	0.017	1.16
-63.5	281.7	0.0234	1.22

Fibre dimensions:

Length = 0.6 cm : Mass/unit length = 6.68 μg/cm.

Density = 1.14 cm^3

$\epsilon' E'_{b20}$ = 6.6. 10^{10} dynes/cm^2.

TABLE XII A.

NYLON 66: Dynamic bending properties and Temperature

Type A.

Temperature °C	Resonant frequency f_o c/s.	tan δ	Relative bending Modulus E'_b/E'_{b20}
160.5	151.4	0.064	0.27
155	155.2	0.071	0.285
151	158.4	0.0782	0.296
147	161.3	0.0868	0.308
141.5	166.5	0.096	0.326
136.5	172.8	0.103	0.35
133	177.8	0.107	0.374
129	182.25	0.106	0.4
127.5	187.2	0.101	0.415
122	195.5	0.092	0.45
117.5	205	0.078	0.496
114.5	208	0.074	0.51
110	218	0.064	0.56
106	224	0.055	0.592
102	231.3	0.0434	0.63
98	238	0.0382	0.67
90	248	0.027	0.73
83.5	254	0.0232	0.76
80	257.85	0.02	0.785
74	262.4	0.0152	0.812
69	265.5	0.014	0.83
58	272.6	0.0106	0.88
47	277.65	0.009	0.91
37	282.2	0.0085	0.94
26.5	286.9	0.0084	0.975
20	290.9	0.00825	1

Fibre dimensions:

Length = 0.53 cm: Mass/unit length = 5.74 µg/cm.

Density = 1.15 gm/cm^3, fo at 20°C = 298 and 291 cps.

$\epsilon' E'_{b20}$ = 6.486. 10^{10} and 6.144. 10^{10} dynes/cm^2.

TABLE XII B.

NYLON 66: Dynamic bending properties and Temperature.

Type B.

Temperature °C	Resonant frequency f_c c/s.	tan δ	Relative bending Modulus E'_b/E'_{b20}
151	157.6	0.078	0.272
146	164.2	0.0854	0.292
143.5	166.5	0.0915	0.304
140.5	169	0.095	0.314
135.5	175	0.103	0.335
132	180.85	0.108	0.358
126.5	189.5	0.114	0.394
121.5	199.3	0.1135	0.435
117	205	0.107	0.46
112	217	0.092	0.508
108	224	0.0855	0.55
104	233	0.075	0.595
100	240.4	0.0655	0.636
94	249	0.05	0.68
88	259.5	0.038	0.735
80	267	0.0225	0.782
75	271.7	0.019	0.808
68	276	0.01485	0.835
63.5	281.5	0.0124	0.85
54	286	0.0105	0.89
44	291	0.01	0.93
34	295.2	0.0095	0.955
27	297.5	0.0099	0.97
22	299.8	0.00935	0.98
20	302	0.0095	1

Fibre dimensions:

Length = 0.535 cm: Mass/Unit length = 6.8 μg/cm.

Density = 1.43 gm/cm^3

f_o at 20°C = 314 and 302 cps.

$\epsilon' E'_{b20}$ = 6.233.10^{10} and 5.768. 10^{10} dynes/cm^2.

TABLE XII C.

NYLON 66: Dynamic bending properties and Temperature.

Type C.

Temperature °C	Resonant frequency f_o c/s.	tan δ	Relative bending Modulus E'_b / E'_{b20}
153	135.8	0.081	0.266
148	138.6	0.0886	0.277
141.5	145.7	0.097	0.305
134	153	0.1145	0.339
128	160.7	0.121	0.372
123.5	169.8	0.118	0.414
120	174.8	0.113	0.442
115	184.1	0.104	0.492
109	195.3	0.092	0.552
105	201.5	0.0845	0.586
96.5	213.5	0.061	0.658
91	222.4	0.05	0.72
85.5	228	0.0377	0.754
80	232.15	0.025	0.78
74	236.3	0.021	0.808
61	244	0.0131	0.862
52	248.1	0.0113	0.896
42	252.6	0.0095	0.925
34	255.5	0.00862	0.945
26.5	258.4	0.0085	0.965
20	263	0.008	1
17	264.2	0.0076	1.01
9.5	267	0.0075	1.03
0	270	0.0085	1.055
-10.5	273.25	0.0095	1.08
-21	275.8	0.0117	1.1
-30	278.3	0.0129	1.12
-40	281.5	0.01425	1.14
-49	285.5	0.0196	1.18
-60	291.85	0.0254	1.23

Fibre dimensions: Length = 0.575 cm: Mass/unit length = 6.8 µg/cm.

Density = 1.142 gm/cc.

f_o at 20°C = 271 and 263 cps.

$\epsilon' E'_{b20}$ = $6.194.10^{10}$ and $5.834.10^{10}$ dynes/cm^2.

TABLE XII D

NYLON 66: Dynamic bending properties and Temperature.

Type BH_1

Temperature °C	Resonant frequency f_o c/s.	tan δ	Relative bending Modulus $E'b/E'_{b20}$
149	130.2	0.096	0.254
146	131.2	0.099	0.257
143	135.5	0.103	0.274
137.5	140.4	0.11	0.294
134	144.5	0.115	0.308
130	150	0.12	0.335
125	156	0.125	0.363
120	163.5	0.126	0.4
114	174	0.102	0.452
106	190	0.083	0.54
98	205.7	0.061	0.63
94	211	0.0475	0.665
89	218	0.0367	0.708
84.5	223.2	0.031	0.742
75	231	0.0208	0.8
68.5	235.6	0.0153	0.85
56.5	242.5	0.0124	0.875
47.5	246.9	0.0975	0.91
38	251	0.0955	0.94
31	253.4	0.087	0.96
26.5	255.9	0.078	0.975
23.5	257	0.078	0.985
20	259	0.08	1

Fibre dimensions.

Length = 0.585 : Mass/unit length = 6.8 µg/cm.

Density = 1.142 g./cm^3.

f_o at 20°C = 246 and 259 cps.

$\epsilon' E'_{b20}$ = $5.46.10^{10}$ and $6.05.10^{10}$ dyn/cm2.

TABLE XII E.

RAYON: Dynamic bending properties and Temperature.

Temperature °C	Resonant frequency f_o c/s.	tan δ	Relative bending Modulus E'_b/E'_{b20}
180	225	0.0525	0.6
170	234	0.0465	0.65
160	239	0.04	0.68
151.5	244	0.0344	0.705
141.5	249.5	0.0297	0.74
131.5	253.75	0.0248	0.765
124	257.5	0.0217	0.785
120.5	259.1	0.0197	0.8
114	261.4	0.0182	0.815
106	264.4	0.0161	0.83
99	267.2	0.0135	0.855
92	269.25	0.0122	0.86
86	271.45	0.0118	0.875
80.5	273.8	0.011	0.89
73	276.65	0.0101	0.915
64.5	278.5	0.0094	0.925
53	281.5	0.00816	0.94
44.5	284	0.0072	0.96
30	287	0.008	0.98
20	290.15	0.00825	1
11	292.3	0.01025	1.015
1	293.9	0.0109	1.022
-9	296.3	0.0135	1.03
-17	298.5	0.0168	1.06
-29	301.8	0.0232	1.03
-40	305.3	0.03	1.11
-47	308.15	0.0335	1.13
-54	310.8	0.0373	1.145
-61	313.8	0.0383	1.17

Fibre dimensions:

Length = 0.53 cm : Mass/unit length = 1.7 μg/cm.

Density = 1.519 gm/cm^3.

f_o at 20°C = 290.15 and 249.6 cps.

$\epsilon' E'_{b20}$ = 36.21. 10^{10} and 26.88.10^{10} dynes/cm^2.

TABLE XIII A.

TERYLENE: Dynamic bending properties and Temperature.

Normal.

Temperature ^{o}C	Resonant frequency f_o c/s.	tan δ	Relative bending Modulus E'_b/E'_{b20}
183	103.5	0.078	0.13
175	112	0.098	0.154
170	115.5	0.3125	0.163
166	121	0.124	0.18
159.5	131.4	0.149	0.21
153	144.8	0.161	0.256
149	157.5	0.166	0.308
146	162.4	0.164	0.322
138	177	0.146	0.388
135	191.5	0.125	0.448
130	206	0.107	0.52
125	225	0.072	0.62
119	235.9	0.049	0.68
115	244	0.0332	0.73
110	250.7	0.024	0.77
106	255.5	0.0157	0.79
98	260.8	0.0152	0.83
89.5	265.3	0.0102	0.86
78	269.3	0.008	0.89
63.5	273.5	0.0095	0.915
50	277.5	0.0132	0.94
36.5	280.7	0.0196	0.965
23	285.4	0.024	0.995
20	286	0.028	1
7.5	290.5	0.0344	1.03
-7.5	295.5	0.0425	1.06
-14.5	301.8	0.0448	1.11
-24.5	308	0.052	1.16
-32.5	314	0.054	1.2
-42	320.5	0.056	1.26
-52	328	0.052	1.31
-63	335	0.048	1.37
-70	342	0.044	1.43

Fibre dimensions: Length = 0.45 cm. Mass/unit length = 2.58 μg/cm.
Density = 1.373 gm/cm^3.

$\epsilon' E'_{b20} = 10.8.10^{10}$ dynes/cm^2.

TABLE XIII B,

TERYLENE: Dynamic bending properties and Temperature.

Heat set at 180° for 1 hour, under 500 mg. load.

Temperature °C	Resonant frequency f_o c/s.	tan δ	Relative bending Modulus E'_b/E'_{b20}
159	109	0.12	0.22
153	115.5	0.139	0.24
148.5	124.5	0.15	0.285
143	134.5	0.15	0.335
139.5	142	0.142	0.37
131	154	0.128	0.435
129.5	166.5	0.102	0.505
124	175.5	0.084	0.562
120	185.5	0.0625	0.63
110	198.5	0.0352	0.72
105.5	202.5	0.025	0.75
97	209.3	0.0143	0.8
88	213.9	0.0124	0.82
77.5	217.9	0.011	0.87
69	220.6	0.0108	0.89
61.5	222.85	0.01075	0.91
53	224.8	0.0115	0.93
44.5	226.55	0.0145	0.945
33	229.4	0.0209	0.97
27	230.8	0.0225	0.98
20	233.5	0.026	1
12	235	0.03	1.018
1	238	0.0376	1.04
-6	241.3	0.044	1.06
-15	246	0.049	1.11
-22	249.5	0.0522	1.14
-30	254.3	0.0542	1.19
-41	260.5	0.05	1.24
-48	264.8	0.0472	1.29
-54.5	268.2	0.0455	1.32
-63.5	271.9	0.0415	1.35
-67	273.5	0.04	1.37

Fibre dimensions: Length = 0.5 cm: Mass/unit length = 2.4 µg/cm.

Density = 1.393 gm/cm^3.

$\epsilon' E'_{b20}$ = 10.86. 10^{10} dynes/cm^2.

TABLE XIII C

TERYLENE: Dynamic bending properties and Temperature.

Heat set at 150°C for 1 hour under zero load.

Temperature - °C	Resonant frequency f_c c/s.	tanδ.	Relative bending Modulus E'_b/E'_{b20}.
162.5	83	0.12	0.187
158	86.3	0.1345	0.202
152	93	0.16	0.235
148.5	98.5	0.176	0.264
144	105.5	0.18	0.28
139.5	112	0.17	0.34
133	124.5	0.137	0.42
129.5	131.5	0.129	0.47
125	142	0.0985	0.55
119	151.9	0.0725	0.625
113	160	0.05	0.692
107	165.6	0.036	0.742
97	173	0.015	0.812
87.5	177	0.0113	0.85
76	181	0.011	0.89
66	183.25	0.0104	0.912
56	185	0.0108	0.93
44.5	187	0.0123	0.95
38	188.1	0.0149	0.96
25	190.65	0.0226	0.985
20	192.2	0.029	1
6	195.3	0.0384	1.04
-6	199.5	0.049	1.08
-19.5	204	0.054	1.13
-31	209.4	0.0575	1.185
-42	214.4	0.058	1.25
-54.5	220.5	0.06	1.32
-70	226	0.057	1.38

Fibre Dimensions. Length = 0.515 cm: Mass/unit length = 2.435μg/cm.

Density = 1.393 gm/cm^3.

$\epsilon' E'_{b20}$ = 8.2.10^{10} dynes/cm2.

TABLE XIV A.

POLYBLEND: Dynamic bending properties and Temperature.

Type BH$_5$.

Temperature ^{o}C	Resonant frequency f_r c/s.	$\tan\delta$	Relative bending Modulus $E'b/'_{b20}$
164	152	0.076	0.215
160.5	156	0.083	0.226
157	160	0.09	0.238
152	166.4	0.096	0.256
149	171.5	0.1	0.272
145	174.5	0.106	0.28
141.5	182	0.11	0.295
134	195	0.104	0.354
130	202	0.101	0.38
124	212	0.094	0.418
118.5	227.5	0.087	0.48
110	244.5	0.0695	0.56
102	261	0.0612	0.63
98	268.5	0.058	0.67
88	285.8	0.035	0.76
81.5	292	0.027	0.79
75	299.6	0.02	0.83
68	304	0.01315	0.86
59	310	0.0128	0.89
50	315	0.0117	0.92
42.5	317.6	0.107	0.94
35	321.3	0.0124	0.96
28	323.9	0.013	0.975
20	328	0.016	1
13	329.5	0.0165	1.01
5	331	0.0172	1.02
-5	334	0.0242	1.04
-12	338	0.0272	1.06
-23.5	342.5	0.03	1.09
-33.5	348.5	0.034	1.13
-44	354.5	0.0382	1.17
-55	362	0.04	1.22
-63	368	0.0422	1.26
-67.5	374	0.044	1.3

Fibre dimensions: Length=0.57 cm: Mass/unit length=6.8 μg/cm.
Density = 1.215 gm/cm^3
$\epsilon'E'_{b20}$ = $7.224.10^{10}$ dynes/cm^2

TABLE XIV B.

POLYBLEND: Dynamic bending properties and Temperature.

Type BH_3.

Temperature °C	Resonant frequency f_o c/s.	tan δ	Relative bending Modulus $E'b/E'_{b20}$
160	110	0.1	0.18
157	113.5	0.1145	0.192
150	121.8	0.12	0.22
146	125.9	0.125	0.235
144	131.35	0.126	0.258
139	140.2	0.123	0.294
131.5	153.5	0.112	0.35
124	165.7	0.099	0.41
120	172.8	0.092	0.445
115	181	0.078	0.49
111	187.5	0.07	0.525
104	195.5	0.058	0.57
100	204.8	0.051	0.625
95.5	210	0.045	0.66
88	222	0.032	0.735
80.5	231	0.022	0.795
73	236.7	0.016	0.84
63.5	241.5	0.0124	0.87
54	245.5	0.0106	0.9
45.5	249	0.0104	0.925
33	253.5	0.009	0.955
26.5	256.2	0.0148	0.982
20	259.9	0.0162	1
6	264.25	0.0208	1.04
-5	267.2	0.0262	1.06
-16.5	271.85	0.0272	1.1
-20.5	273.5	0.0278	1.12
-26	277.2	0.0315	1.14
-35.5	280.5	0.032	1.17
-57	289	0.033	1.24
-65	291.5	0.033	1.27

Fibre dimensions: Length = 0.6 cm: Mass/unit length = 6.8 µg/cm.
Density = 1.21 gm/cm^3

$\epsilon'E'_{b20} = 7.58.10^{10}$ dynes/cm^3.

TABLE XIV C.

POLYBLEND: Dynamic bending properties and Temperature.

Type BH_4.

Temperature °C	Resonant frequency f_s c/s.	tan δ	Relative bending Modulus $E'b/E'_{b20}$.
160	88.5	0.11	0.135
152	93	0.14	0.15
146.5	105	0.16	0.19
140	10	0.19	0.2
136	113	0.197	0.22
129	134.5	0.186	0.312
124	145.5	0.165	0.365
120	153	0.14	0.408
114	168.75	0.11	0.494
108.5	179	0.0895	0.56
100	196.3	0.051	0.665
96.5	202.2	0.0396	0.71
88	210.7	0.0246	0.77
80.5	216.6	0.0184	0.81
70	219.3	0.0137	0.83
62.5	225.1	0.1065	0.88
53	228.2	0.00875	0.91
47	230.1	0.007	0.93
40	232.3	0.0085	0.94
30	235.7	0.00765	0.965
20	240.5	0.00915	1
14	243.4	0.0095	1.012
-7.5	246.1	0.00975	1.042
-14	248.2	0.00965	1.062
-23.5	250.1	0.012	1.08
-33.5	252.5	0.01425	1.1
-41.5	254.5	0.0157	1.12
-55	258.4	0.0193	1.16
-63.5	260.6	0.023	1.18

Fibre dimensions: Length = 0.592 cm: Mass/unit length = 6.8 μg/cm.

Density = 1.152 gm/cm^3.

$\epsilon' E'_{b20}$ = 5.566. 10^{10} dynes/cm^2.

TABLE XIV D.

DACRON: Dynamic bending properties and Temperature.

Temperature °C	Resonant frequency f_o c/s.	tan δ	Relative bending Modulus E'_b/E'_{b20}
180	97	0.1	0.13
176.5	100	0.112	0.138
170	107.5	0.126	0.16
160.5	124.5	0.152	0.215
154	133	0.165	0.244
152	142.5	0.17	0.28
147	152	0.164	0.32
140	172	0.14	0.41
132	201.5	0.11	0.56
125	216.5	0.08	0.65
120	225	0.06	0.7
112.5	233	0.0258	0.75
108	237	0.021	0.78
100	242.5	0.0124	0.815
95	245.2	0.0114	0.832
81.5	250	0.0108	0.862
71	253.3	0.0103	0.885
60	256	0.0117	0.91
49	259	0.0135	0.93
40	261	0.0153	0.942
36	264.3	0.022	0.955
26	266	0.0287	0.98
20	269	0.032	1
10	273	0.0402	1.025
0	278	0.048	1.07
-11.5	288	0.0556	1.142
-21	297	0.0605	1.22
-32	306	0.06	1.29
-40	310	0.052	1.33
-49	317	0.044	1.39
-58	323	0.0372	1.44

Fibre dimensions: Length = 0.595 cm: Mass/unit length = 6.5 μg/cm.
Density = 1.383 gm/cm^3.

$\epsilon E'_{b20} = 10.83.10^{10}$ dynes/cm^2.

TABLE XV A

NYLON 66 Type A: Dynamic tensile properties, Temperature and Relative humidity.

Fibre 1.

% R.H.	Temperature °C.	tan δ	Dynamic tensile Modulus E' 10^{10} dynes/cm^2.
45	93	0.1	3.4
	87	0.085	3.5
	79	0.075	3.65
	72	0.065	4.85
	66	0.06	4
	56	0.055	4.3
	46	0.045	4.6
	40	0.04	4.8
	32	0.035	5.2
	20	0.03	6.6
65	88	0.053	3.15
	80	0.0575	3.3
	72	0.065	3.4
	64.5	0.07	3.5
	60	0.0675	3.55
	55.5	0.065	3.6
	50	0.0625	3.75
	44	0.06	3.9
	35	0.0525	4.2
	27	0.045	4.8
	20	0.0425	5.8
85	91.5	0.0575	2.6
	82	0.0525	2.7
	69	0.0575	2.8
	57	0.0625	2.95
	50	0.07	3
	45	0.075	3.1
	39	0.08	3.2
	34	0.075	3.4
	30	0.07	3.65
	27	0.065	4
	20	0.06	4.6

TABLE XV B

NYLON 66 Type A: Dynamic Tensile properties, Temperature and Relative humidity.

Fibre 2.

% RH.	Temperature °C	tan. δ	Dynamic tensile Modulus E'10^{10} dynes/cm^2.
0	143	0.0425	3.25
	140	0.045	3.3
	135	0.05	3.35
	130	0.06	3.4
	125	0.07	3.5
	122	0.075	3.6
	120	0.0825	3.65
	118	0.09	3.7
	114	0.0975	3.8
	110	0.085	4
	108	0.08	4.1
	105	0.0725	4.3
	100	0.06	4.5
	95	0.0525	4.7
	90	0.045	5
	85	0.0375	5.25
	80	0.03	5.55
45	95	0.0675	3.5
	90	0.0775	3.6
	87	0.085	3.8
	80	0.075	4
	75	0.0675	4.2
	70	0.0625	4.35
	65	0.0575	4.5
	60	0.055	4.6
	55	0.0525	4.8
	50	0.0475	4.9
	45	0.045	5.1
	40	0.0425	5.3
	35	0.0375	5.5
	30	0.035	5.8
	25	0.0325	6.3

TABLE XV B.

CONTINUED:

65	95	0.05	2.8
	90	0.0525	2.95
	85	0.055	3.1
	80	0.06	3.2
	75	0.0625	3.3
	70	0.0675	3.45
	65	0.0725	3.55
	60	0.0675	3.7
	55	0.065	3.8
	50	0.06	3.9
	45	0.0575	4.05
	40	0.055	4.2
	35	0.05	4.4
	30	0.0475	4.65
	25	0.045	5
	20	0.0425	5.7
85	95	0.05	2.6
	90	0.0475	2.65
	85	0.045	2.7
	80	0.045	2.8
	75	0.045	2.85
	70	0.0475	3
	65	0.05	3.05
	60	0.0525	3.1
	55	0.055	3.2
	50	0.06	3.25
	45	0.0675	3.35
	40	0.075	3.5
	35	0.0675	3.6
	30	0.0625	3.8
	25	0.0575	4.1
	20	0.055	4.5

TABLE XV C.

NYLON 66 Type B: Dynamic tensile properties, Temperature and Relative humidity.

Fibre 1.

% RH.	Temperature °C	tan δ	Dynamic tensile Modulus E' 10^{10} dynes/cm^2.
0	125	0.075	3.3
	120	0.085	3.55
	117.5	0.09	3.7
	115	0.095	3.8
	113	0.1	4
	110	0.105	4.1
	107	0.105	4.3
	100	0.0925	4.7
	95	0.0825	5
	90	0.075	5.35
	85	0.07	5.6
	80	0.06	5.8
	76	0.055	6.1
	67	0.045	6.35
	62	0.04	6.4
	55	0.035	
	50	0.03	
45	93	0.05	2.95
	88	0.055	3
	80	0.0625	3.2
	73	0.0675	3.5
	58	0.0625	3.8
	60	0.0575	4.35
	55	0.055	4.75
	50	0.05	5.2
	40	0.04	5.7
	30	0.035	6
	20	0.04	6.1

TABLE XV C.

CONTINUED.

65	90 85 80 73 65 59 53 50 45 40 35 30 20	0.055 0.0575 0.06 0.065 0.0725 0.0775 0.0775 0.0725 0.0675 0.0625 0.06 0.0475 0.045	2.6 2.6 2.7 2.75 2.85 2.95 3.2 3.3 3.7 4.2 4.6 4.9 5.1
85	95 90 80 70 60 55 48 42 35 30 20	0.04 0.0375 0.0375 0 04 0.045 0.05 0.0575 0.065 0.0775 0.085 0.875	2.3 2.35 2.4 2.4 2.5 2.5 2.6 2.75 2.8 3.1 3.6

TABLE XV D.

NYLON 66 Type B: Dynamic tensile properties, Temperature and Relative humidity.

Fibre 2.

% RH	Temperature °C	tan δ	Dynamic tensile Modulus $E' 10^{10}$ dynes/cm^2
0	141	0 045	3.2
	137	0.05	3.3
	133	0.055	3.4
	130	0 06	3.5
	126	0,065	3.6
	122	0.07	3.8
	117	0.0775	4
	113.5	0.08	4.2
	110	0.08	4.3
	107	0.075	4.45
	102	0.065	4.65
	100	0.06	4.8
	95	0.0525	5
	90	0.045	5.3
	85	0.0375	5.5
	80	0.03	5.8
45	95	0.05	3.1
	87	0.055	3.2
	80	0.0625	3.4
	75	0.0675	3.6
	70	0.065	3.9
	65	0.06	4.2
	60	0.0575	4.55
	55	0.0525	4.85
	50	0.05	5.1
	47	0.0475	5.3
	40	0.0425	5.6
	35	0.04	5.8
	30	0.0375	5.9
	25	0.035	

TABLE XV D.
CONTINUED:

65	95	0.05	2.4
	90	0.0475	2.5
	85	0.05	2.6
	80	0.0525	2.7
	75	0.055	2.8
	70	0.06	2.9
	65	0.0625	3
	60	0.0675	3.2
	56	0.07	3.3
	50	0.065	3.5
	45	0.06	3.7
	40	0.0575	4
	35	0.055	4.2
	30	0.0525	4.5
	20	0.05	4.9
85	95	0.04	2
	90	0.0375	2.1
	85	0.035	2.15
	75	0.0375	2.2
	70	0.04	2.2
	65	0.0425	2.2
	60	0.045	2.3
	55	0.05	2.35
	50	0.055	2.4
	45	0.0625	2.45
	40	0.07	2.5
	35	0.075	2.7
	30	0.0825	2.8
	27	0.09	3
	20	0.0875	3.4
	17	0.08	3.5

TABLE XV E.

NYLON 66 Type C: Dynamic tensile properties, Temperature and Relative humidity.

Fibre 1.

%RH.	Temperature °C	tan δ	Dynamic Tensile Modulus $E' 10^{10}$ dynes/cm^2.
0	133	0.07	3.4
	128	0.075	3.4
	121	0.0825	3.55
	114	0.09	3.8
	110	0.095	4
	106	0.09	4.2
	101	0.0825	4.45
	95	0.075	4.8
	90	0.07	5.1
	87	0.065	5.35
	83	0.06	5.55
	78.5	0.055	5.7
	74	0.05	5.9
	70	0.045	6
	65.5	0.04	6.1
	60	0.035	6.15
45	93	0.06	3.1
	87	0.065	3.2
	83	0.0675	3.3
	78 5	0.0725	3.4
	71	0.0675	3.6
	67	0.0625	3.9
	60	0.055	4.2
	55	0.05	4.4
	50	0.045	4.7
	45	0.04	5
	40	0.035	5.3
	30	0.0275	5.8

TABLE XV E.

CONTINUED:

	98	0.045	2.4
	90	0.0475	2.5
	85	0.05	2.55
	79	0.055	2.6
	72	0.06	2.7
	67	0.065	2.9
65	60	0.07	3.1
	55	0.065	3.3
	49	0.06	3.5
	43	0.055	3.8
	37	0.05	4.2
	30	0.0475	4.6
	27	0.0475	4.8
	20	0.055	5.2
	92	0.0375	2.2
	82	0.0375	2.3
	72	0.0425	2.4
	63	0.0475	2.55
85	54	0.05	2.6
	43	0.06	3.2
	40	0.065	3.35
	37	0.07	3.5
	33	0.075	3.65
	29	0.08	3.8
	20	0.075	4.1

TABLE XV F.

NYLON 66 Type C: Dynamic tensile properties, Temperature and Relative humidity.

Fibre 2.

% RH	Temperature °C	tan δ	Dynamic tensile modulus E'10^{10} dynes/cm^2
0	142	0.04	3.1
	136	0.045	3.2
	132	0.05	3.3
	127	0.0575	3.4
	123.5	0.0625	3.5
	120	0.0675	3.6
	117	0.0725	3.8
	114	0.08	3.9
	108	0.0775	4.2
	103	0.065	4.5
	100	0.06	4.65
	95	0.0525	4.9
	90	0.045	5.2
	87	0.04	5.4
	80	0.0325	5.7
45	95	0.055	3
	90	0.06	3.1
	85	0.0625	3.2
	80	0.0675	3.4
	75	0.0725	3.45
	70	0.0675	3.7
	64	0.06	4
	57	0.0525	4.4
	47	0.0425	4.9
	39	0.035	5.4
	32	0.03	5.8

TABLE XV F

CONTINUED:

65	95	0.0525	2.5
	90	0.05	2.55
	85	0.0525	2.65
	80	0.055	2.7
	75	0.0575	2.8
	70	0.0625	2.9
	62	0.07	3.1
	55	0.0675	3.3
	50	0.065	3.45
	43.5	0.0575	3.8
	38	0.0525	4.1
	32	0.0475	4.4
	27	0.045	4.6
	20	0.045	4.7
85	95	0.0375	2.1
	90	0.035	2.2
	85	0.0375	2.25
	80	0.04	2.3
	70	0.045	2.4
	64	0.0475	2.5
	57	0.0525	2.65
	51	0.0575	2.8
	43	0.065	3
	34	0.075	3.4
	30	0.08	3.55
	26	0.085	3.7
	23	0.08	3.8
	20	0.075	3.95
	17.	0.07	4

TABLE XVI.

HEAT SETTING CONDITIONS.

Fibre type:	Treatment.
Acrilan 16A.. .. .. Nylon 66 type 900A ..	.Heat set at 150°C in an oven for 1 hour .under 10% extension and slowly cooled to room temperature.
Acrilan 16B..	.Similar treatment as above but at 130°C
Acrilan C .. .. .. Nylon 66 type 900B ..	.Heat set in boiling water at 100°C for .1 hour under 10% extension and then cooled and dried at 20°C and 65% RH.
Acrilan D .. .. .. Nylon 66 type 900C ..	.Heat set at 150°C in an oven for 1 hour .under zero tension and slowly cooled to room temperature.
Terylene A..	.Single filament heat set at 180°C for 1 hour over P_2O_5 in the apparatus(bending) under 200 mg.load/Denia and cooled to room temperature
Terylene B	.Heat set at 180°C in an oven for 1 hour under zero tension and slowly cooled to room temperature.

TABLE XVII.

Measured values of Optical birefringence and Density.

Fibre type.	Optical Birefringence at 20°C & 65% RH.	Density g./cm^3 at 20°C & 0% RH.
Acrilan 16		1.1845
Acrilan 16A		1.179
Acrilan 16B		1.187
Acrilan 16C		1.186
Acrilan 16D		1.1845
Polypropylene A	0.025*	0.92
Polypropylene B	0.025 *	0.915
Polypropylene C	0.029 *	0.905
Nylon 66 A	0.0672	1.15
Nylon 66 B	0.0672	1.143
Nylon 66 C	0.0675	1.144
Nylon 66 BH_1	0.0656	1.142
Nylon 66 type 900	0.0664	1.144
Nylon 66 type 900 A	0.0683	1.147
Nylon 66 type 900 B	0.0683	1.149
Nylon 66 type 900 C	0.0642	1.1485
Terylene	0.1828	1.373
Terylene A	0.209	1.393
Terylene B	0.173	1.393
Dacron	0.1854	1.383
Rayon		1.519
Polyblend BH_2	0.104	1.215
Polyblend BH_3	0.1025	1.21
Polyblend BH_4	0.0686	1.152

* determined by the Becke line method of refractive index measurements using polarised light.

KEY TO TABLES XVIII A & B.

FIBRE TYPE	CODE No.
Acrilan 16	1
Acrilan 16, heat set at 150°C for 1 hour under 10% extension.	2
Acrilan 16, heat set at 130°C for 1 hour under 10% extension.	3
Acrilan 16, heat set in boiling water at 100°C for 1 hour under 10% extension.	4
Acrilan 16, heat set at 150°C for 1 hour under zero tension.	5
Polypropylene A	6
Polypropylene B	7
Polypropylene C	8
Nylon 66 type A	9
Nylon 66 type B	10
Nylon 66 type C	11
Nylon 66 type BH_1	12
Nylon 66 type 900	13
Nylon 66 type 900, heat set at 150°C for 1 hour under 10% extension.	14
Nylon 66, type 900, heat set in boiling water at 100°C for 1 hour under 10% extension.	15
Nylon 66 type 900, heat set at 150°C for 1 hour under zero tension.	16
Dacron	17
Rayon	18
Polyblend type BH_2	19
Polyblend type BH_3	20
Polyblend type BH_4	21

TABLE XVIII A.

Optical, Physical and Mechanical properties of some synthetic fibres.

Code No.	Optical birefringence at 20°C & 65% RH.	Density g/cm.^{3} at 20°C & 65% RH.	Initial Modulus E'10^{10} dynes/cm^2 at 20°C & 65% RH.	Yield point at 20°C & 65% RH		Breaking point at 20°C & 65% RH.	
				stress 10^9 dyn/cm^2	% extension	Stress 10^9 dyn/cm^2	% Extension.
1.		1.1845	3.5	1.15	3.5	2.35	50
2.		1.179	5.15	1.3	3.5	2.4	42
3.		1.187	5.15	1.36	3.5	2.54	31
4.		1.186	5.15	1.18	3	2.49	37
5.		1.1845	3.75	1.18	3.5	2.34	46
6.	0.025	0.92					
7.	0.025	0.915					
8.	0.029	0.905					
9.	0.0672	1.15	4.2		no yield point	9.85	14.5
10.	0.0672	1.143	2.95	8.2	16.5	8.55	21.6
11.	0.0675	1.144	3.25	9	16.5	9.25	24
12.	0.0656	1.142					
13.	0.0664	1.144	2.5	8.5	16.5	8.8	25.5
14.	0.0683	1.147	3.3	8.7	12	9.3	20.4
15.	0.0683	1.149	3.3	9	12	9.4	19
16.	0.0642	1.1485	2.75	7.6	20	8.35	28.7
17.	0.1854	1.385	5.4	7.8	15	8.5	18.6
18.		1.519	14.25	1.5	1	7.5	15.6
19.	0.104	1.215					
20.	0.1025	1.21					
21.	0.0686	1.152					

TABLE XVIII B.

Dynamic Mechanical properties of some synthtic fibres.

≠ tanδ continues to rise above the temps. mentioned.

+ at 3 - static strain & 0·1 dyn. strain

Code No.	Dynamic bending modulus $E'_{b}{}_{20}10^{10}$ dyn/cm² at 20°C and 65%RH.	Dynamic tensile modulus $E'10^{10}$ dyn/cm² at 20°C and 65%RH.	Mechani-cal dispe-rsion.	Temp. at which a maximum in tanδ occurs.				
				Dynamic bending experiments in vacuo at 40- 500 c/s.	Dynamic tensile experiments at 20c/s. 2% static, 0·1% dyn strain.			
					%RH			
					0	45	65	85
1	11·9	5·9	α	≠100°C	≠ 90°C	≠ 77°C	≠ 68°C	≠ 65°C
			β	64°C				
3	9·74	6·25	α	≠ 100°C				
			β	55°C				
4	8·36	6	α	≠100°C				
			β	50°C				
6	3·9		α	17°C				
7	4·9		α	17°C				
8	5·5		α	25°C				
9	6·1 to 6·5	5·7	α	132°C	115°C	86°C	65°C	39·5°C
10	5·8 to 6·2	5	α	125°C	110°C	75°C	56°C	24°C
11	5·8 to 6·2	5	α	126°C	112°C	75°C	60°C	26°C
12	5·5 to 6		α	126°C	106°C			
13			α		109°C	74°C	57°C	23°C
14		6·6	α		119°C	79°C	60°C	27°C
15		6·9	α		115°C	84°C	67°C	37°C
16		3·9	α		114°C	78°C	61°C	28°C
17	10·8	9·8	α	150°C	144°C			
			β	-23°C				
18	26·9 to 36·2	+ 10		tanδ rising above & below 40°C	≠120°C	≠75°C	≠55°C	≠40°C
19	7·2		α	142°C	134°C			
			β	-60° to -70°C				
20	7·6		α	144°C	134°C			
			β	-30°C				
21	5·6		α	135°C	134°C			

TABLE XIX.

Moisture regain of some Man-made fibres.[114]

Type of fibre.	Temperature °C	% R H.			
		40	65	75	90
Acrilan 16	21	0.9	1.4	1.7	2.1
	35.6	0.9	1.4	1.7	2.4
Nylon 66	21	2.4	3.9	4.5	6.5
	35.6	2.9	3.7	5.0	7.3
Polyester	21	0.3	0.3	0.4	0.4
	35.6	0.2	0.3	0.4	0.5
Viscose rayon.	21	8.8	12.1	15.3	20.8
	35.6	8.4	12.4	15.6	25.1

CHAPTER V. SUMMARY AND CONCLUSION.

SUMMARY AND CONCLUSION.

The work that is presented in this thesis has been aimed at determining the dynamic mechanical properties of several natural and synthetic fibres of normal textile counts over a wide range of temperature and/or humidity. For this purpose two experimental techniques have been developed in the Fibre Science laboratory at the University of Strathclyde. One of the experimental techniques used for measuring the dynamic bending properties of dry fibres in vacuo is similar to that used by Meredith and Hsu[40], but with certain minor modifications in the design of the fibre holder made of quartz rod carrying a suitable metal clip for mounting the fibre. The use of the quartz rod was to minimise conduction losses through the fibre mounting unit. The basic principle of this method consists of a clamped fibre in the form of a cantilever in an electrostatic field between two electrodes, brought to resonance in the transverse direction by superimposing on the electrodes an alternating field of the right frequency supplied from a variable frequency oscillator. On this apparatus dynamic bending properties of dry fibres can be measured at 50 - 600 cps fairly quickly and very accurately over a wide range of temperature but, when dealing with normal textile counts the measurements have to be made in vacuo to avoid correction for damping. Meredith and Hsu have worked out theoretical correction for damping, nevertheless, the magnitude of correction is larger than the quantities that one is interested in measuring.

This means of course, that it is difficult by this method to obtain accurate results other than in dry state.

The other experimental technique used for measuring the dynamic mechanical properties of fibres of normal textile counts over a wide range of temperature and/or humidity is similar to that employed by Yoshino and Takayanagi[75]. The principle of this method is to fix both ends of the sample to two strain gauges of unbonded type. One of the strain gauges is used to transform the sinusoidal displacement into an electrical quantity proportional to the displacement and the other is a transducer of generated force. The absolute values of these electrical vectors representing force and displacement are adjusted to unity (full scale of deflection on voltmeter) and vector reduction is achieved by changing the connection of the output circuit of the two strain gauges. By this operation the value of $\tan\delta$ can be directly read off the voltmeter. Regulation of the magnitude of the vector is brought about conveniently by controlling D.C input of the strain gauges. The dynamic tensile modulus is calculated from the ratio of the input voltages of the strain gauges $^{V}2/v_1$. When output voltages are regulated to unity, the dynamic tensile modulus $E' = k\ (^{V}2/v_1)$, where k is a constant relating to the dimensions of samples and strain gauges. In this method since sinusoidal forces are applied longitudinally to the fibre air damping has no influence. Therefore, dynamic tensile properties can be studied very

accurately over a wide range of temperature and humidity.

Since Yoshino and Takayangi made dynamic tensile measurements on polymer films, the electrical strain gauge system they used for detecting the in-phase and out of phase deformational responses of the specimen subjected to an alternating stress was rather coarse (250 gms.maximum load) and hence was not sensitive enough for handling normal textile counts It will therefore be appreciated that an apparatus had to be designed and built with very fine strain gauges (20 gms.maximum load) in order to make measurements possible on fine textile counts. However, it may be useful to mention that since this work began Japanese workers have introduced an apparatus into the market suitable for fine textile counts called 'Vibron' which works on similar principle to the one described above.

In summarising the results it should be mentioned that much information on the dynamic mechanical properties over a wide range of temperature and humidity of several textile fibres and fibres from tyre cords has been obtained in this work which was hither to not available in great detail. The results on tyre cord fibres are expected to be of significant practical value in the development of better tyre cord reinforcement.

The work on dynamic bending properties on dry fibres in vacuo at

50 - 600 cps over a range of temperature from -70° to 170°C has been concentrated on several groups of fibres e.g. Protien, Cellulosic and regenerated cellulosic, modified regenerated cellulosic, polyacrylonitrile, polyolefin and finally polyamide, polyester and polyblend fibres. Protien fibres such as wool, silk and Fibrolane, cellulosic and regenerated cellulosic fibres such as ramie, Fortisan and viscose rayon and modified regenerated cellulosic fibres namely, acetate and Tricel have been studied. Included in the synthetic fibres studied are Acrilan 16, Orlon, three types of polypropylene, eight types of nylon 66, Terylene, Dacron and three types of polyblend fibres.

Nylon 66, Acrilan 16 and Terylene fibres heat set under various conditions have also been studied. All the results have been graphically represented and discussed in the preceding chapter.

The salient feature in these results is that each group of fibres shows characteristic response to dynamic mechanical testing over the range of temperature studied. This response may be seen to occur consistently even in natural fibres like wool, silk and ramie. Although the multiple transition phenomena in polycrystalline materials observed by this method alone are not fully susceptible to interpretation at a molecular level nevertheless, they form a useful basis for further work using the current techniques of infra-red spectroscopy and nuclear magnetic resonance spectroscopy.

In the study of the structure of high polymers these three far-reaching techniques are the most popular to date.

From the results it will be noticed that the glass transition temperature for fibres are considerably higher than thos reported for polymer rods[29]. e.g. for dry nylon 66 fibres the glass transiton temperature occurs at about 120° to 135°C, where as for nylon 66 rods it is reported to occur at about 80°C. This difference is of course, attributableto high degree of orientation and crystallinity in fibres compared with rods.

The other features that are noticeable are that the dynamic mechanical properties of polar polymers are extremely sensitive to moisture At 85% RH the glass transition peak for nylon 66 fibres occur almost at room temperature. This behaviour of nylon 66 fibres is comparable with that of dry polypropylene fibres which also exhibit a glass transition peak around room temperature. It is further evident from the dynamic mechanical behaviour of rayon, nylon 66, Acrilan 16 and Dacron that at temperatures above room temperature segmental motion increases with moistur regain and polar polymers which have higher moisture regains exhibit glass transition peaks at comparatively lower temperatures than polymers with lower moisture regain. Since glass transition peaks are generally associated with sharp changes in moduli, under wet conditions the working modulus range over the temperature scale will be poor for fibres with high moisture regain. Therefore, it is apparent that under wet

conditions tyres reinforced with Dacron cords would show better dynamic mechanical performance than those reinforced with rayon or nylon cords. However, good response of tyre cords to dynamic stresses and strains over a range of temperature and humidity is but one of the many desirable properties in deciding the choice of fibres for tyre cord manufacture. In this respect the new polyblend fibres which are possibly being developed for tyre cords seem to combine the properties of polyamides and polyesters and therefore may prove suitable for the manufacture of better tyres that do not produce 'flat spots' (as in tyres reinforced with nylon cords) and show better performance under various weather conditions. Since the composition of these fibres have not yet been made known, it is as yet early to predict the potentialities of these newer fibres for tyres.

Finally it should be mentioned that nylon 66 fibres heat set in boiling water at 100°C for one hour under 10% extension show glass transition peaks and associated changes in moduli at higher temperatures over the range of temperature and humidity investigated. This behaviour is attributed to the larger size of crystallites that are possibly formed in nylon 66 in the presence of water. The effect of heat setting on the dynamic mechanical properties of Acrilan 16 and Terylene are not as marked as in nylon 66.

REFERENCES

1)	SAUER J.A., and WOODWARD A.E.	Review of Modern Physics, 32. No.1. Jan.1960.
2)	MANFRED GORDON	High Polymers (Structure & Physical properties), published for the Plastics Institute, 1963.
3)	FERRY J.D.	Viscoelastic Properties of Polymers, WILEY, 1961.
4)	NIELSON L.E.	Mechanical properties of polymers, Ed.Nielson L.E., Reinhold publishing Corp., 1962.
5)	BUECHE F.	Physical Properties of Polymers, Ed.Bueche, F.,John Wiley and Sons,1962.
6)	TOBOLSKY A.V.	The Properties and structure of Polymers, Ed.Tobolsky, A.V. John Wiley and Sons,1960.
7)	GOODMAN I.	Chap.4. in Fibre Structure, Ed. Hearle, J.W.S. & Peters, R.H. The textile Institute, Butterworths, 1963.
8)	YASAKA WADA.	J.Phy.Soc.Japan,16,No.6, 1961.
9)	TRELOAR L.R.G.	Chap.9 in Fibre Structure, Eds.Hearle, J.W.S. & Peters R.H. The Textile Institute, Butterworths, 1963.
10)	WILLBOURNE A.H.	Trans.Faraday Soc.,54 717,1958.
11)	PEIRCE F.T.	J.Text, Inst., T 153, 1929.

12)	WARBURTON, F.L.	J.Text.Inst.,39,297,1948.
13)	WOODS, H.J.	Leeds Lit. and Phil Soc., 3 , 577, 1940.
14)	SPEAKMAN J.B.	Trans.Faraday Soc. 25 , 92, 1929.
15)	LOCHNER J.P.A.	J.Text.Inst. 40 , T.220, 1949.
16)	LINCOLN B.	J. Text.Inst. 43 , T.158, 1952.
17)	VAN WYK C.M.	S.Afr.J.Sci. 45 , 127,1951.
18)	HORIO, M.,ONOGI,S.NAKAYAMA & YAMAMOTO K.	J.Appl.Physics, 22 966, 1951
19)	HORIO,M.,ONOGI S.	J.Appl.Physics 22 , 977, 1951.
20)	STOKES G.G.	Mathematical and Physical Papers, Vol.111 Uni.Press Cambridge, pp.38-67, 1901.
21)	KÄRRHOLM E.M. & SCHRODER B.	Text.Res.J., 23,207,1953.
22)	KÄRRHOLM E.M.	Text.Res.J., 25 756, 1955.
23)	OKAJIMA S. and SUZUKI S.	J.Soc.Text.and cell., Ind. Japan,15, 809,1959.
24)	SCHRODER G.	Melliand Textilberichte, 5,418, 1953.
25)	WAKELIN J.H., VOONG E.T.L., MONTGOMERY D.J., and DUSSENBURY J.H.	J.Appl.Physics, 26,786, 1955.

26)	MARLOW P.E.	J.Text.Inst., 49, T40, 1955.
27)	ADAMS N.	J.Text.Inst., 47, T.531, 1956.
28)	KAWAGUCHI T.	J.Appl.Polymers Sec., 2 56-61, 1959.
29)	WOODWARD A.E., CRISSMAN J.M., and SAUER J.A.	J.Polymer Sci., 44, 23-34, 1960.
30)	WOODWARD A.E., SAUER J.A., DELLY, C.W., and KLINE D.E.,	J.Polymer Sci. 12 363, 1957.
31)	DEELY, C.W., WOODWARD A.E., and SAUER J.A.	J.Appl. Physics, 28, 1124, 1957.
32)	KAWAGHCHI, T.	J.Polymer Sci., 32, 417-424, 1958.
33)	KLIEN D.E., and SAUER J.A.	Polymer 2 No.4. pp.401-408, 1961.
34)	WARD I.M.	Die Makromoekulare Chemie, 38, 147-158, 1960.
35)	THOMPSON A.B., and WOODS D.W.	Trans.Faraday Soc.52 1383, 1956.
36)	REDDISH	Trans.Faraday Soc., 46, 459, 1950.
37)	DUETSCH K., HOFF, E.A.W., and REDDISH W.	J.Polymer Sci., 13, 565, 1954.
38)	HOFF E.A.W., ROBBINSON D.W., and WILLBOURN A.H.	J. Polymer Sci., 18, 161, 1955.

39)	SAUER, J.A. ,WALL R ., FUSCHILLO N. ,and WOODWARD A.E.	J. App. Physics., 29, 1385, 1958.
40)	MEREDITH R ,and BAY-SUNG HSU:	J.Polymer Sci. ,61, 271-292, 1962.
41)	MEYER K.H.,and LOTMAR W.	Helv.Chim. Acta., 19 68, 1936.
42)	TIPTON H.	J. Text.Inst., 46, T323, 1955.
43)	PALANDRI G.	Rubber Age, 64-65, 45, 1948-49.
44)	de VRIES H.	In 'On the Elastic and Optical properties of Cellulose Fibres' Schotanns and Jens, Utrecht 1953 ,
45)	de VRIES H.	Ann.Sci.Text.Belges ,No.4. , 286, 1955
46)	HAMBURGER, W.J.	Text.Res. J.,15, 295,1948
47)	FUJINO K.,KAWAI H., and HORIO T.	Text.Res. J.,25, 722, 1955.
48)	KAWAI H., and TOKITA N.	J.Phys. Soc.Japan, 5, 17, 1950
49)	DUNNEL B.A., and DILLON J.H.	Text.Res.J., 21, 393, 1951.
50)	LYONS,WJ,and PRETTYMAN I.B.	J.App. Physics, 19 , 473, 1945.
51)	CHAIKIN M,and CHAMBERLAIN N.H.	J.Text. Inst., 46, T25, and 44, 1955.
52)	ASMUSSEN R.W., and ANDERSEN F.	Dan.Acad. Tech. Sci., No.5, 1947.

53) ANDERSEN F. Ibid., No.13, 1950.

54) BALLOU,J.W.,and SILVERMAN S. Text.Res. J.,14 ,282, 1944.

55) DUNELL B.A.,and PRICE S.J.W. J.Polymer Sci.,18 ,305, 1955.

56) TOKITA N. J.Polymerman, Sci., 20, 515, 1956.

57) RUSSEL J.,and VAN KERPEL R.G. J.Polymer Sci.,25, 77, 1957.

58) NAKAMURA K. Chem. High Polymers Japan, 13, 47, 1956.

59) TOKITA N.,and KANAMURA K. J.Polymer Sci.,27,255, 1958.

60) MACKAY B.H.,and DOWNES J.C. J.App. Polymer Sci, 2, 32, 1959.

61) REE T.,CHEM M.C.,and EYRING H. Text. Res. J.,21 ,789,and 799, 1951.

62) SMITH J.C.,McCRACKIN F.C., and SCHIEFER H.J. J.Text.Inst,50,755,1959.

63) EYRING,H.,ALDER M.G.,ROSSMASSLER S.A.,and CHRISTENSEN C.J. Text, Res, J.22,223, 1952.

64) OGAWA S.,OSAWA N.,and KAWAKAMI T. Bull. Text. Res. Inst. Japan 32, 23, 1955.

65) DOLE, M.,MARX, P.,WILLHOIT R.C., and WORTHINGTON A.E., Bol. Soc. Quim.,Peru, 19,149, 1953.

66) FUJINO K.,KAWAI, H.,and HORIO T., and HIYAMOTA K. Text. Res. J.,26, 852, 1956

67) KAWAGUCHI T. Chem. High Polymers, 14, 176, 1957.

68)	NOHARA S.	Kobunshi Kagaku, 14, 318, 1957.
69)	BRICE S.J.W., McINTYRE, A.D., PATTISON J.D., and DUNNELL B.A.	Text. Res. J., 26, 276, 1956.
70)	QUISTWATER J.M.R., and DUNELL B.A.	J.Polymer Sci., 28, 309, 1958.
71)	BULL H.B.	J.Am. Chem.Soc., 66, 1499, 1944.
72)	FORWARD M.V., and SMITH S.J.	J.Text.Inst., 46, T158, 1955.
73)	SCHMIEDER K., and WOLF K.	Kolloid Z, 134, 149, 1953.
74)	QUISTWATER J.M.R., and DUNNEL B.A.	J.Appl. Polymer Sci., 1, 267, 1959.
75)	MASATSUGA YOSHINO, and MOTOWA TAKAYANAGI,	Rheology, 8, No.67, Apr.1959.
76)	CRISSMAN J.M., SAUER J.A., and WOODWARD A.E.	J.Polymer Sci. Part A, 2, pp 5075-5091, 1964
77)	ATSUO KONDA, YASHUI WATANABE, SUMI FUJINO, RYUZO ONOOKA and TADAO AGATSUMA,	Bull, Text. Res.Inst., 6, No.8. 1964.
78)	WILLIAM M. KUBIE.	Ph.D.thesis University of Glasgow, Oct.1961.
79)	ROBERT E. WEBER	'Temperature measurement and control' published by the Blakiston Company, Philadelphia, (pp.406), 1941
80)	STAUFF, W.D. and MONTGOMERY D.J.	J.Appl. Phys., 26, 540, 1955.
81)	JONES J.E.	J.Sci.Instrument, 38, 367, 1961.

82)	QUYNN and STEELE.	Text.Res. J, 23, No.4, pp.258-259, 1953
83)	KING A.T.	J.Text.Inst., 17, T.153, 1926.
84)	MAN-MADE TEXTILE ENCYCLOPEDIA	Ed.Press J.Inter science publishing Co. Inc., New York, 1959.
86)	p.66 in CONTRIBUTION TO THE PHYSICS OF CELLULOSE FIBRES.	Ed.Hermans P.H., Elsevier publishing Co. Amsterdam, 1946.
87)	HERMANN, P., and HERZOG A.	in Mikroscopische und Mechanis Techinsche Textiluntersuchunge 1931
88)	p.88 in ARTIFICIAL FIBRES.	Ed. Moncrieff, R.W., London National Trade Press Ltd., 1954
89)	PAULING L., and COREY R.	Proc.Natl.Acad.Sci. ,U.S. , 37, 205, 261, 729, 1951.
90)	PAULING L., and COREY R.	Proc.Natl.Acad.Sci., U.S. 37, 251, 1951.
91)	PETERS L., and WOODS H.J.	Chap.VIII in 'Mechanical Properties of Textile fibres' Ed.R.Meredith, N.Holland publishing Co., Amsterdam, 1956.
92)	P.70 in 'CONTRIBUTION TO THE PHYSICS AND CHEMISTRY OF CELLULOISE FIBRES'	Ed.Hermanns, P.H. Elsevier, N.Y., 1946.
93)	PHILIPP, H.J., NELSON M.C., and ZIEFLE, H.M.	Text.Res.J., 17, 585, 1947.
94)	MARK H.	Ind.Eng.Chem., 34, 1343, 1942.

95)	WABHA M.	J.Text.Inst,56,T.218,No.4., 1965.
96)	WOODING N.S.	Chap.13 in 'Fibre Structure' Ed.Hearle,J.W.S. and Peters, R.H.,Publishers,The Text. Inst.1963.
97)	MANDELKERN C.,and FLORY P.J.	J.Amer.Chem.Soc., 73, 3206, 1951.
98)	DAANE J.H., and BARKER R.E.	J.Polymer Sci.,B, 2,343-347, 1964.
99)	LIANG CY., and KRIMM S.	J.Polymer Sci., 31, 513,1958.
100)	STE'FANI,R,CHEVERTON H., TERRIER,J, and EYRAUD C.	Compt.Rend., 248,2006,1959.
101)	STE'FANI R,CHEVERTON,H., CARNIER,M.,and EYRAUD C.	Compt.Rend., 251, 2174,1960.
102)	MENCIK Z.	Vysokomolekul Soedin, 2, 1935, 1960.
103)	BOHN C.R., SCHAEFGEN and STATTON,	J.Polymer Sci, 55,531, 1961.
104)	TADOKORO,H.,MURAHASHI, S., YAMADERA, R.,NAMEI T.	J.Poly.Sci.A, 1, No.10., pp.3029-3042,1963
105)	GENERAL PROPERTIES OF ACRILAN 16.	Technical Information Bulletin Chemstrand, A643.
106)	BACCAREDDA,M.and BUTTA E.	Chim.e' ind (Milan), 40,6, 1958.
107)	MUUS,McCRUM, and McCREW.,	Spe.Journal 15, 368,1959.
108)	SLICHTER W.P.,and MANDELI E.R.	J.Appl.Phys., 29,1438,1958.

109)	McDONALD M.P., and WARD I.M.	Pro.Phys.Soo., 80, 1249-1263, 1962.
110)	HYNDMAN D., and ORIGLIO, G.F.	J.Polymer Sci, 39,556, 1959.
111)	NISHIOKA, A.,KOIKE,Y, OWAKI,M,NARABA,T.,and KATO,Y,	J.Phys.Soc.Japan, 15 , 416, 1960.
112)	GRUPTA R.P.	Kolloidzscher, 174, 73, 1961.
113)	WOODWARD A.E.,ODAJIMA A., and SAUER J.A.	J.Phys.Chem., 65,1384, 1961.
114)	pp.6-7	Technical Information from Chemstrand on Acrilan 16, A.64/3.
115)	HOLLIDAY P.	Discussion Farad.Soc.,9, 325,1950.
116)	TRIFAN D.S., and TERENZI, J.F.	J.Polymer Sci., 28, 443, 1958.
117)	MIYAKE,A.,	J.Polymer Sci.,, 44, 223, 1960.
118)	GLICK,R.E., and PHILLIPS, R.C.	J.Polymer Sci.,part A, 3 , No. pp.1885-1894, 1965.